EXAMINATION OF THERAPEUTIC POTENTIAL OF LUTEOLIN ON ACUTE LYMPHOBLASTIC LEUKEMIA CELLS AND CHANGES IN MACROMOLECULES

A Thesis Submitted to
the Graduate School of Engineering and Sciences of
İzmir Institute of Technology
in Partial Fulfillment of the Requirements for the Degree of

MASTER OF SCIENCE

in Molecular Biology and Genetics

by
Melisa ÇETİNKAYA

July 2023
İZMIR

We approve the thesis of **Melisa ÇETİNKAYA**

Examining Committee Members:

Prof. Dr. Yusuf BARAN
Department of Molecular Biology and Genetics, Izmir Institute of Technology

Prof. Dr. Bünyamin AKGÜL
Department of Molecular Biology and Genetics, Izmir Institute of Technology

Prof. Dr. Afig BERDELİ
Department of Internal Medicine Sciences, Ege University

03 July 2023

Prof. Dr. Yusuf BARAN
Supervisor, Department of Molecular Biology
and Genetics, Izmir Institute of Technology

Prof. Dr. Özden YALÇIN ÖZUYSAL
Head of the Department of Molecular
Biology and Genetics

Prof. Dr. Mehtap EANES
Dean of the Graduate School of
Engineering and Sciences

ACKNOWLEDGMENTS

My deepest thank and gratitude would be to my supervisor, Prof. Dr. Yusuf BARAN, for his endless and priceless support, encouragement, and guidance in my studies and life. Since I met him, which was around in high school, he has been a perfect role model for me with his ideal career path and his career and encouraged me to study Molecular Biology and Genetics. I am so lucky and grateful to work with him as he was my supervisor and became my family member in the last six years. The things I have learned from him and his everlasting life energy will continue to enlighten my life and career path.

I would like to thank my committee members Prof. Dr. Bünyamin AKGÜL and Prof. Dr. Afig BERDELİ, for their critical and valuable support, suggestions, and contributions.

I would like to thank Assoc. Prof. Dr. Çağatay CEYLAN for his contributions, suggestions, and support for the FTIR experiments.

I would like to also thank former members of Baran Lab and my friends, Nuisabah ABDULHADI, Muharrem Şevki PAZARÇEVİREN, Polen YUNUS, Hatice Damla DAĞ, and Gönül ÖFKELİ for their valuable support in the laboratory and their friendship.

I would like to thank my dearest friend Taha Buğra GÜNGÜL for his never-ending love, support, encouragement, motivation, and unconditional belief in me even though we are in different cities or on other continents. Also, I am so grateful to my beautiful friends Zehra Elif GÜNYÜZ, İlayda ERAKIN, and Elif ÖNSÖZ, who have been in my life for a long time. I would like to thank them for their unlimited support and love.

I am also very grateful to my family, my mom Oya KIZILCAN; my grandfather Şekim KIZILCAN, my grandmother Betül KIZILCAN; and my cousin Defne EMİROĞLU for their unconditional love, support, understanding, and motivation, throughout my life.

I would like to thank the Department of Molecular Biology and Genetics and IZTECH Biotechnology and Bioengineering Research and Application Center specialists for their valuable help and support of my studies.

ABSTRACT

EXAMINATION OF THERAPEUTIC POTENTIAL OF LUTEOLIN ON ACUTE LYMPHOBLASTIC LEUKEMIA CELLS AND CHANGES IN MACROMOLECULES

Acute lymphoblastic leukemia (ALL) is a genetic disease that arises from the various recurrent genetic alterations blocking the differentiation of the precursor B-and T-cells, resulting in the aberrant proliferation and survival of immature lymphoblasts within the peripheral blood and bone marrow. T-ALL is an aggressive type of ALL, and the current treatment strategies, including the high-intensity combination chemotherapy, result in different side effects which are difficult to accept or ultimately lead to the death of patients as substantial toxicity of those chemotherapeutics is known to healthy cells alongside with the cancer cells. Therefore, there is a need to identify nontoxic, cost-effective, potent, and readily available treatment options for T-ALL patients.

One alternative option is the flavonoids in cancer therapeutics, which are secondary metabolites of plants mainly responsible for plants' colors and flower aromas. Luteolin is an extensively researched member of the flavonoids with anticancer properties shown in various cancer types, except for the T-ALL.

This study demonstrated Luteolin's time- and dose-dependent antiproliferative, cytostatic, and apoptotic effects on T-ALL cells for the first time in the literature. Also, the macromolecular changes caused in response to Luteolin treatment in T-ALL cells were examined for the first time. As a consequence, it was found that Luteolin had antiproliferative, apoptotic, and cytostatic effects on T-ALL cells, suggesting its therapeutic potential and was demonstrated to cause an increase in the lipid-to-protein ratio and the hydrocarbon chain length of the lipid acyl chains in a dose-dependent manner on T-ALL cells.

ÖZET

LUTEOLIN'İN AKUT LENFOBLASTİK LÖSEMİ HÜCRELERİ ÜZERİNDEKİ TERAPÖTİK POTANSİYELİNİN VE MAKROMOLEKÜLER ETKİLERİNİN İNCELENMESİ

Akut lenfoblastik lösemi (ALL) genetik bir hastalık olup öncül B ve T hücrelerinin farklılaşmasını bloke eden çeşitli tekrarlayan genetik değişikliklerden kaynaklanır ve olgunlaşamamış lenfoblastların anormal çoğalması ve hayatta kalmasıyla ve kan iliği, periferik kan gibi bölgelerde birikimi ile sonuçlanır. T-ALL, ALL'nin agresif bir türüdür ve mevcut tedavi stratejileri arasında kullanılan kombinasyon kemoterapisi, hastalarda ölüme yol açan veya kabul edilmesi zor olan yan etkilere sebep olmaktadır. Bunun nedenlerinden biri de kemoterapötiklerin kanser hücreleri yanı sıra sağlıklı hücrelere de önemli düzeyde toksisiteye sebep olmasıdır. Bu nedenle, T-ALL hastaları için toksik olmayan, maliyeti uygun, etkili ve kolayca bulunabilen tedavi seçeneklerinin geliştirilmesine acil bir ihtiyaç vardır.

Kanser için alternatif terapötik ajan olarak son yıllarda bitkilerin ikincil metabolitleri olan flavonoidlerin kullanımının, esas olarak bitkilere renk ve aroma vermekle sorumludurlar, araştırmaları önem kazanmıştır. Luteolin, T-ALL hariç diğer kanser çeşitlerinde antikanser özelliği kapsamlı bir şekilde gösterilmiş olan bir flavonoiddir.

Bu çalışma ile, literatürde ilk kez Luteolin'in T-ALL hücreleri üzerindeki doza ve zamana bağlı antiproliferatif, apoptotik ve sitostatik etkileri gösterilmiştir. Ayrıca, yine literatürde ilk defa Luteolin tedavisine yanıt olarak T-ALL hücrelerinde oluşan makromoleküler değişiklikler incelenmiştir. Sonuç olarak, Luteolin'in T-ALL hücreleri üzerinde antiproliferatif, apoptotik ve sitostatik etkilere sahip olduğu bulunmuş olup, bu da Luteolin'in T-ALL için terapötik potansiyelini işaret etmektedir. Aynı zamanda, Luteolin'in T-ALL hücrelerinde doza bağlı olarak lipid-protein oranında ve lipidlerin asil zincirlerindeki hidrokarbon zincir uzunluğunda artışa sebep olduğu gösterilmiştir.

To My Beloved Grandfather Şekim KIZILCAN…

To My Lovely Mother Oya KIZILCAN…

To Patients Fighting with Leukemia…

TABLE OF CONTENTS

LIST OF FIGURES

Figure **Page**

LIST OF TABLES

LIST OF ABBREVIATIONS

ABL1, Abelson murine leukemia 1

ADCC, Antibody-dependent Cellular Cytotoxicity

ADCP, Antibody-dependent Cellular Phagocytosis

AEG-1, Astrocyte-elevated Gene-1

ALL, Acute Lymphoblastic Leukemia

ATR, Attenuated Total Reflection

BAX, BCL2-Associated X

BCL-2, B-cell leukemia/lymphoma 2

BCL-xL, B-cell lymphoma-extra large

BCR, Breakpoint Cluster Region

CAR, Chimeric Antigen Receptor

CDC, Complement-dependent Cytotoxicity

CML, Chronic Myeloid Leukemia

COMTs, Catechol-O-methyltransferases

CVAD, Cyclophosphamide, Vincristine, Doxorubicin, Dexamethasone

CXCR4, C-X-C Chemokine Receptor Type 4

DMSO, Dimethylsulfoxide

DMSZ, German Collection of Microorganisms and Cell Cultures

DR, Death Receptor

EMT, Epithelial-mesenchymal Transition

ERK, Extracellular Signal-regulated Kinase

FAB, French–American–British

FcγR, Fc Gamma Receptor

FDA, Food and Drug Administration

FGFR, Fibroblast Growth Factor Receptor

FLT3, FMS-like Tyrosine Kinase 3

FTIR, Fourier Transform Infrared

H2AX, H2A Histone Family Member X

IC_{50}, The half maximal inhibitory concentration

IL, Interleukin

JNK, c-Jun N-terminal Kinase

MDM2, Mouse Double Minute 2

MMP, Matrix Metalloproteinase

mTOR, Mammalian Target of Rapamycin

PARP, Poly (ADP-ribose) Polymerase

PBD, Pyrrolobenzodiazepine

PBS, Phosphate Buffered Saline

PDGFR, Platelet-derived Growth Factor Receptor

PI, Propidium Iodide

PI3K, Phosphoinositide 3-kinase

RET, Rearranged during Transfection

ROS, Reactive Oxygen Species

Ph, Philadelphia chromosome

pNA, p-nitroanilide

TIMP, Tissue Inhibitor of Metalloproteinase

TNFR, Tumor Necrosis Factor Receptor

UGTs, UDP-glucuronosyltransferases

VEGF, Vascular Endothelial Growth Factor

WHO, World Health Organization

CHAPTER 1

INTRODUCTION

1.1. Acute Lymphoblastic Leukemia (ALL)

Acute lymphoblastic leukemia (ALL) is a hematological malignancy and a type of leukemia that is related to the transformation and proliferation of lymphoblasts in a malignant way, resulting in the accumulated lymphoid cells, which are poorly differentiated and known to be malignant, in the bone marrow, peripheral blood, and other extramedullary sites like thymus, spleen, and central nervous system (DeAngelo, Jabbour, and Advani 2020). The lymphoblast precursor cells' early development is identified to be blocked by the accumulation of recurrent genetic abnormalities or epigenetic alteration, including aneuploidies, chromosomal rearrangements, and secondary mutations in the period of hematopoiesis, resulting in the suppression of other normal cells of the blood and normal immune response (Terwilliger and Abdul-Hay 2017; DeAngelo, Jabbour, and Advani 2020).

According to GLOBOCAN 2020 statistics, leukemia accounted for 2.5% of the new cancer incidence globally, and the mortality caused by leukemia was around 3.1% (Ferlay J et al. 2020). On the other hand, ALL comprises 10% of diagnosed leukemias, and each year nearly 6000 cases are newly diagnosed with ALL in the USA (Siegel et al. 2022). ALL is one of the most commonly observed cancers in children, with a prevalence of almost 25% of the cancers, and the incidence of the disease is observed to be peak between 1 year old and 4 years old; however, most of the deaths caused by ALL, four out of five deaths from ALL, are observed in adults (Malard and Mohty 2020; Board 2022). Also, ALL has been identified to have primarily arisen in healthy people, with predisposing factors like inherited genetic abnormalities or environmental exposure determined in a few (Malard and Mohty 2020).

1.1.1. Classification of ALL

Until today, the classification of ALL has been done differently by various groups from different perspectives (Abdul-Hamid 2011). One of the earlier classifications was done by a group of French- American- British scientists, French–American–British Cooperative Group (FAB), in the 1970s, and their classification of leukemia was based on the morphology and cytochemical studies on the leukemia cells, which categorized ALL into three subtypes as L1, L2, and L3 (Bennett et al. 1976). Also, according to the traditional categorization of ALL, the enhanced lymphoblast number in the bone marrow or peripheral blood that was required to diagnose ALL was determined as 30% or more (Lai, Hirsch-Ginsberg, and Bueso-Ramos 2000; Bennett et al. 1976).

In 1997, the World Health Organization (WHO) offered a more comprehensive classification of ALL sourced on the morphology, genetics, cytogenetics, and immunophenotypic studies that classified ALL into three subtypes, which were B lymphoblastic, T lymphoblastic, and Burkitt-cell Leukemia (N. L. Harris et al. 1999). Furthermore, according to WHO, if the number of lymphoblasts was higher than 20%, it could be considered sufficient for diagnosis (Lai, Hirsch-Ginsberg, and Bueso-Ramos 2000; N. L. Harris et al. 1999).

The classification of ALL by WHO has been revised several times in recent years. In 2008, Burkitt-cell Leukemia was removed from the classification of ALL since the subtype was considered to be not a type different subtype of Burkitt Lymphoma. Also, based on the 2008 revision, B-lymphoblastic leukemia was further split into two subgroups, which were B-ALL, not specified otherwise, and B-ALL with recurrent genetic abnormalities, and the latter category was further subcategorized based on the present specific chromosomal rearrangements (Vardiman et al. 2009). In 2016, the latest revision to ALL classification was done by WHO, and based on the newest revision, two novel entities were listed to the recurrent genetic abnormalities as provisional entities, and the hypodiploid was defined again with low hypodiploid or hypodiploid along with TP53 mutations. Also, according to the latest revision, a temporary entity entitled Early T-cell precursor lymphoblastic leukemia was included; a subset was characterized by a genuine genetic and immunophenotypic profile that indicated solely limited early differentiation of T-cell along with retaining cell characteristics of myeloid

and stem cell (Arber et al. 2016). In brief, with the latest revisions to the classification, according to WHO, ALL is divided into two main subcategories, B-ALL and T-ALL, and the B-ALL is further divided into the presence of specific recurrent genetic abnormalities and B-ALL with no specified otherwise (Table 1.1.) (Arber et al. 2016).

Table 1.1. The classification of ALL based on WHO (Source: (Luca 2021))

B-lymphoblastic leukemia/lymphoma
- B-lymphoblastic leukemia/lymphoma, not otherwise specified (NOS)
- B-lymphoblastic leukemia/lymphoma with recurrent genetic abnormalities:
  - * B-lymphoblastic leukemia/lymphoma with t(12;21) (p13.2;q22.1); *ETV6-RUNX1*
  - * B-lymphoblastic leukemia/lymphoma with hyperdiploidy
  - † B-lymphoblastic leukemia/lymphoma with t(9;22) (q34.1;q11.2); *BCR-ABL1*
  - † B-lymphoblastic leukemia/lymphoma with t(v;11q23.3); *KMT2A*-rearranged
  - † B-lymphoblastic leukemia/lymphoma with hypodiploidy
  - † B-lymphoblastic leukemia/lymphoma, *BCR-ABL1*–like
  - † B-lymphoblastic leukemia/lymphoma with iAMP21
  - ‡ B-lymphoblastic leukemia/lymphoma with t(1;19) (q23;p13.3); *TCF3-PBX1*
  - ○ B-lymphoblastic leukemia/lymphoma with t(5;14) (q31.1;q32.1); *IGH/IL3*
- B-lymphoblastic leukemia/lymphoma with newly described oncogenic fusions (unofficial)
- B-lymphoblastic leukemia/lymphoma with other significant mutations (unofficial)

T-lymphoblastic leukemia/lymphoma
- T-lymphoblastic leukemia/lymphoma, NOS
  §Early T-cell precursor lymphoblastic leukemia

NK-lymphoblastic leukemia/lymphoma

*, favorable; †, unfavorable; ‡, intermediate; ○, probably indifferent; §, debatable.

Most ALL cases are from the B-cell lineage, approximately 80%, while the rest are of the T-cell lineage, and the T-ALL is defined as an aggressive form of the ALL. Also, determining the genetic alterations is crucial for treating ALL patients as the genetic abnormalities are known to affect the progress of treatment, the patient response to therapy, and the efficacy of the therapeutic drugs used for treating adult and children patients (Roberts 2018). In general, the trisomy of chromosome numbers, 4,10, and 21, hyperdiploid, hypodiploid, and chromosomal translocations like t(9;22) BCR-ABL1, t(4;11) MLLAF4, t(1;19) E2A-PBX1, and t(12;21) ETV6-RUNX1 are considered as the B-ALL genetic determinants (Terwilliger and Abdul-Hay 2017).

Moreover, the reciprocal translocation among chromosome number 9 and 22 resulted in the generation of the fusion gene, BCR-ABL1, and the Philadelphia chromosome, a changed version of chromosome 22, that bears the fusion gene is

considered one of the critical genetic determinants in the B-ALL genetics and based on the presence of this translocation and transcriptional profile of leukemic blasts, B-ALL can be categorized as; Philadelphia chromosome-positive B-ALL (Ph-Positive B-ALL), Philadelphia-like (Ph-like) B-ALL, and Philadelphia chromosome-negative B-ALL (Nowell 2007; Den Boer et al. 2009). The Ph-like B-ALL is one of the newly identified subtypes that had entered the classification with the 2016 revision to the WHO classification and characterized with a congener profile of transcription to Ph+ B-ALL; however, in this subtype, there is no t(9;22) BCR-ABL1 (Arber et al. 2016).

1.1.2. Present Treatment Strategies for ALL

The first-line treatment for ALL generally comprises four phases lasting over 2 to 3 years, and the four phases of the chemotherapy treatment that are considered the first-line treatment are induction, consolidation, intensification, and long-term maintenance with a targeted therapy provided to avoid central nervous system relapse (Narayanan and Shami 2012). Induction chemotherapy focuses on achieving complete remission and restoring normal hematopoiesis and involves using a combination of chemotherapeutic agents, including anthracycline, vincristine, L-asparaginase, and glucocorticoid. After induction therapy, patients eligible for allogeneic stem cell transplantation can continue the allogeneic stem cell transplantation treatment, while others continue the chemotherapy's consolidation, intensification, and long-term maintenance phases (Capria et al. 2020; Samra et al. 2020). Consolidation therapy generally involves the usage of similar agents used in the induction and comprises intrathecal chemotherapy with the appliance of cranial radiation therapy at different times for central nervous system prophylaxis (Schrappe and Stanulla 2010). The intensification therapy is followed after consolidation and involves the usage of drugs that have been used during the induction treatment. Maintenance therapy contains the administration of mercaptopurine on a daily basis and methotrexate weekly along with or not vincristine and glucocorticoid every 1 to 3 months, and the maintenance therapy is continued for 2-3 years (Malard and Mohty 2020). Also, special consideration must be taken when treating Ph-positive ALL.

Even though the children's 5-year overall survival rate had reached up to 90%, solely 25% of the adult patients (more than 50 years old) did not die five years after the diagnosis with ALL, which highlights the importance of the discovery of new therapeutic strategies for the treatment (Hunger et al. 2012).

1.1.2.1. Tyrosine Kinase Inhibitors

The usage of molecular biology techniques has an important part in the classification of malignancies, which provided the discovery of the signaling pathways that can be used to target the treatment of the disease. One important example was the refinement of the tyrosine kinase inhibitors for the targeted therapy of Ph-positive chronic myeloid leukemia (CML) and ALL by targeting BCR/ABL fusion protein as this fusion protein was found as a molecule that is the primary regulator of the disease prognosis (Pottier et al. 2020).

Tyrosine kinase inhibitors' discovery was a massive landscape of treating Ph-positive ALL as, before the addition of the tyrosine kinase inhibitors to the treatment, Ph-positivity was considered a terrible player both in terms of prognosis and treatment with the previous 1-year survival of the patients was around 10% and the 5-year survival rate was approximately 5-20% (Dombret et al. 2002; Faderl et al. 2000).

The first-generation tyrosine kinase inhibitor, named Imatinib mesylate (Gleevec, STI571, Novartis), took approval from Food and Drug Administration (FDA) in the year 2001 (Cohen et al. 2002). This drug's mode of action was based on the principle of BCR/ABL1 protein's constitutive activation with the binding of ATP to the domain of the fusion protein, which Imatinib mesylate binds, in particular, to the domain of ATP binding of BCR/ABL1 and competitively inhibits phosphorylation and activation of BCR/ABL and the related pathways; however, it has also been identified to suppress the tyrosine kinase activity of c-KIT and the Platelet-derived Growth Factor Receptor (PDGFR) (Druker et al. 2001; 1996). Adding Imatinib to conventional chemotherapy resulted in improved outcomes; however, resistance to the treatment was observed in some patients. The resistance to Imatinib was found to be related to the mutations in the ABL kinase domain, such as F317L or T315I, activating loop or P-loop mutations (Azam, Latek, and Daley 2003; Shah et al. 2002). Also, combining Imatinib

with conventional chemotherapy failed due to the central nervous system relapse observed after the decrement in the penetration of Imatinib (de Labarthe et al. 2007; Jones et al. 2008; Daver et al. 2015). Ultimately, the second and third generations of tyrosine kinase inhibitors started to be developed after the observation of no response in some patients who were administered Imatinib in the first-line treatment and the development of resistance to Imatinib (Jabbour, Kantarjian, and Cortes 2015).

One of the second-generation tyrosine kinase inhibitors, Dasatinib (Sprycel, BMS-354825, Bristol-Myers Squibb), was designed to bind to forms of BCR/ABL protein, which are inactive and active with higher efficacies compared to Imatinib mesylate and approved by FDA in 2006. Also, Dasatinib was demonstrated to inhibit kinases like c-KIT, Ephrin A receptor kinases, SRC and PDGFRβ. Dasatinib was found to be highly efficacious in CML patients with Imatinib resistance with several mutations in BCR-ABL, but the activity of Dasatinib was prevented in the cells that carried the T315I mutation (Shah et al. 2004). Moreover, Dasatinib was found to have an improved penetration ability to the central nervous system compared to Imatinib (Porkka et al. 2008).

The treatment with Dasatinib plus conventional chemotherapy resulted in similar complete remission rates with Imatinib. However, the outcome which is long-term of the treatment was demonstrated to be better than Imatinib in children with Ph-positive ALL, in which the 5-year overall survival was 86% for patients that received Dasatinib and around 70% for the ones that received Imatinib, yet there is no prospective study that compares Imatinib and Dasatinib (Schultz et al. 2014; Slayton et al. 2018; Ravandi et al. 2015).

On the other hand, Nilotinib (Tasigna, AMN107, Novartis) is another second-generation tyrosine kinase inhibitor designed as the aminopyrimidine derivative of Imatinib and approved by the FDA in 2007, and it can bind to the ABL's inactive kinase domain with higher affinity compared to Imatinib (Hazarika et al. 2008). Moreover, Nilotinib can inhibit the c-KIT and PDGFR activity (Saqlio 2010). Although both Dasatinib and Nilotinib as second-generation inhibitors were identified as more effective than the first-generation Imatinib and they have been found to overcome almost entire mutations that occur in BCR/ABL1, they were determined to be not able to overcome T315I mutation, leading to the third-generation tyrosine kinase inhibitors' development (Bradeen and Eide 2006; Jabbour, Cortes, and Kantarjian 2011; Saqlio 2010).

Ponatinib (AP24534) is a third-generation tyrosine kinase inhibitor approved by FDA in 2016, and this pan-tyrosine kinase inhibitor is specifically known for its ability to inhibit the T315I mutation in the ABL kinase domain of the BCR/ABL protein, but also it can inhibit the activity of tyrosine kinases including, Fibroblast Growth Factor Receptor (FGFR), Vascular Endothelial Growth Factor Receptor (VEGFR), SRC, Rearranged during Transfection (RET), and FMS-like tyrosine kinase 3 (FLT3) (Zhou et al. 2011; Pulte et al. 2022). It has been found that Ponatinib was effective in the treatment of patients with T315I mutation, as the 47% of the patients who previously had no response to therapy with Nilotinib or Dasatinib showed significant cytogenic responses to Ponatinib (Cortes et al. 2013). Moreover, a study that compared the two non-randomized studies demonstrated that frontline with Ponatinib therapy was found to improve event-free and overall survival compared to frontline with Dasatinib in Ph-positive ALL patients (Sasaki et al. 2016).

Even though the usage of tyrosine kinase inhibitors in combination with conventional chemotherapy has been considered as a strategy that is the most efficient for treating ALL patients with Ph-chromosome positive, the urge for developing novel options for overcoming the tyrosine kinase inhibitors resistance, the relapse of the disease and other patients that have Ph-negative ALL continues (Malard and Mohty 2020).

1.1.2.2. Monoclonal Antibodies

The regimen of conventional chemotherapy can result in some disadvantages like the relapse of disease, treatment of only a proportion of patients, complete remissions that are not successful, and side effects, leading to the refinement of novel therapeutic strategies, specifically, therapy options that are targetted (Rosenblatt and Avigan 2010). In addition to the need for targeted therapeutic approaches, identifying the cell surface markers present on the surface of the cancer cells has opened up a new era in the development of agents in terms of immunotherapeutic strategies for the treatment of several cancer types, such as ALL. The forenamed immunotherapy strategies are categorized into two main categories: antibody-based and cell-based immunotherapies (Shang and Zhou 2019; Davis and Mackall 2016). The antibody-based

immunotherapies can be further classified into monoclonal antibodies, bispecific T-cell engaging (BiTE) antibodies, and antibody-drug conjugates, subtypes based on the properties of antibodies used in the treatment, and the cell-based therapy consists of Chimeric Antigen Receptor (CAR) T cells for the cure of ALL (Lussana, Gritti, and Rambaldi 2021; Shang and Zhou 2019).

The strategy behind the usage of monoclonal antibodies as a cancer immunotherapeutics is the ability of monoclonal antibodies to bind to the antigens present on the surface of the cancer cells, thereby avoiding the interaction with the ligands or inhibiting the receptor clustering and stimulation, ending up with the apoptosis of the target cancer cells (Golay and Introna 2012). Furthermore, monoclonal antibody-based therapeutics result in the activation of effector mechanisms, including antibody-dependent cellular cytotoxicity (ADCC), complement-dependent cytotoxicity (CDC), and antibody-dependent cellular phagocytosis (ADCP), resulting in the killing of the cells expressing antigen via engagement of Fc gamma receptors (FcγRs) present on the surface of immune cells or complement factors with the Fc regions (Taylor and Lindorfer 2016). Therefore, the therapeutic strategy using monoclonal antibodies eliminates cancer cells by specifically targeting them, separating the non-cancerous cells from cancer cells (Charles et al. 2022).

Monoclonal antibody-based treatment has been considered an important advance in ALL therapy, as the directed delivery of monoclonal antibodies according to the recognition of the cell surface receptors of leukemic cells resulted in enhanced efficacy and decreased off-target toxicity. The well-searched antigens to which the monoclonal antibodies have been directed are CD19, CD20, and CD22, all used for treating B-ALL (Farhadfar and Litzow 2016). Unlike B-ALL, the refinement of the monoclonal antibodies in order to target and treat T-ALL is lagging because of the common expression of surface antigens among normal and leukemic T cells. Although researching and identifying targets selective for blasts of T-ALL not expressed by healthy T-cells is a fundamental challenge in developing the monoclonal antibodies for the T-ALL treatment, up to the present two monoclonal antibodies that target surface antigens, CD38 and CD52 on the T-ALL blasts have been developed (Caracciolo et al. 2023).

CD20, an antigen that is specific in the B-cell lineage, expressed at almost all differentiation stages on the healthy and malignant B-cells' surfaces, has been identified to be expressed in 30-50% of B-ALL patients and has been linked in poor in adult

patients (Maury et al. 2010; Thomas et al. 2009). Moreover, CD20 signaling has been found to play roles in the progression of the cell cycle, apoptosis, and differentiation (Thomas et al. 2009). Adding the first-generation anti-CD20 monoclonal antibody, Rituximab, to the chemotherapy used in first-line yielded promising results for adult patients with ALL that is relapsed or refractory (Chevallier et al. 2012). Also, combining the hyper-cyclophosphamide, vincristine, doxorubicin, and dexamethasone (CVAD) with Rituximab has been found to be linked with decreased relapse rates and enhanced overall survival and event-free survival in comparison to the patients that had administered with only conventional chemotherapy (Thomas et al. 2010).

Even though Rituximab resulted in promising results, in some patients, resistance to the Rituximab therapy was observed, leading to the development of Ofatumumab, a second-generation anti-CD20 monoclonal antibody that has a diversified binding site from the Rituximab (Wierda et al. 2011). In a Phase II study (NCT01363128), Jabbour et al. showed that Ofatumumab, in combination with hyper-CVAD, had resulted in improved 1-year complete remission duration and survival rates overall in patients with who are diagnosed recently with CD20-positive B-ALL or patients who had finished one course of the chemotherapy regimen (Jabbour et al. 2013). Furthermore, Obinutuzumab is a different novel anti-CD20 monoclonal antibody, which has resulted in promising results in various preclinical settings for treating CD20-positive B-ALL (Abuasab, Rowe, and Tvito 2021).

CD22 has been identified to be expressed in almost 90% of B-ALL, and the antigen is an ideal target for immunotherapeutic strategies as binding an antibody to the antigen CD22 results in the rapid internalization of CD22 (Malard and Mohty 2020). Epratuzumab is a monoclonal antibody that directs CD22 that is unconjugated and was extensively searched in specifically adult relapsed ALL and pediatric ALL. In pediatric settings, Raetz et al. examined the effect of Epratuzumab as part of the salvage therapy regimen in 15 patients. In the clinical study, Epratuzumab was administered as the only agent first and then combined with conventional reinduction chemotherapy, resulting in the complete remission of 9 patients, as 7 achieved complete minimal residual disease clearance after reinduction (Raetz et al. 2008). Moreover, in a Phase II study (NCT00945815), Advani et al. demonstrated that adding Epratuzumab to the Clofarabine/Cytarabine therapy resulted in an improved response rate compared to the only Clofarabine/Cytarabine therapy in adult relapsed or refractory ALL patients (Advani et al. 2014).

A distinct anti-CD22 monoclonal antibody is Inotuzumab Ozogamicin, which is a monoclonal antibody in conjugation with a compound that is cytotoxic and promotes double-strand DNA breaks, Calicheamicin. The immunoconjugate's internalization results in the binding of DNA by Calicheamicin, causing double-stranded DNA breaks that promote apoptosis (DiJoseph et al. 2004; Hinman et al. 1993). The Phase I and Phase II studies (NCT01363297, NCT01925131) of Inotuzumab Ozogamicin yielded promising results that encouraged the Phase III studies of the immunoconjugate (H. Kantarjian et al. 2013; DeAngelo et al. 2017). In the Phase III trial (NCT01564784) of administration weekly of the Inotuzumab Ozogamicin, the immunoconjugate was contrasted with the normal chemotherapy regimen in adult patients with relapsed/refractory ALL, and clinical trials resulted in the improved complete remission rate in patients receiving Inotuzumab Ozogamicin (81%) compared to patients that had received only conventional chemotherapy (29%), with the enhanced median overall and median progression-free survival (H. M. Kantarjian, DeAngelo, et al. 2016). The results were confirmed by the Phase III study with longer follow-up, which resulted in the fast-track approval of single-agent Inotuzumab Ozogamicin to treat adult patients with relapsed disease from the FDA (H. M. Kantarjian et al. 2019). Furthermore, different anti-CD22 targeted therapies, including Combotox and Moxetumomab pasudodotox, have been ameliorated and researched in various settings of preclinical and clinical studies (Terwilliger and Abdul-Hay 2017).

CD19 is another B-cell lineage-specific antigen demonstrated to be expressed in nearly 90% of B-ALL patients (Ning et al. 2005). The broad expression of CD19 has been shown in entire differentiation stages. Its expression is lost in the B-cells' maturation to plasma cells, and CD19 is known to be serving as the co-receptor for the B-cell surface immunoglobulin. The signaling of CD19 is responsible for the differentiation and proliferation due to the phosphorylation of different cascades, including Src-family kinases, c-MYC, and Phosphoinositide 3-kinase (PI3K) (Chung et al. 2012). Coltuximab ravtansine (SAR3419) is an anti-CD19 monoclonal antibody that is known to be conjugated to an anti-tubulin semisynthetic compound called Maytansinoid. The effect of Coltuximab ravtansine was investigated in patients with CD19-positive B-cell lymphoma in Phase I clinical trial (NCT00539682), and it was found that in 74% of patients, the tumor size reduction was observed, including 47% of patients that were resistant to Rituximab; however dose-limiting toxicities were observed, including neuropathy and reversible blurred vision (Younes et al. 2012).

However, an initial Phase II clinical trial (NCT01440179) on the effect of Coltuximab ravtansine in patients with ALL that is relapsed was ended due to the low response rate, which was 25% (H. M. Kantarjian, Lioure, et al. 2016). Denintuzumab mafodotin (SGN-CD19A) is another anti-CD19 monoclonal antibody that is in conjugation with Monomethyl Auristatin F (MMAF), a drug that disrupts microtubule, has currently being developed, and the Phase I study (NCT01786096) of Denintuzumab mafodotin in the patients with B-ALL which are relapsed or refractory had yielded a 35% response rate in complete (Fathi et al. 2015). One of the newest anti-CD19 monoclonal antibodies that have been entered into the development is Loncastuximab tesirine (ADCT-402), which is a humanized anti-CD19 monoclonal antibody in conjugation with pyrrolobenzodiazepine (PBD), an inhibitor of cell division via binding in the minor groove of DNA, and resulting in DNA strands' cross-linking. The Phase I study (NCT02669264) of Loncastuximab tesirine in relapsed or refractory B-ALL was terminated in the stage for an escalation of dose due to slow accrual (Jain et al. 2020).

CD52, a surface glycoprotein, is not expressed in normal hematopoietic progenitors; however, it is profoundly expressed in lymphocytes, B-cells, T-cells, macrophages, and monocytes (Oehler et al. 2010). Furthermore, in some cases of T-ALL, the high expression of CD52 has been reported, but it has been found that the pre-T leukemic blasts demonstrated a lower expression profile compared to mature cells, showing that the immunotherapeutics targeting CD52 can be limited with the mature subtypes (Tibes et al. 2006; Lozanski et al. 2006).

The function of CD52 has been studied in some studies, and it has been reported that CD52 can result in the promotion of the activation of T-cells and stimulate CD4+ regulatory T-cells' production, thereby activating the immunosuppressive mechanisms, but its function was not clearly understood (Bandala-Sanchez et al. 2013). Alemtuzumab (CAMPATH-1H) is an antibody that is monoclonal and targets the CD52 on diseases associated with T-cells involving T-ALL. The Phase II clinical trial (NCT00089349) of Alemtuzumab in children patients with relapsed/refractory T-ALL resulted in poor results, as the activity of solely Alemtuzumab was found to be tethered in those settings, even though one of the patients showed complete response (Angiolillo et al. 2009). Also, a Phase I clinical trial (NCT00061945) focused on delivering Alemtuzumab's effectiveness in combination with chemotherapy on the patient profile that had above 10% CD52-positive lymphoblasts for the destruction of the minimal residual disease in patients with T-ALL resulted in no advantageous outcomes

compared to available therapies and various side effects, resulting in the closure of clinical studies that involves CD52 (Stock et al. 2009).

CD38, a type II transmembrane glycoprotein found to be expressed at the early stages of development of T-and B-cell, is identified to be expressed merely in lymphocytes, which are mature and naïve, as re-expressed following the event that T-cells are activated and found to be lost in the compartment of T-cell memory (Vale and Schroeder Jr 2010; Malavasi et al. 2008). The function of CD38 in T-cells is that its signaling is related to the T-cell receptor function, promoting intracellular molecules' activation, including Zap70, Akt, and ERK, and the ligation of CD38 results in the inducement of T-cell precursors' death, thereby contributing to the thymocyte selection inside the thymus (Zubiaur et al. 2002).

Furthermore, CD38 has been identified to be widely expressed in hematological malignancies (Jiao et al. 2020), and more recently, Tembhare et al. demonstrated its broad expression in different T-ALL subtypes via flow cytometry, resulting in the finding that patients with relapsed T-ALL or who haven't responded to conventional chemotherapies can be treated with anti-CD38 monoclonal antibodies as a treatment option (Tembhare et al. 2020).

The efficacy of Daratumumab, which is an anti-CD38 monoclonal antibody, has been well reported in preclinical settings for treating T-ALL, as the expression of CD38 was demonstrated in Earlier T-cell Precursor ALL patient leukemic cells and in non-Early T-cell Precursor ALL cells, and nearly entire patient-derived xenografts of T-ALL were identified to be sensitive to Daratumumab (Bride et al. 2018). Moreover, Gurunathan et al. demonstrated in a case report that a patient with refractory T-ALL who was 19 years old had tolerated Daratumumab well, and it caused a reduction which was found to be temporary in the T-cell lymphoblasts present in the bone marrow (Gurunathan, Emberesh, and Norris 2019).

More recently, Daratumumab has been demonstrated to eradicate the minimal residual disease successfully in patients with T-ALL who suffered a relapse after the allogeneic stem cell transplantation (Ofran et al. 2020). Also, a Phase II clinical trial (NCT03384654) is currently going on to investigate the effectiveness of combining Daratumumab and conventional chemo for treating children and young adult patients with T-ALL or B-ALL relapsed or refractory (Ruhayel and Valvi 2020).

1.1.2.3. Chimeric Antigen Receptor (CAR) T cells

Chimeric Antigen Receptor (CAR) T cells are T-cells that are engineered in a genetic manner to express the antigen-binding domain of an immunoglobulin which is in link to a costimulatory molecule and the domain of the intracellular T-cell receptor signaling, and they can recognize the antigens which are not processed, and they can be activated in a way that is not dependent on the major histocompatibility complex (Mohanty et al. 2019). Even though the first-generation CAR T cells are designed to comprise the intracellular signaling moieties, which are known to be solely derived from the complex of T-cell receptor/CD3, the addition of costimulatory signals in the gene constructs of the CAR is included in the second and third generations, and the more recent design, the fourth-generation CAR T cells, cytokine-expressing cassette have been included (Mehrabadi et al. 2022). Furthermore, the developed autologous CAR T-cell treatment consists of collecting T-cells from patients, delivering the construct of CAR and CAR T cells' autologous administration to the patients (Pettitt et al. 2018).

For treating B-ALL, the CD19-directed CAR T cell therapy has been considered a promising strategy, as the broad expression of CD19 on almost entire B-ALL cells made it an ideal target for developing anti-CD19 CAR T cells and has been widely studied. In a pilot Phase 1/2 clinical study (NCT01626495 and NCT01029366), Maude et al. gave the CAR T cells after the depletion chemotherapy of T-cells to 30 children and adult patients who have relapsed/refractory B-ALL, and complete remission was observed in 90% of the participants with negative minimal residual disease ratio of 88% alongside complete remission (Maude et al. 2014). In a subsequent Phase II study (NCT02435849) which was more extensive, among 75 children and adolescents and young adult patients, 61 showed complete remission with negative minimal residual disease (Maude et al. 2018). After one year, 76% of patients demonstrated overall survival, 50% had accomplished event-free survival, and preliminary research indicated that complete remission could be achieved in 88% (14 out of 16 patients with relapsed/refractory ALL) via using a different anti-CD19 CAR T-cell construct (Davila et al. 2014), which was updated and followed by a larger cohort, 53 patients, for a more extended period and resulted in the complete remission of 83%, overall survival for 12.9 months and event-free survival for 6.1 months (Park et al. 2018). As a result, CAR T-

cells were approved by the FDA for the therapy of relapsed or refractory disease patients, which are children or adolescents and young adults after administering two rounds of different treatments or after the hematopoietic cell transplantation (Davis and Mackall 2016).

Based on the promising results gathered from treating B-ALL, various trials have also been started to use CAR T cells for T-ALL therapeutics (Bayón-Calderón, Toribio, and González-García 2020). CD4 is known to be a prior molecule researched to be CAR T cell therapy's target for treating T-ALL, as it is identified to be expressed in a reliable T-ALL portion (K. Pinz et al. 2016). In the preclinical settings, Pinz et al. developed a third-generation of CD4 CAR that contained 4-1BB and CD28 costimulatory domains and demonstrated in the *in vitro* and *in vivo* models of peripheral T cell lymphoma efficacy when CAR was carried by NK92 and T cells (K. G. Pinz et al. 2017; K. Pinz et al. 2016). Based on the preclinical success, a Phase I trial (NCT04162340) was started to investigate the antitumor efficacy and safety of CD4 Car T cells for treating malignancies of CD4+ T-cell, such as T-ALL (Bayón-Calderón, Toribio, and González-García 2020). Another ideal target for treating T-ALL by using CAR T cell therapy was the CD5, the most prevalent surface marker of T-cells, which are malignant and identified to be expressed in 80% of T-ALL (Pui, Behm, and Crist 1993). For this purpose, in the preclinical settings, Mamonkin et al. demonstrated that a second-generation CD5 CAR alongside the costimulatory domain of CD28 had yielded the downregulation of CD5 and transient fratricide. Also, the generated CD5 CAR T cells were found to be significantly effective in the elimination of T-ALL lines *in vitro* and controlled the onset of disease *in vivo* (Mamonkin et al. 2015), leading to the Phase I clinical study (NCT03081910) to investigate this therapeutic approach effectiveness and safety for the patients with T-ALL who have refractory or the relapsed disease (Dai et al. 2021).

CD7 is another important CAR T cell therapeutics target due to its profound expression in T-ALL (Campana et al. 1991). In the preclinical studies of the CD7 CAR T cell therapy, reduction in the levels of CD7 on the CAR T cells which were transduced was observed to be incomplete, resulting in the fulminant fratricide and making the expansion in the *ex vivo* settings impossible, thereby it was suggested that the CD7' surface expression should be avoided in the engineered CAR T cells for avoiding the persistent self-targeting that occurs in CAR T cells (Png et al. 2017; Cooper et al. 2018). The eradication of the CD7 expression via avoiding the protein

trafficking of CD7 to the cell's surface or via gene editing resulted in the decrement of fratricide and enhanced the CD7 CAR T cells' expansion by causing a no change in the proliferation or short-term effector function and yielded in the significant antitumor activity in the preclinical settings that are against CD7+ T-ALL (Png et al. 2017; Cooper et al. 2018; Gomes-Silva et al. 2017).The findings from the preclinical studies opened up the way for the Phase I clinical study (NCT03690011), which examines the safety profile and effectiveness of the CD7 CAR T cells that are edited by CD7-CRISPR-Cas9 for treating CD7+ T-ALL patients (Watanabe et al. 2023).

Although CAR T cell therapeutics can be seen as an encouraging approach for ALL, some considerations still need to be taken care of. For instance, the designed CAR T cells directing CD19 have been identified to be related to severe side effects such as cytokine release syndrome and neurotoxicities, which are very threatening to patients' lives. For CAR T cell therapeutics to be efficient, these severe complications must be managed in a way leading to the publication of consensus guidelines in 2018 by The American Society for Blood and Marrow Transplantation (D. W. Lee et al. 2019). Tocilizumab, a monoclonal antibody against the IL6 receptor, can be used to manage cytokine release syndrome, as it is significantly tolerated by patients and quickly effective for the purpose (Le et al. 2018). Also, for neurotoxicity, the usage of steroids has been found to be effective, yet precautions should be taken into account since steroids can decrease the antitumor potential of CAR T cells (Karschnia et al. 2019).

1.2. Flavonoids

The plant kingdom has been for a long time considered an indispensable source for therapies based on natural manner to treat neoplasms that are benign or malignant. Plant-derived bioactive compounds' mechanistic and structural features have initiated extensive research for using them to prevent or moderate diseases, including neurodegenerative and cardiovascular diseases, inflammation, and, particularly, cancer, leading to the initiation of investigation in preclinical settings (Dehelean et al. 2021). There among the initiated studies, a program was conducted to screen the plant-derived compounds' anticancer characteristics that were given start in 1961 by the United States National Cancer Institute has been considered an important one as the study has led to

the discovery of various novel natural products that have currently critical roles in the chemotherapeutics, like vincristine, vinblastine, and paclitaxel. As mentioned earlier, the study is also considered a highlight in the field as it has enlightened the path for using the natural structures that plants provide to humankind to serve and develop efficient therapeutics that can be used as particularly anticancer agents (Sak 2022).

Flavonoids are a group that is among the bioactive compounds derived from plants with more than ten thousand members that are widely distributed in various vegetables, fruits, roots, flowers, stems, bark, and particular beverages. They are the secondary metabolites of plants in the polyphenolic structure and are classified into six primary subclasses: flavanones, isoflavones, flavanols, anthocyanins, and flavones, found in the human diet (Panche, Diwan, and Chandra 2016). Flavonoid research has identified their beneficial roles in human health, as they have remarkable antiviral, anti-inflammatory, antihypertensive, neuroprotective, anticancer, and antioxidant properties (Dias, Pinto, and Silva 2021; Ullah et al. 2020). Among the various valuable parts of flavonoids in human health, their anticancer properties of them were known to be well-researched in different *in vitro* and *in vivo* settings. Their anticancer properties have been identified to be mainly associated with their ability in terms of regulation oxidative stress in cells (Dias, Pinto, and Silva 2021; Slika et al. 2022). Luteolin, an extensively studied member of flavonoids, is a flavonoid that belongs to the flavone member and is found to be widely occurring in different plant species (Çetinkaya and Baran 2023).

1.2.1. The Physiochemical and Biological Properties of Luteolin

Luteolin (3′,4′,5,7-tetrahydroxyflavone) is an example of a plant-derived chemical compound. This broad study flavone is the subclass of flavonoids that consists of a C6-C3-C6 carbon skeleton alongside the two rings of benzene fused, which are known to be connected together with a heterocyclic ring structure (Figure 1.1.), and it is an integral part of the Chinese traditional medicine as the plants that are wealthy in terms of Luteolin is known to be used for treating cancer, hypertension, and inflammatory diseases (Harborne and Williams 2000). As the chemical, Luteolin is known to appear as a yellow crystalline with a $C_{15}H_{10}O_6$ molecular formula and 286.24 g/mol molecular weight, and it has low water solubility (K. Yang et al. 2013).

Interestingly, Luteolin was found to be a naturally heat-stable compound not lost during cooking (Le Marchand 2002). Furthermore, the Luteolin molecule has been identified to be broadly shed in plants as primarily an aglycone molecule which is known to have no moiety of sugar, called aglycone form, and as a molecule of glycoside, so-called the LUT-7-O-glucoside. The glycoside form of Luteolin includes a bounded sugar moiety, mainly glucose, and it differs from the aglycone in terms of its chemical structure, in which one or more hydroxyl groups bound the sugar moieties in the glycoside form (López-Lázaro 2009). Moreover, LUT-7-O-glucoside is the most prevalent Luteolin compound that has been present in diets consisting of foods depending on fruits, vegetables, and beverages, like apples, pomegranates, lettuce, grapes, oranges, lemons, spinach, parsley, carrots, leaves of onions, nuts, green tea, seaweed, coffee, dark chocolate, and thyme (Caporali et al. 2022).

The biological functions of Luteolin have been exhibited in a variety of studies, and the highlighted Luteolin's biological effects include its neuroprotective, antiallergy, anti-inflammatory, antiviral, and anticancer properties (Muruganathan et al. 2022). Also, it has been found that Luteolin can serve as an antioxidant based on Luteolin′s chemical structure. The structure-activity relation studies have shown that Luteolin′s potent antioxidant activity because of the hydroxyl groups at different locations (Lin et al. 2008). Moreover, Luteolin and its glycoside form as an antioxidant were identified to be related to scavenging free radicals formed by oxidative damage, chelating ions of metals, inhibiting pro-oxidant enzymes′ activities, which would result in the production of free radicals, and promoting the activity of antioxidant enzymes (Q. Cai, Rahn, and Zhang 1997; Choi et al. 2007; López-Lázaro 2009).

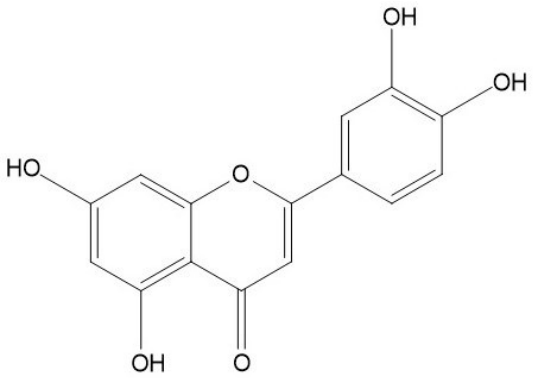

Figure 1.1. Luteolin′s chemical structure

The structure-activity studies have revealed more helpful information about Luteolin; for instance, the carbonyl oxygen that is present at the C4 position is related to the effectiveness of Luteolin toward the microorganisms, and the double bond alongside the C2 and C3 in its structure was found to be attributed to its biocidal activity (Lin et al. 2008). Also, the studies that are related to the comparison of the potency of the biological activities of Luteolin′s different forms have revealed that the Luteolin′s aglycone form can more strongly demonstrate the actions of anti-inflammatory, antioxidant, and antidiabetic compared to its state of LUT-7-O-glucoside (Y. Zang, Igarashi, and Li 2016). Moreover, the identified biological effects of Luteolin were determined to be interconnected with each other, as the anticancer activity of Luteolin, for example, is associated with anti-inflammatory functions (Lin et al. 2008).

1.2.2. The Pharmacokinetic Profiles of Luteolin

The several biological properties of Luteolin have led to the development of its commercial use as a food and its inclusion into products used in cosmetics. Studies about the safety profile of Luteolin have demonstrated its nontoxic side effects, with the oral median lethal dose established to be higher than 5000 and 2500 in rats and mice, respectively, that was equivalent for humans nearly 219.8−793.7 mg/kg, leading to construction and investigation of more studies related to the pharmacokinetic profile of Luteolin as the information of its pharmacokinetics constitutes a significant standing for the understatement and understanding the relation among its *in vitro* and *in vivo* activities (Aziz, Kim, and Cho 2018).

As a class, generally, flavonoids are identified to be absorbed from the intestinal tract either in the glycosylated or free form and metabolized to sulfate or glucuronide conjugates (Sayre et al. 2012). Specifically, for Luteolin, Chen et al. showed that following the oral administration of Luteolin, the absorption of it took place rapidly in rates, as the level of it reached its maximum plasma peak at the hour of 1.1 following the administration (T. Chen et al. 2007). Supportively, Yasuda et al. exhibited that the plasma concentration of Luteolin which is free in rats, fastly enhanced following 30 minutes of its administration, reaching its peak concentration within 1 hour, suggesting its efficient absorption after ingested orally (Yasuda et al. 2015). Differently, Shimoi et

al. demonstrated the absorption of Luteolin′s glycosylated form and found that its glycosylated form is first hydrolyzed by enterobacteria or lactase phlorizin hydrolase (LPH) to free form and then absorbed (Shimoi et al. 1998); however, the findings of Yin et al. exhibited another route that its glucoside form can be directly absorbed via the sodium-glucose co-transporter 1 present on the intestinal cells′ surface (Yin et al. 2013).

After that, the intestinal absorption of Luteolin, the profound portion of it, is conjugated, with the small part found in the excretion of the urinal and fecal (T. Chen et al. 2007). Kure et al. revealed that Luteolin and its glycosylated forms′ bioactivities were associated with their metabolites, where the Luteolin glucuronides, in particular, the Luteolin-3′-O-glucuronide exhibiting Luteolin's active molecule as identified with Luteolin's anti-inflammatory effects in studies with rats (Kure et al. 2016). Additionally, it has been shown by Wang et al. that the metabolites of Luteolin were primarily catalyzed via the activity of catechol-O-methyltransferases (COMTs) and UDP-glucuronosyltransferases (UGTs), as the methylation and glucuronidation reactions were believed to be two profound pathways for the disposition of and Phase II metabolism of Luteolin and its glucoside form (L. Wang et al. 2017). Interestingly, in a prior study conducted in rats and humans by Shimoit et al., after the administration of Luteolin, the free state of Luteolin, along with Luteolin's conjugates and conjugates which are methylated, were identified in rats′ plasma, as the presence of a free form Luteolin in the plasma suggesting the possible escape of a Luteolin proportion from the conjugation occurs in the intestine, or possibly from the methylation or sulfation, that further supported by the findings from humans with the presence of Luteolin in free form along with the monoglucuronide form in the serum following the ingestion (Shimoi et al. 1998).

The low bioavailability of flavonoids is among the essential concerns associated with using them for therapeutic purposes, which is related to the structural composition of flavonoids as they are polyphenolic compounds, and their bulky structure restricts their lipoidal cell membrane permeability (Gaikwad et al. 2021). In addition to their sturdy design, their low solubility in water is a roadblock limiting the absorption of flavonoids into the circulation to approach the necessary levels in plasma for achieving their action in terms of therapeutics, highlighting the importance of the bioavailability concern, which has to be managed carefully to achieve efficient and potent therapeutics by using them. Moreover, for Luteolin, which is rapidly absorbed, within 30 minutes, after oral administration, the detected concentration of it in the plasma is scanty and

emergently goes through the kidney excretion, suggesting insufficient systemic absorption of it as it has low water solubility (X. Wang, Wang, and Morris 2008; Gaikwad et al. 2021). Also, the comprehensive pre-systemic metabolism of Luteolin is another limitation to its therapeutic usage, leading to the construction of various pharmaceutical studies for increasing Luteolin′s solubility and bioavailability for retarding the degradation of it in the blood that would enhance its circulation time (T. Chen et al. 2007).

One of the strategies for enhancing Luteolin′s bioavailability and solubility was proposed by Khan et al., which they had designed a phospholipid complex for the encapsulation of it to treat inflammatory liver damage and revealed that this complex caused a remarkable increment of the *in vivo* bioavailability of Luteolin to 535.31% compared to the free Luteolin (Khan, Saraf, and Saraf 2016). A different strategy by Dang et al. in which their study demonstrated the usage of nanoparticles for improving Luteolin's pharmacokinetic profile and bioavailability in the *in vitro* and *in vivo* studies and presented that the designed nanoparticles, which were loaded with Luteolin had resulted in the increment in the plasma concentration of Luteolin with five times higher bioavailability compared to its free form (Dang et al. 2014).

Later on, Qing et al. suggested the usage of different copolymer micelles to achieve improving the release of *in vitro* and solubility of Luteolin, in which they found that the encapsulation of the Luteolin inside the mPEG5K-PCL10K copolymer micelle resulted in more stability with significant encapsulation effectiveness (Qing et al. 2017). Moreover, as mentioned before, another limitation causing Luteolin's low bioavailability, and restricting its clinical application, is its extensive glucuronidation via the activity of enzymes, including UGT1As.

For this limitation, a way-out approach has been offered by the study of Wu et al., in which they used the compound, Resveratrol that can inhibit the activity of enzymes UGT1A1 and UGT1A9, thereby remarkably enhancing Luteolin's bioavailability in rats via minimizing the occurrence of significant glucuronidation metabolite (Wu et al. 2022).

1.2.3. Luteolin in Cancer: Literature Overview

Plant-based agents are considered to be essential for therapies and compounds which are dietary by manipulating signaling pathways in cells for ages. Specifically, Luteolin has been identified to have profound anticancer features, which have been attributed to Luteolin′s inhibition ability of proliferation, metastasis, invasion, and angiogenesis via several mechanisms, such as the induction of apoptosis, suppression of the specific protein kinases and transcription factors and regulation of the cell cycle progression (Figure 1.2.) (Singh Tuli et al. 2022). The regulation of apoptosis and its promotion by Luteolin has been found to be related to its ability to cause an increment of expressions of p53, JNK, Bax, and Death receptors, and the levels of cleaved PARP and Caspase 3, 8, and 9, and by downregulating the proteins which are considered antiapoptotic, including Bcl-xL and Bcl-2 (Prasher et al. 2022). Furthermore, in general, the inhibition of the progression of the cancer cell cycle by Luteolin is related to the inhibition of proteins like Cyclin D1, CDC2, and Cyclin and Survivin, causing the increase in the p21 levels (Imran et al. 2019). The suppression of the angiogenesis by Luteolin, on the other hand, was found to be related to its ability to cause inhibition in angiogenic proteins' expression, including Matrix Metalloproteinase-2 (MMP-2), VEGF, Astrocyte-elevated gene-1 (AEG-1), and VEGFR2, and inhibition of the metastasis via suppressing the expression of proteins that take a role in the metastasis, including MMP-2/-9, C-X-C chemokine receptor type 4 (CXCR4), Extracellular signal-regulated kinase-1/-2 (ERK1/2), PI3K/Akt (Prasher et al. 2022; Çetinkaya and Baran 2023).

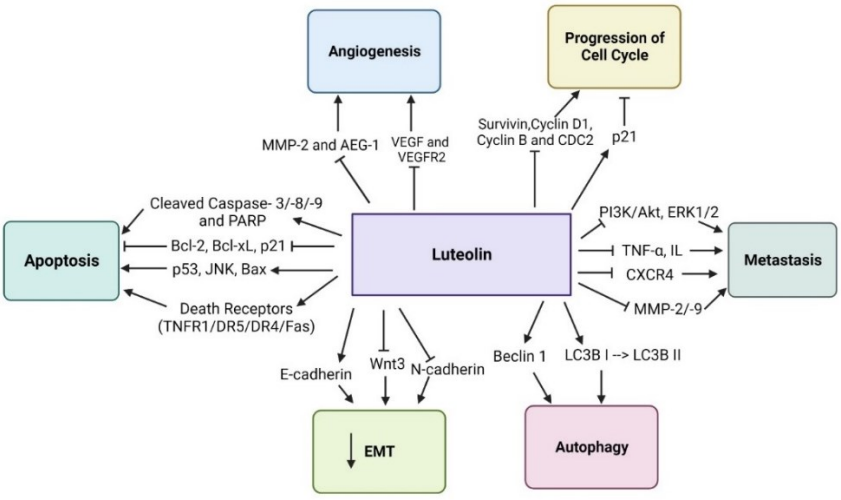

Figure 1.2. The summary of the possible roles of Luteolin in cancer cells

Regulation of apoptosis by Luteolin has also been extensively investigated and demonstrated in different studies, and it has been identified that Luteolin was determined to cause regulation of intrinsic and extrinsic pathways of apoptosis (Figure 1.3.) (Çetinkaya and Baran 2023). For the extrinsic pathway, it was found and thought that Luteolin could induce the extrinsic apoptotic path by enhancing the levels of death receptors and downstream effectors of them and suppressing different signaling pathways of death receptors that contribute to the survival of cells (Ambasta et al. 2019). On the other hand, Luteolin was known to take roles in the regulation of the membrane potential of mitochondria, release cytochrome c, and suppress the antiapoptotic proteins' expression for the intrinsic pathway. Moreover, it can also cause the inhibition of Ras-activated mouse double minute 2 (Mdm2), where Mdm2 has been shown to induce the degradation of p53, a well-known tumor suppressor that regulates apoptosis via enhancing Bax expression, a proapoptotic protein, and minimize the levels of Bcl-2. Moreover, the direct regulation of apoptosis by Luteolin has been found to involve the modulation of DNA damage induced via reactive oxygen species (ROS), and DNA damage signaling was identified as causing the induction of the production and activity of p53 (Franza et al. 2021; Imran et al. 2019).

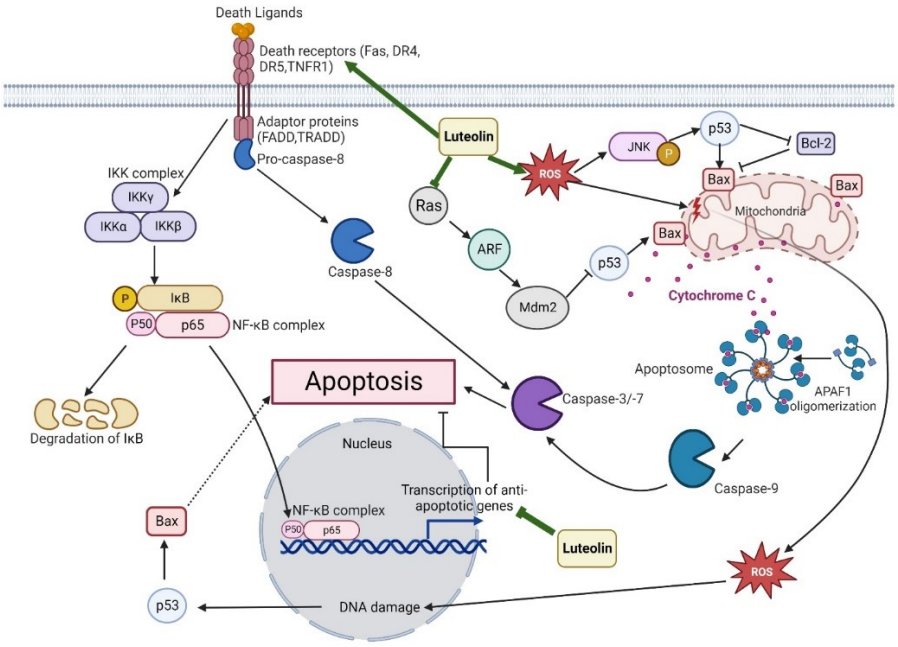

Figure 1.3. The illustration of mechanisms possible for Luteolin-induced apoptosis in cancer (Source: (Çetinkaya and Baran 2023))

Luteolin's anticancer potential has been identified in several types of cancer, including glioblastoma, prostate, colon, breast, liver, and gastric cancer. In glioblastoma cells, A172 and U-373MG, Lee et al. have revealed that Luteolin could cause a decrease in the viability of cancer cells significantly, and the half maximal inhibitory concentration (IC_{50}) was calculated as 89.84 μM for A172 cells and 76.80 μM for U-373MG cells at 72 hours. In the same study, Luteolin concentrations higher than 100 μM have been identified to result in apoptosis-related factors like cleavage of Caspase-3 and PARP and apoptosis-related morphological changes like nuclear fragmentation (H.-S. Lee et al. 2021). Furthermore, Franco et al., the antiproliferative effect of Luteolin extracted from *Fridericia platyphylla* was investigated on six different glioblastoma cell lines and revealed that Luteolin was able to suppress the proliferation with the most sensitive glioblastoma cell line towards Luteolin were identified to be U-251 with the IC_{50} value of 6.6 μM at 48 hours exposition. In a mechanistic manner, Luteolin was identified to inhibit the tumorigenesis and migration of the U251 cell line profoundly and enhanced the apoptosis via disrupting the membrane potential of mitochondria, Caspase-9, and PARP cleavage, increasing the DNA damage by phosphorylating an H2A histone family member X (H2AX), and phosphorylating ERK proteins (Franco et al. 2021). In the study by Wang et al., Luteolin inhibited the proliferation of U251MG cells at concentrations higher than 40 μM and for U87MG cell lines at a concentration of 80 μM for exposure lasting 24 hours. Also, they have shown that Luteolin downregulated the expression of MMP-2 and 9 and upregulated the tissue inhibitor of metalloproteinase (TIMP)-1 and -2, suppressing migration U87Mga and U251MG. In these human glioblastoma cells, the signaling pathway of phosphorylated insulin-like growth factor 1 receptor (p-IGF1R)/PI3K/Akt/mammalian target of rapamycin (mTOR) was found to be a potential target for decreasing the migration of cells (Q. Wang et al. 2017).

Luteolin's effect on prostate cancer has also been well-examined. In one of the earlier studies, Pratheeeskumar et al. demonstrated the anti-angiogenic activity of Luteolin on prostate cancer by *in vitro*, *in vivo,* and *ex vivo* assays, in which they found that Luteolin could remarkably suppress the proliferation of endothelial cells induced by VEGF, invasion, migration in response to a chemical, angiogenesis, and formation of the tube via targeting the Akt/ERK/mTOR pathway regulated by VEGFR2, resulting in the suppression of angiogenesis and prostate tumor growth (Pratheeshkumar et al. 2012). They also exhibited that Luteolin was able to decrease prostate cancer growth via

inducing apoptosis and inhibiting the angiogenesis *in vivo*, resulting in the decrement of cytokines which are proinflammatory, including TNF-α - IL-6,-8, and -1β, generation in PC-3 cells (Pratheeshkumar et al. 2012). Furthermore, Tsui et al., in their study, exhibited that Luteolin, at 30 μM, could inhibit the prostate carcinoma cell line's growth, LNCaP, by increasing the levels of prostate-derived Ets factor (PDEF), decreasing the androgen receptor (AR) expression and inducing apoptosis. More mechanistically, it was found to cause an increase in the expressions of Maspin, NDRG1, and B-cell translocation gene 2 (BTG2), where the co-transfection of the expression vector of PDEF resulted in the increment of activities of promoters of genes, NDRG1, Maspin, and BTG2. Recently, Luteolin was exhibited by Han et al. to inhibit the Wnt signaling pathway by increasing the levels of the negative regulator of the β-catenin's activity of transcription, frizzled class receptor 6 (FZD6), resulting in the inhibition of stemness of cells of prostate cancer (Han et al. 2018).

In liver cancer, in one of the pioneer studies, it was demonstrated to suppress liver cancer cells' BEL-7402 and SMMC-7721 proliferation in a dose- and time-dependently, as it resulted in G1/S stage arrest of the cell cycle and caused the reduction of the membrane potential of mitochondria and enhanced apoptosis with the increment in the cleaved Caspase-3 and Bax levels, and decrement of Bcl-2 protein levels in the liver cancer cell lines (Ding et al. 2014). Interestingly, the role of Luteolin in autophagy regulation was also studied in liver cancer, where Cao et al. found that the application of Luteolin caused an increment of the number of intracellular autophagosomes and the expressions of Beclin-1 and promoted the microtubule-associated protein-I light chain 3 (LC3B-I) to -II conversion in SMMC-7721, hepatocellular carcinoma cells (Cao et al. 2018). Also, Cao et al. revealed that decrement in SMMC-7721 cells viability increment in the apoptosis, as they had demonstrated with the increased Caspase-8 and decreased Bcl-2 levels and remarkable induction of arrest of the cell cycle at the stage of G0/G1(Cao et al. 2018).

Additionally, for gastric cancer, Luteolin was found by Zang et al. to cause a suppression in the proliferation, migration, and invasion of Hs-746T and MKN28 gastric cancer cell lines and resulted in increased apoptosis in a manner that is dose- and time-dependent and also in mice model of human gastric cancer, Luteolin was revealed to reduce *in vivo* growth of the tumor. Moreover, the application of Luteolin resulted in the reversion of epithelial to mesenchymal transition, as seen in a shrinkage of the cytoskeleton and an increment in the E-cadherin expression, epithelial marker, and a

decrease in the Snail, Vimentin, and N-cadherin, mesenchymal biomarkers, expressions and, in addition, the signaling pathway of Notch1 was revealed to be suppressed when Luteolin was applied (Ming-de Zang et al. 2017). Also, Luteolin application had caused a profound decrease in the vasculogenic mimicry that is formed by gastric cancer cells, Hs746T, and VEGF that has been secreted from Hs-746T cells, all related to the suppression of Notch1 in return to the Luteolin (Mingde Zang et al. 2017), demonstrating the potential function of Luteolin in inhibition of angiogenesis and formation of vasculogenic mimicry in gastric cancer via suppression of the secretion of VEGF depending on the Notch1 expression.

1.3. Aim of the Study

T-ALL is an ALL subtype that is very aggressive and associated with the abnormal proliferation of thymocytes which are immature. Even though the survival in overall terms of children patients with T-ALL has been determined as 80%, nearly 20% of the patients finally die from the relapsed/refractory disease (Cordo' et al. 2021), highlighting the importance of developing novel therapies. The T-ALL's current therapy comprises the usage of chemotherapeutic drugs at high concentrations, with which most of the patients demonstrate early and late complications regardless of the therapeutic method choice, and the use of high-intensity combination chemotherapy can result in side effects that are difficult to accept or even can result in the death of patients as they demonstrate substantial toxicity to healthy cells as well. Therefore, a nontoxic, readily available, cost-effective, and effective treatment is highly desirable for treating T-ALL.

One alternative option for cancer treatment is using flavonoids due to their plant-based origin, safety profile, cost-effectiveness, and substantially low toxicities to healthy cells. Luteolin, the flavonoid used in this project, is a well-searched flavonoid with proven anticancer properties, including apoptotic, antiproliferative, anti-angiogenic, antimetastatic, and cytostatic in various solid tumors. Yet, there are few studies regarding the anticancer potential of Luteolin in hematological malignancies, even with no research about its usage as a therapeutic agent for the T-ALL. Therefore, in this study, the anticancer potential of Luteolin was aimed to be examined *in vitro* in a T-ALL cell line, MOLT-4.

In this study, the antiproliferative, apoptotic, cytotoxic, and cytostatic effects of Luteolin on T-ALL cells, MOLT-4 cells, will be determined by using different methods, including MTT cell proliferation assay, method of Trypan blue dye exclusion, JC-1 dye-based mitochondrial membrane potential measuring, Annexin V/PI double staining, colorimetric detection of activity of Caspase-3, and the analysis of cell cycle profile via PI staining for the first time in the literature. Furthermore, the macromolecular changes regarding the application of Luteolin to T-ALL cells will be investigated by Fourier-Transform Infrared (FTIR) Spectroscopy. As described previously, flavonoids exhibit enormous effects on cellular processes, as they are found to affect entire cancer progression and development by changing the levels of several essential proteins that participate in different signaling paths. However, the molecular pathways related to the anticancer features of flavonoids depend on various factors. The factors are the specific molecule studied, concentrations of the molecule used in different assays, and types of cancer cells or tissues.

Consequently, all these factors make it very challenging to classify and compare these compounds based on changes in a particular metabolite or a specific protein's expression levels. In this light, strategies which are systemic, such as proteomics and metabolomics, are a great approach to achieving more global information about the biological processes mediated by flavonoids, as the analyses with FTIR spectroscopy of different flavonoids exposed-cancers in the *in vitro* settings can result in gathering a more comprehensive signature for the changes in macromolecules related to the exposure of flavonoids.

CHAPTER 2

MATERIALS AND METHODS

2.1. Materials

The materials which were used in this study, including cell lines and the chemicals utilized for the propagation of cells and examination of anticancer properties of Luteolin on cells, were listed below in groups.

2.1.1. Cell Line

The T-cell leukemia cell line, MOLT-4 (ACC 362, DMSZ no), was taken from the German Collection of Microorganisms and Cell Cultures (DSMZ), Germany, and the cell line used in the project was from the stocks stored in the -80°C fridge.

2.1.2. Chemicals

Luteolin powder was purchased from Santa Cruz Biotechnology, USA, and its solution used as the stock was prepared as 20 mM using *Dimethyl sulfoxide* (DMSO) was stored at -20°C, and the sterile DMSO was obtained from the Merck Group, Germany.

Fetal Bovine Serum (FBS) and RPMI 1640 media (1X) were purchased from Gibco, UK. Dulbecco's Phosphate-buffered saline (PBS) (1X) was obtained from Capricorn Scientific, Germany, and Penicillin-Streptomycin (100X) solution was obtained from Euroclone, Italy.

3-(4,5-Dimethylthiazol-2-yl)-2,5-Diphenyltetrazolium Bromide (MTT) powder was obtained from Invitrogen, USA, and the stock solution of MTT was prepared in order to achieve 5 mg/mL concentration in 1X PBS, which was stored at -20°C.

Trypan blue powder was purchased from Sigma Aldrich, USA, and the Trypan blue's stock solution was prepared in order to achieve 0.4% in 1X PBS.

FITC Annexin V Apoptosis Detection Kit I used for the apoptosis studies was purchased from BD Biosciences, USA.

Mitoprobe^{TM} JC-1 Assay Kit used for analysis with flow cytometry was purchased from Invitrogen, USA.

The Caspase 3 Activity Colorimetric Assay Kit was purchased from Elabscience Biotechnology, USA.

The Propidium Iodide (PI) powder was purchased from AppliChem, and the stock solution of PI was prepared to be 1 mg/mL in distilled water, and the solution was stored at 4°C.

Triton X-100 solution was purchased from AppliChem, and RNase A, DNase, and protease-free endonuclease (10mg/mL) was obtained from Thermo Scientific, USA.

2.2. Methods

2.2.1. Conditions of Cell Cultures

MOLT-4 cells were grown in RPMI 1640 medium containing 10% Fetal Bovine Serum (FBS) and 1% Penicillin-Streptomycin in 25 cm^2 cell culture flasks, and cells were incubated in the CO_2 incubator (Nüve, Turkey), at the following conditions; 5% CO_2, 37 °C. MOLT-4 cells were subcultured when the cell number reached 1.5×10^6 cells/mL every three days after cell seeding.

2.2.2. Thawing of Frozen Cells

MOLT-4 cells were stocked and frozen at -80°C, and when the cell line was required, the stock was taken from the fridge, and when the ice crystals were melted, the content inside the cryovial tube was taken into a test tube with 2 mL corresponded complete fresh medium. The cryovial tube was rinsed two times with 1 mL complete medium, and the falcon tube was included with the remnant content in the cryovial. The process was performed quickly to achieve the highest viable cell percentage. The test tube was centrifuged at 800 rpm for 5 minutes for MOLT-4 cells. After the centrifugation period, the supernatant was discarded, and the cell pellet was resuspended in the complete medium, cultured in the 25 cm^2 cell culture flask, and incubated in the CO_2 incubator.

2.2.3. Maintenance of MOLT-4 Cells

The subculturing of MOLT-4 cells was performed every two to three days when their density had reached 1.5×10^6 cells/mL, and during the culturing process, firstly, the collected MOLT-4 cells from the 25 cm^2 cell culture flask were put to a test tube and centrifuged at 800 rpm for 5 minutes. Afterward, the removal of supernatant took place, and the cell pellet was resuspended in the 2 mL RPMI 1640 complete medium.

30 µl from the cell suspension was taken and mixed with 30 µl Trypan Blue, and from the mixture, 10 µl was loaded into the Neubauer Haemocytometer, and cells that were placed at the larger squares located at corners were counted under the light microscope (Carl-Zeiss 12 V DC 30W) at 10 X magnification of objective lens (100X total magnification). Then, the average of the cell number counted on the four large squares was calculated and multiplied by the factor of dilution (2) and 10^4, the constant given in the instructions, to determine the number of cells per mL. After determination of the number of cells/mL, 0.4×10^6 MOLT-4 cells per mL were seeded into the 25 cm^2 culture flask containing RPMI 1640 medium, which made 2×10^6 cells in 5 mL medium.

2.2.6. The Freezing of Cells

MOLT-4 cells were frozen in cryovial tubes to use in further studies for which high cell numbers were needed. Two freezing mixes, Freezing Mix 1 and 2, were prepared to use in the freezing process of cells. In each cryovial tube, 2×10^6 cells were frozen in 1mL, and the 1 mL solution was included with 500 µL of Freezing Mix 1 and 500 µL of Freezing Mix 2. Freezing Mix 1 was formed with 6 mL of media free of serum (60%) and 4 mL of FBS (40%). On the other hand, Freezing Mix 2 was prepared with 8 mL of media free of serum (80%) and 2 mL of DMSO (20%).

The cells cultured in culture flasks were collected, and the cell suspension was centrifuged for 5 minutes at 800 rpm. After the centrifugation, the supernatant was carefully discarded, the cell pellet was resuspended in Freezing Mix I, and the cell number was counted based on the cell number; the volume of Freezing Mix I was adjusted as each cryovial tube was supposed to include 500 µL of Freezing Mix I. The total content was separated into cryovial tubes, and 500 µL of Freezing Mix I was added into each cryovial tube drop by drop, and cryovial tubes were immediately put in the -80 °C fridge.

2.2.5. Preparation of the Stock Solution of Luteolin

The 10.3 mg of the Luteolin powder with a molecular weight of 286.24 g/mol was weighed and dissolved in 1.799 mL DMSO to prepare a stock solution of 20 mM. The DMSO volume which was needed to dissolve the Luteolin powder was calculated using the molarity (M) formula using the mole and volume. The stock solution of Luteolin was stored at -20 °C in the dark. In the other experiments, when it was needed to apply the Luteolin, the 20 mM stock solution was utilized to form the concentrations which were required to test (5- 50 µM) to determine the concentration that inhibited 50% of the growth of cells (IC_{50}) value, and the concentrations were prepared via using the calculated volume from the stock and mixing it with the medium which was complete.

2.2.6. Measurement of Cell Proliferation by MTT Cell Proliferation Assay

The effect of Luteolin on MOLT-4 cell proliferation was determined using the MTT Cell Proliferation assay. For this purpose, 1×10^4 cells/well for MOLT-4 cells were seeded into the wells of 96-well plates that were included with 100 µL medium with four technical replicates. Luteolin drug solutions were prepared as 5-,10-,15-,20-,25-,30-,35-,40-,45-, and 50 µM concentrations with the control group that was not included with any Luteolin solution but only with complete medium, and from the drug solutions 100 µL was applied to each corresponding wells of the 96-well plate. DMSO's final concentration in each well was calculated, and it was below 0.1%, but also, for each plate, the DMSO control as the negative control was added based on the DMSO volume at the highest Luteolin concentration applied. After the Luteolin application, 96-well plates were incubated in the incubator at afore told conditions for 48 and 72 hours.

After incubating cells with Luteolin for the required period, 20 µL of MTT solution that had the concentration of 5mg/mL was added into each well and incubated for 4 hours in the incubator. After incubation, 96-well plates were centrifuged at 4 °C and 1400 rpm for 10 minutes for precipitation of the formazan crystals. Later, the supernatant was carefully removed, and to each well of the 96-well plate, 100 µL of DMSO was added to solubilize the formed formazan crystals. 96-well plates were put in the rotator shaker at room temperature for 15 minutes, and after that, 96-well plates were read in the microplate reader (Thermo Scientific, Multiskan GO, Finland) at 570 and 670 nm wavelengths.

After measuring the absorbance values, the proliferation percentages of Luteolin-treated experimental sample groups were calculated relative to the control MOLT-4 cells and also based on the absorbance values and plotted cell proliferation versus Luteolin concentrations graphs, the IC_{25}, $IC_{50,}$ and IC_{75} values of Luteolin for MOLT-4 cells were calculated.

2.2.7. Measurement of Cell Viability by Trypan Blue Dye Exclusion Method

The influence of Luteolin MOLT-4 cells' viability was determined using the Trypan Blue Dye Exclusion method. For this purpose, 2×10^5 MOLT-4 cells were seeded into each well of the 12-well plate in 2 mL RPMI 1640 medium with three replicates, and for trials of 48 hours of incubation, 5-,10-,15-,20-,30-, and 40 µM Luteolin was applied to MOLT-4 cells, whereas for 72 hours of incubation, 5-, 10-,15-,20-, and 25 µM Luteolin was applied to the cell with control groups and the cells were incubated in the CO_2 incubator for intended times. After each incubation period, cells were gently pipetted, and 30 µL of the cell suspension was taken from each well and mixed with 30 µL of Trypan Blue dye. From the mixture, 10 µL was loaded into a Neubauer hemocytometer, and cells located in four large squares in the hemocytometer were counted under the Zeiss light microscope at 100X total magnification. The counted cells' average number was calculated and multiplied by two, the dilution factor, and 10^4, the constant given in the instruction. Based on the multiplication result, the average cell number per mL was calculated, and the result was multiplied by two to get the total cell number for MOLT-4 cells in each well. The cell number for control and Luteolin-treated groups at different concentrations was calculated.

2.2.8. Measuring the Apoptosis Ratio by Annexin V/PI Double Staining

The probable influence of Luteolin on apoptosis of MOLT-4 cells was examined by Annexin V/PI Double Staining and analysis via BD Flow Cytometry. 1×10^5 MOLT-4 cells/mL were seeded as 2×10^5 cells inside the 2 mL of complete RPMI 1640 medium into the wells of the 6 well-plate. Later, the Luteolin application was performed in 3-,8-, and 16 µM concentrations, and in the experiment setup, two control groups that were not included with any agent and a negative control group with DMSO were included. Then, cells were incubated at 5% CO_2, 37°C, in the incubator for 48 and 72 hours.

After incubation, sample and control groups were collected in test tubes and centrifuged at 1000 rpm for 10 minutes. Right after supernatants were carefully removed, pellets of each sample and control group were dissolved in 1 mL cold 1X PBS, and the two control groups without any reagent were divided into two Falcon tubes. Afterward, tubes with samples and control groups were centrifuged at 1000 rpm for 10 minutes, and supernatants were discarded. Each pellet was resuspended in the 200 µL 1X Annexin Binding Buffer. 2 µL Annexin V and 2 µL PI were added to samples, including Luteolin at different concentrations, to the negative control group and one of the control groups. One of the control groups was stained with only 2 µL Annexin V, the other control group was included with only 2 µL PI dye, and one control group was stained with any of the dyes, named as unstained. The monochrome and unstained control groups were used to analyze samples in the flow cytometry to introduce the dyes to the program. After the 15-minute incubation of cells with the dyes at room temperature, samples were examined with flow cytometry in two channels (BD FACS Canto, USA) in the BIOMER facility of TAM in IZTECH. The analysis of the cells was based on the principle of the interaction between Annexin V with the flip-flopped phosphatidylserine located at the outer part of the cell membrane and the interaction of PI with the DNA fragments at the nucleus. After the analysis, the cells that were dyed either Annexin V or PI or with both or none located at the different quadrants, as described in Figure 2.1. and their percentages were used to interpret the samples for apoptosis analysis.

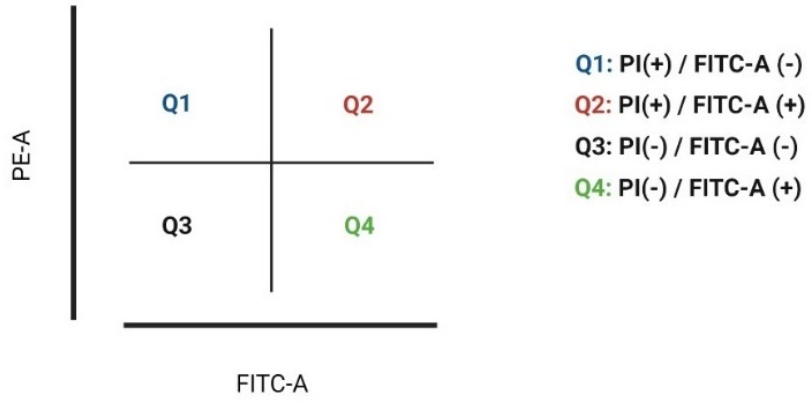

Figure 2.1. The illustration of the Annexin V/PI double staining interpretation

Regarding the interaction between the Annexin V protein and phosphatidylserine, the cells that were only Annexin V-positive, located at the Q4, had shown the cells at the early stages of apoptosis. In contrast, cells that were PI-positive and Annexin V- positive, as represented in the cells in Q2, were at the late stages of apoptosis. Cells that were positive for only PI, as described in the cells in Q1, were undergoing necrosis, while cells that were negative for both dyes, as located in Q3, were the healthy cells.

2.2.9. Determination of the Caspase-3 Activity by Caspase-3 Colorimetric Assay

The changes caused by Luteolin on the activity of Caspase-3 of MOLT-4 cells were measured by the Caspase-3 Colorimetric Assay Kit (Elabscience Biotechnology, USA), which was dependent on the detection of the p-nitroanilide (pNA), a chromophore, spectrophotometrically, that is released from the DEVD-pNA, a labeled substrate, right after the cleavage by caspases.

MOLT-4 cells were seeded as 8×10^5 cells in the 2mL of RPMI-1640 complete medium in each well of the 6-well plate, and Luteolin was applied in 3-, 8-, and 16 µM concentrations with the control groups. Later, cells were incubated at the CO_2 incubator for 72 hours. After 72 hours, sample and control groups were collected into test tubes and centrifuged at 1000 rpm for 10 minutes. Then, supernatants were removed, 50 µL of chilled Lysis Buffer was put into each sample and control group, and tubes were incubated on ice for 10 minutes. After 10 minutes, samples were centrifuged for 1 minute at 10000 g, and supernatants were collected into new test tubes. Afterward, to set up the reaction, from each sample, 50 µL was put into the wells of a 96-well plate, and instead of putting the sample, 50 µL Lysis Buffer was added for the blank. Then, each well was added with 50 µL 2X Reaction Buffer containing 10 mM DTT and 5 µL of the 4 mM DEVD-p-NA (final concentration of 200 µM). The 96-well plate was incubated at 5% CO2, 37°C, for 3 hours.

After 3 hours, the 96-well plate was read in the microplate reader at 405 nm. Ultimately, the total protein concentrations in the control and experimental group samples were measured by Bradford Protein Assay by measuring the absorbance values

at the 595 nm and the total protein concentrations were used to normalize the absorbance values of the Caspase-3 activity. The calculated value of the control sample, without any agent, was accepted as 1, and the relative fold changes in the activities of the Caspase-3 in the samples were calculated via comparison to the control.

2.2.10. Examination of the Mitochondrial Membrane Potential by JC-1 Dye

Luteolin's impact on the membrane potential of mitochondria of MOLT-4 cells was examined via JC-1 dye-based assay, which was MitoProbe™ JC-1 Assay Kit that is used for the analysis with the flow cytometry. Firstly, MOLT-4 cells were seeded as 2×10^5 cells in the 2mL medium into each well of 6-well plates; the Luteolin application occurred in 3-, 8-, and 16 µM concentrations. In the experimental setup, two control groups that weren't included with any agents and one negative control group that included cells with DMSO were added. After that, cells were incubated at the CO_2 incubator for 72 hours.

After 72 hours of incubation, 2 µL of 50 mM CCCP (carbonyl cyanide 3-chlorophenylhydrazone) solution, which was known as the mitochondrial membrane potential disrupter (with a final concentration of 50 µM), was added to one of the controls, and cells were incubated at 37°C for 5 minutes. Then, 20 µL of 200 µM JC-1 dye (with a final concentration of 2 µM) was put into each well, and the 6-well plate was incubated in the CO_2 incubator for 20 minutes. After that, cells were gathered into test tubes and centrifuged for 5 minutes at 1000 rpm. Then, the supernatant was removed, the cell pellet was sensitively dissolved in 500µL 1X PBS for each group, and the changes in the membrane potential of mitochondria were examined by flow cytometry. Standard compensation was performed for each treatment using the CCCP-treated sample.

2.2.11. Analysis of the Cell Cycle Profile by Propidium Iodide (PI) Staining

The possible impact of Luteolin on the cell cycle profile of MOLT-4 was examined by PI staining and analysis by flow cytometry. MOLT-4 cells were seeded as 2×10^5 cells in the 2 mL medium into each well of 6-well plates, and the Luteolin application was carried on in concentrations of 3-, 8-, and 16 μM. In the experimental setup, one control group that wasn't included with any agents and one negative control group that included cells with DMSO were added. Then, cells were incubated in the CO_2 incubator at the abovementioned conditions for 72 hours.

After 72 hours, for cell fixation, firstly, MOLT-4 cells were collected to test tubes, and centrifugation was performed at 1000 rpm for 10 minutes. Later, supernatants were immediately removed, pellets were dissolved in 1mL of 1X cold PBS, and tubes were incubated for 15 minutes on ice. After the incubation, 4mL absolute ethanol, which was stored at -20°C, was added to each test tube, and test tubes were incubated for at least one day at -20°C.

On the day of the measurement for staining the cells with PI, firstly, tubes were centrifuged for 10 minutes at 1000 rpm, supernatants were removed, and cell pellets were resuspended in 5 mL 1X cold PBS. Then, they were centrifuged again at 1000 rpm for 10 minutes, and after removing supernatants, pellets were resuspended in 200 μL 0.1% TritonX 100 in 1X PBS. Later, 4 μL of RNase-A (200 ug/ml) was put into each tube and incubated at 37°C, 5% CO_2, for 30 minutes. Afterward, 20 μL of the PI solution (1mg/mL) was put into test tubes, which were incubated for 10 minutes at room temperature.

Ultimately, the cell cycle profile of Luteolin-treated cells and control groups was examined by flow cytometry. Based on the cell cycle profile of cells gathered from the PI staining by flow cytometry, the percentage of cells in the different stages of the cell cycle as in G1, S, and G2 phases were determined, and the possible cell cycle arrest caused by Luteolin was evaluated by comparing the percentage of cells for the control group.

2.2.12. Measurement of Macromolecular Changes by FTIR Spectroscopy

The macromolecular changes caused by the Luteolin in MOLT-4 cells were determined by using Fourier-Transform Infrared (FTIR) Spectroscopy. For this purpose, samples were first prepared for the FTIR spectroscopy, then the FTIR spectrum was accumulated, and the gathered data was processed.

2.2.12.1. Sample Preparation for the FTIR Spectroscopy

For the sample preparation, 8×10^5 MOLT-4 cells were seeded in the 2 mL of the complete medium into each well of 6-well plates, and Luteolin was added in concentrations of 3-, 8-, and 16 μM, with the control group that was not included with any agent. Then, cells were incubated in the CO_2 incubator at the abovementioned conditions for 72 hours. After the incubation process for the corresponding time interval, cells were collected in test tubes and centrifuged for 10 minutes at 1000 rpm. Later, supernatants were carefully and thoroughly removed from each test tube, and cell pellets were overnight lyophilized in a freeze-drier (LABCONCO-FREEZONE 6) to be disposed of from the water in the BIOMER facility of the TAM, IZTECH. After the overnight incubation, tubes were collected from the free-drier and directly preceded to FTIR spectral analysis.

2.2.12.2. Accumulation of FTIR Spectrum and Processing of Data

The spectral analysis was done using the FTIR (PERKIN ELMER – UATR TWO) machine in conjugation with the Attenuated Total Reflectance (ATR) accessory. The FTIR spectra of each sample and control group were recorded among the 4000 and 450 cm^{-1}, the average of the interferograms was taken at the resolution of 4 cm^{-1} for 20

scans, and the spectrum gathered from the background was removed from the samples' spectra, and for data manipulations, the Spectrum 10 software (Perkin Elmer) was used.

The identical spectra were gathered from each sample with at least three different scans, which were used for averaging each sample, and the average spectra obtained were used for the analysis of data and statistics. Smoothing of the spectra was performed over different points using the Savitsky-Golay algorithm, and the spectra were interactively baselined from the two arbitrary points. Ultimately, the normalization of the spectra in specific regions was performed.

2.2.13. Statistical Analysis

For statistical analysis and drawing graphs, the GraphPad Prism 9.0 program was utilized, and the statistical analysis performed was the paired t-test used for the comparison control group and experimental groups. The one-way-ANOVA test was performed to compare the whole experiment. $p<0.05$: *, $p<0.01$: **, $p<0.001$: ***, $p<0.0001$: **** values were accepted as statistically significant, and with the error bars demonstrated on the graphs, the standard deviations were represented.

CHAPTER 3

RESULTS AND DISCUSSION

3.1. The Effect of Luteolin on the Proliferation of MOLT-4 Cells

The impact of Luteolin at increasing concentrations (5-, 10-, 15-, 20-, 25-, 30-, 35-, 40-, 45-, and 50 μM) with control groups that were non-treated on the proliferation of the MOLT-4 cells was examined using MTT Cell Proliferation Assay at the 48 and 72 hours exposure times.

The results gathered from the MTT Cell Proliferation Assay identified that Luteolin has a remarkable antiproliferative effect on MOLT-4 cells, and this antiproliferative effect has increased with the increasing doses of Luteolin applied to MOLT-4 cells at both 48 and 72 hours. However, when the results of 48 hours and 72 hours were compared, it was found that the antiproliferative effect of Luteolin was significantly higher at 72 hours compared to 48 hours (Figure 3.1.).

Based on the plotted graphs, the IC_{25} values of Luteolin on MOLT-4 cells were calculated as 5.4 μM and 3 μM for 48 and 72 hours, respectively. The IC_{50} values, on the other hand, of Luteolin on MOLT-4 cells were determined as 17.1 μM and 8 μM for 48 and 72 hours, respectively. Also, the IC_{75} value of Luteolin on MOLT-4 cells could not be determined for 48 hours as the proliferation of MOLT-4 cells was found to be higher than 50% at even the 50 μM Luteolin concentration, the highest applied dose; thus, it can be said that for 48 hours the IC_{75} value of Luteolin is higher than 50 μM on MOLT-4 cells. For 72 hours, on the other hand, the IC_{75} of Luteolin on MOLT-4 cells was calculated as 16 μM.

Based on Figure 3.1., it has been found that Luteolin has significantly inhibited the proliferation of MOLT-4 cells, and this antiproliferative impact was identified to depend on the dose of Luteolin and time of exposure.

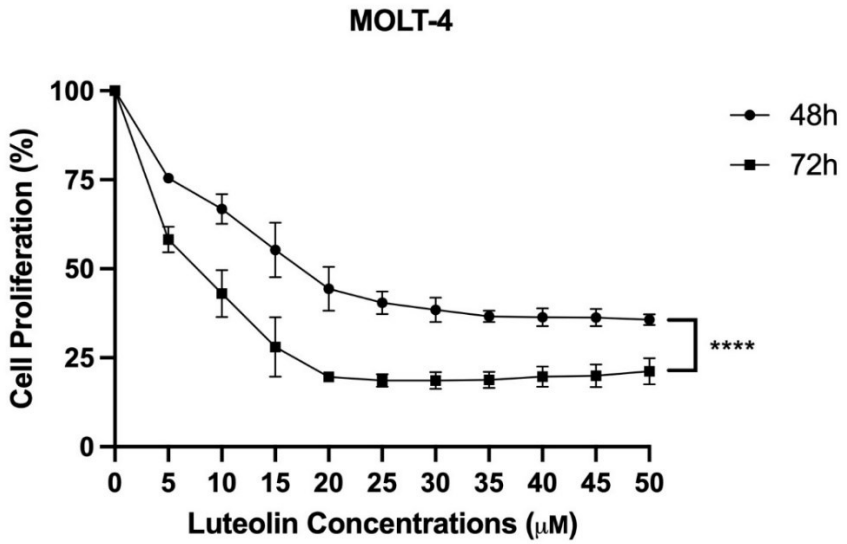

Figure 3.1. The effect of Luteolin on the proliferation of MOLT-4 cells at 48 and 72 hours. The MTT experiments were independently performed three times (n=3), with the statistical analysis which was performed by using a paired t-test, where $p<0.0001$:**** was accepted to be significant, and the error bars, which represented the standard deviation (SD), at some points, are not seen since they are smaller than the symbols themselves.

The acquired data is remarkably in agreement with the previous research done by other researchers; for instance, in the study by Sak et al., when the antiproliferative impact of Luteolin was investigated in human chronic lymphocytic leukemia cells, HG-3 cells when Luteolin was applied in increasing concentrations in between 10 nM to 500 μM for 24, 48 and 72 hours, the significant antiproliferative impact of Luteolin was pointed out in a manner that was dependent on time and dose, where the IC_{50} values of Luteolin on HG-3 cells were calculated, respectively as, 109 μM, 33 μM and 24 μM for 24, 48 and 72 hours of exposure (Sak, Kasemaa, and Everaus 2016). In a more current study by Chen et al., similar results were also obtained, that Luteolin significantly reduced the proliferation of THP-1, a human acute myeloid leukemia cell line, in a fashion that was dependent on dose and time when applied at 25-, 50-, 100-, and 150 μM concentrations for 24, 48, and 72 hours, where the value of IC_{50} was calculated as 46.16 μM for THP1 cells (P.-Y. Chen et al. 2018). Also, in comparison to the findings by Chen et al. and Sak et al. (P.-Y. Chen et al. 2018; Sak, Kasemaa, and Everaus 2016), Luteolin was identified to be more effective in this study in the T-ALL cells, the MOLT-4 cells compared to acute myeloid leukemia and chronic lymphocytic leukemia cells.

3.2. The Effect of Luteolin on MOLT-4 Cells' Viability

The effect of Luteolin at concentrations that gradually increased (5-,10-,15-,20-,30-, and 40 μM for 48 hours and 5-, 10-,15-,20-, and 25 μM for 72 hours) on the viability of MOLT-4 cells' was determined via counting the number of alive cells with the help of the Trypan Blue Dye Exclusion method.

The gathered results indicated that the increasing concentrations of Luteolin resulted in a significant reduction of the viability of MOLT-4 cells after 48 (Figure 3.2.A.) and after 72 hours of exposure of MOLT-4 cells to Luteolin (Figure 3.2.B.). Compared to the control group, after 48 hours of exposure to Luteolin at gradually increasing concentrations, the MOLT-4 cells viability was progressively decreased (Figure 3.2.A.), however as can be seen in Figure 3.2.B., a sharp reduction of the cell viability was found, at the 10 μM Luteolin application, and also after the application of 20 μM Luteolin, the decrement in the cell viability of MOLT-4 cells minimized, with the meager amount of viable cells left after the 20 μM and 25 μM Luteolin exposure. The decrease in the antiproliferative effect of Luteolin after 20 μM concentration was also observed with the MTT results at 72 hours (Figure 3.1.), which correlated with the results from MOLT-4 cells' viability with the Trypan Blue experiment (Figure 3.2.B).

Consequently, it was shown that with the Trypan Blue experiments, Luteolin had a cytotoxic effect on MOLT-4 cells viability at both 48 and 72 hours of exposure (Figure 3.2.), and the results were pretty much in similarity to the MTT results, which indicated the antiproliferative effects of Luteolin at both 48 and 72 hours (Figure 3.1.), showing that Luteolin has a cytotoxic effect both on proliferation and viability of MOLT-4 cells.

The decreasing influence of Luteolin on cancer cells' viability has been demonstrated in various cancer cells, including breast, colon, gastric, liver, pancreas, lung, breast, and even on a variety of leukemia, including acute myeloid leukemia and chronic lymphoblastic leukemia cells (Çetinkaya and Baran 2023; Sak, Kasemaa, and Everaus 2016).

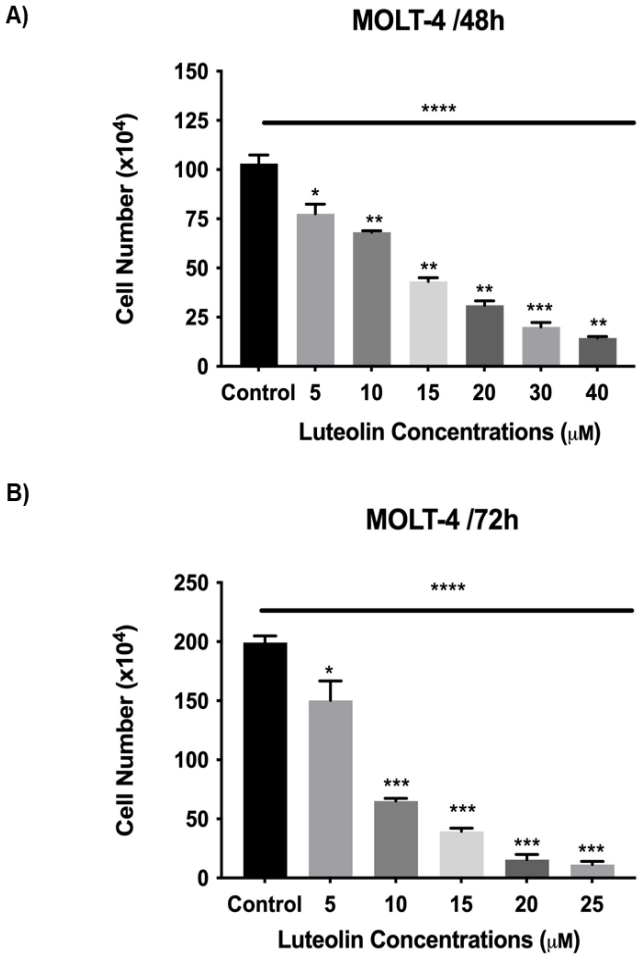

Figure 3.2. The impact of Luteolin on the MOLT-4 cells' viability at A) 48 and B) 72 hours. Trypan Blue experiments were independently performed three times (n=3). The statistical analysis was performed by a paired t-test to for comparing experimental groups with the control group and using one-way ANOVA to compare all groups, where $p<0.05$:*, $p<0.01$: **, $p<0.001$: ***, and $p<0.0001$:**** was accepted to be significant, and with the error bars, standard deviation (SD) is represented.

3.3. The Effect of Luteolin on Apoptosis of MOLT-4 Cells

Apoptotic effects of Luteolin after 48 and 72 hours of application at the determined IC_{25} (3 μM), IC_{50} (8 μM), and IC_{75} (16 μM) values by the MTT Cell proliferation assay at 72 hours were investigated by the Annexin V/PI Double Staining and analysis by flow cytometry.

The X-axis in dot plots in Figure 3.3. and Figure 3.4. represented the channel of Annexin-FITC, where the Y-axis represented the channel of PI, and the quadrants in the

figures demonstrated the cells which are alive or dead as a result of the dye binding concerning their properties.

The quadrant of Q3 represented the percentage of viable MOLT-4 cells, measured as 95.2% for the control (Figure 3.3.A), 92.6% for the 3 μM Luteolin application (Figure 3.3.B), 86.7% for the 8 μM Luteolin exposure (Figure 3.3.C), and 69.8% for the 16 μM Luteolin application (Figure 3.3.D) to MOLT-4 cells when exposed for 48 hours, indicated that increasing concentrations of Luteolin caused a reduction in the viability of MOLT-4 cells, where increased the percentage of apoptosis of MOLT-4 cells as shown by the Q2 and Q4 quadrants (Figure 3.3.).

The Q2 quadrant represents the cells dyed with both PI and Annexin V, demonstrating late apoptosis, and the Q4 quadrant represents the cell population stained with only Annexin V, showing the cells undergoing early apoptosis and the total of the percentage of cells in Q2 and Q4 gave the apoptosis ratio.

The statistical analysis of the three experiments performed independently is shown in Figure 3.3.E. The significant enhancement of the apoptosis rate was seen gradually with the increment in the Luteolin concentration after 48 hours of Luteolin exposure to MOLT-4 cells.

The total percentage of apoptosis of control MOLT-4 cells was, on average, 4.8%, which was found to be increased by 2.6% on the 3 μM Luteolin treated MOLT-4 cells and reached 7.4% on average. The apoptosis ratio increased to 11.7%, on average, with the application of 16 μM Luteolin, and compared to the control MOLT-4 cells, it was found to be significantly increased by 6.9%. Furthermore, the apoptosis ratio was found to be remarkably increased from 4.8%, which was for control MOLT-4 cells, to 29%, on average, in the three biological replicates with the application of 16 μM Luteolin to MOLT-4 cells (Figure 3.3.E.).

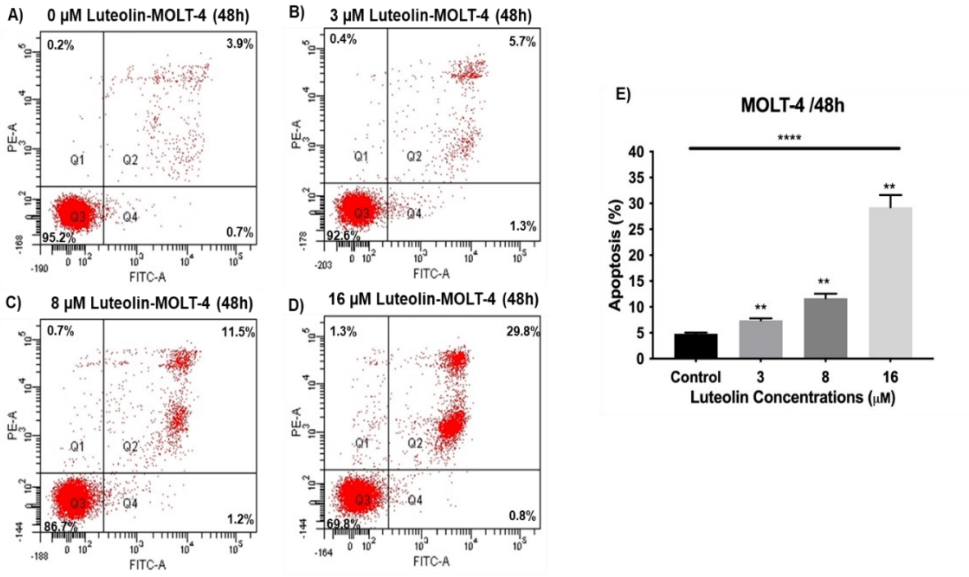

Figure 3.3. The influence of Luteolin at different concentrations on the apoptosis of MOLT-4 cells at 48 hours of exposure. Experiments were independently performed three times (n=3). The statistical analysis was performed by using a paired t-test to compare the experimental groups with the control group and using one-way ANOVA to compare all groups, where $p<0.05$:*, $p<0.01$: **, and $p<0.0001$:**** was accepted as significant, and error bars represent the standard deviation (SD).

The apoptosis induction of Luteolin after the treatment for 48 hours is in line with the previous research; for instance, Chen et al. showed with A549, human lung adenocarcinoma cells that 20, 40, and 60 µM application of Luteolin for 48 hours significantly induced apoptosis, where the 20 µM Luteolin application resulted in total apoptosis ratio of 16.27%, compared to the untreated control group which had 10.31% apoptosis ratio (Q. Chen et al. 2012). Furthermore, in more current research by Raina et al., it was found that Luteolin caused an increase in the percentage of early apoptosis of the human cervical cancer cell line, HeLa cells, from 2.9% in the sample of control to 9.8% when cells were exposed to 10 µM Luteolin for 48 hours, and to 12.4% when treated with 20 µM. Also, they showed that Luteolin had caused a profound enhancement in the HeLa cells, which were prone to late apoptosis, as the ratio increased from 1.89% to 7.85% in response to 10 µM Luteolin and to 14% with the treatment of 20 µM Luteolin (Raina et al. 2021).

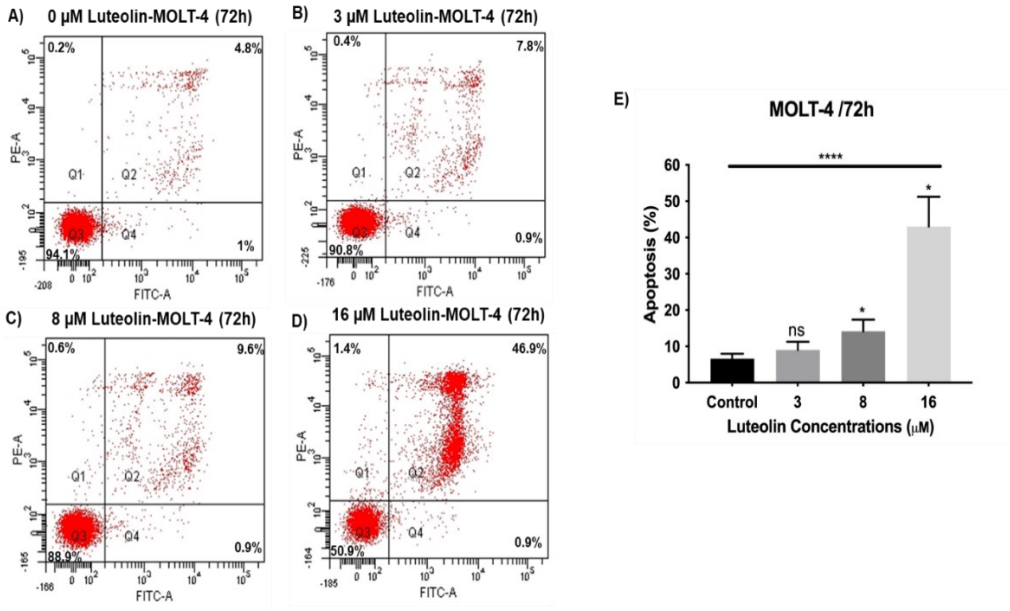

Figure 3.4. The influence of Luteolin at different concentrations on the apoptosis of MOLT-4 cells at 72 hours of exposure. Experiments were independently performed three times (n=3). The statistical analysis was performed by using a paired t-test to compare the experimental groups with the control group and using one-way ANOVA to compare all groups, where $p<0.05$:*, and $p<0.0001$:**** was accepted to be significant, and ns is used for the abbreviation of non-significant, and with the error bars, standard deviation (SD) is represented.

On the other hand, when Luteolin was applied for 72 hours, viable MOLT-4 cells' percentage, represented by quadrant Q3, was measured as 94.1% for the control (Figure 3.4.A), 90.8 % for the 3 µM Luteolin application (Figure 3.4.B), 88.9% for the 8 µM Luteolin exposure (Figure 3.4.C), and 50.9% for the 16 µM Luteolin application (Figure 3.4.D) to MOLT-4 cells, suggesting that increasing concentrations of Luteolin caused a reduction in the viability of MOLT-4 cells, where enhanced the percentage of apoptosis of MOLT-4 cells as represented by the Q2 and Q4 quadrants after 72 hours (Figure 3.4.). The percentage of MOLT-4 cells that were undergoing late apoptosis, as measured by the Q2, increased from 4.8% in the control group to 7.8%, 9.6%, and 46.9% when MOLT-4 cells were applied to 3,8 and 16 µM of Luteolin for 72 hours in order. Moreover, the total percentage of apoptosis, the sum of Q2 and Q4, had increased from 5.8% to 8.7% when Luteolin was applied at 3 µM concentration, to 10.5% when used at 8 µM and profoundly increased to 47.8 when applied in 16 µM for 72 hours (Figure 3.4.).

As the statistical analysis of the three experiments performed independently showed in Figure 3.4.E., 8 and 16 µM of Luteolin caused significant apoptosis induction in 72 hours of Luteolin exposure to MOLT-4 cells. In contrast, the apoptosis induction at 3 µM Luteolin exposure was found to be statistically non-significant in comparison to the control (Figure 3.4.E).

The promotion of apoptosis by Luteolin after 72 hours of exposure was exhibited in different cancer cells, such as esophageal carcinoma (P. Chen et al. 2017) and lung cancer cells (Zhang et al. 2021) by other groups. Chen et al. demonstrated that the total apoptosis rate significantly increased in the EC1 and KYSE450 human esophageal carcinoma cells when treated with 20 µM and 40 µM Luteolin compared to the ratio of apoptosis in total (the summation of the percentages in early and late apoptosis) in control cells (P. Chen et al. 2017). Furthermore, the study of Zhang et al. showed that the application of 5, 10, 20, and 40 µmol/L of Luteolin concentrations to NCI-H1975 and NCI-H1650, non-small cell lung cancer cells, for the exposure time of 72 hours resulted in a remarkable induction of apoptosis in each cell line in a fashion that was dependent on the dose (Zhang et al. 2021).

Moreover, when the time-dependent apoptosis effect of Luteolin was compared in a dose-based fashion, a significant increment in the concentration of 16 µM Luteolin between 48 and 72 hours, while the changes in the apoptosis ratio between 48 and 72 hours in other groups were non-significant (Figure 3.5.)

In the literature, most studies related to the induction of apoptosis in response to Luteolin have been demonstrated in different cancer cells at either 24 or 48 hours (Prasher et al. 2022). However, in one study carried out by Norzila et al., the application of 8.02 µg/mL Luteolin extracted from the leaves of Malaysian *Brucea javanica* to human cervical cancer cells, HeLa cells, resulted in an increase in the percentage of late apoptosis at 72 hours, when compared to 24 and 48 hours of application (Norzila, Shajarahtunnur, and Hasmah 2016).

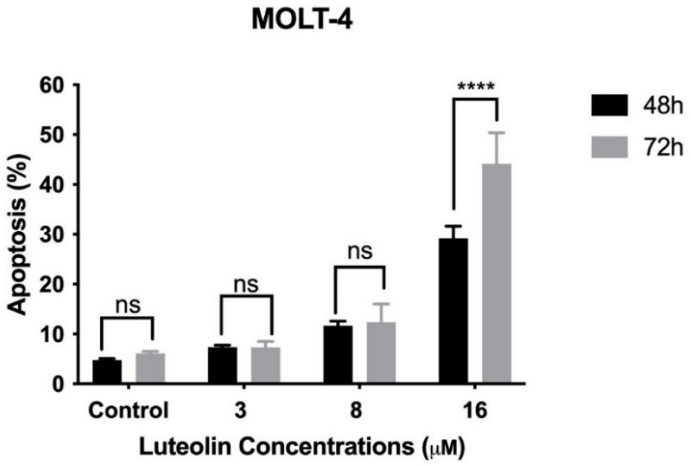

Figure 3.5. The time-dependent dose-based apoptotic effects of Luteolin on MOLT-4 cells. Experiments were independently performed three times (n=3). The statistical analysis was done using two-way ANOVA, where $p<0.05$:*, and $p<0.0001$:**** was accepted to be significant, and ns is used for the abbreviation of non-significant, and with the error bars, standard deviation (SD) is represented.

However, whether the increase was statistically significant compared to other time applications is unknown; also, whether the application of different doses of Luteolin might have affected the dose-based time-dependency of apoptosis induction was not investigated. For instance, Liao et al., in their study about the apoptotic effects of Luteolin on the macrophage cells, ANA-1, demonstrated that the application of 5,10 and 20 μM Luteolin did not significantly change the apoptosis ratio when compared in 24 and 48 hours. However, a considerable difference in early and late apoptosis ratios was observed between 24 and 48 hours in the 40 μM Luteolin application (Liao et al. 2018). Indicating that maybe incubating cells with a specific time of Luteolin (i.e., 72 hours, as shown in Figure 3.5.) caused the reaching of the maximum effect on the apoptosis for typical doses within the first 48 hours, and after that point, the saturation of the apoptosis pathways might take place so that any significant change in apoptosis could not be observed, or maybe other alternative pathways might have been activated. Even though, in Figure 3.3. and Figure 3.4., it can be said that Luteolin significantly affects the apoptosis induction in the MOLT-4 cells after incubation for 48 and 72 hours.

3.4. The Effect of Luteolin on the Caspase-3 Activity of the MOLT-4 Cells

The influence of various Luteolin concentrations (3-, 8-, and 16 µM) on the activity of Caspase-3 of MOLT-4 cells after 72 hours of exposure was measured by the Caspase-3 Colorimetric Assay Kit.

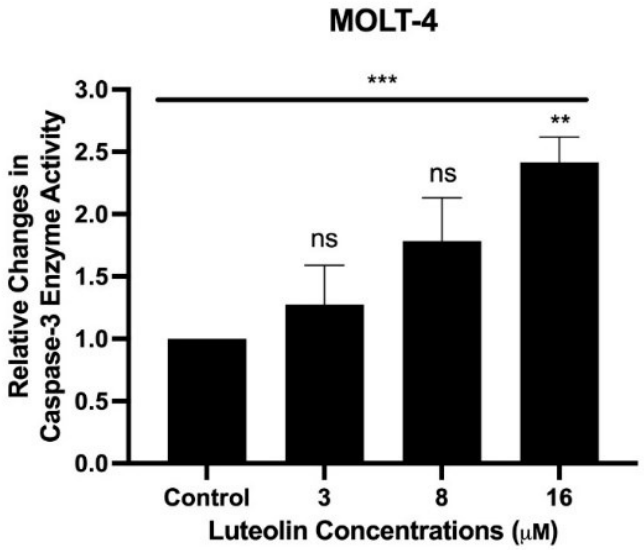

Figure 3.6. The effect of Luteolin on the Caspase-3 activity of MOLT-4 cells after 72 hours of exposure. Experiments were independently performed three times (n=3). The statistical analysis was performed by using a paired t-test to compare the experimental groups with the control group and using one-way ANOVA to compare all groups, where $p<0.05$:*, $p=0.0067$:** and $p=0.0007$:*** was accepted to be significant, and ns is used for the abbreviation of non-significant, and with the error bars, standard deviation (SD) is represented.

As seen in Figure 3.6., Luteolin application caused changes in the Caspase-3 enzyme activity in comparison to the control, with a significant change in the MOLT-4 cells exposed to 16 µM of Luteolin for 72 hours. The application of 16 µM of Luteolin (at the IC_{75}) caused a 2.42-fold change in the Caspase-3 activation compared to the control that was not included with Luteolin, whereas 3 µM of Luteolin forced a 1.27-fold change and 8 µM of Luteolin resulted in 1.78-fold more Caspase-3 activation in MOLT-4 cells (Figure 3.6.).

Caspase-3 is an executioner caspase in apoptosis that can be activated both by intrinsic and extrinsic apoptotic pathways in the cell, and the increase in its activity, in the means of its cleavage, indicates that apoptosis is induced in the cells (Eskandari and Eaves 2022) seen in Figure 3.6., Luteolin caused an increment in the activity of Caspase-3 of MOLT-4 cells, significantly at the 16 μM application after 72 hours, suggesting that it caused induction of apoptosis in MOLT-4 cells, which supported the Annexin V/PI Double Staining results of the MOLT-4 cells (Figure 3.5.). Therefore, it can be said that Luteolin has an apoptotic effect on the MOLT-4 cells, by which it could exert its anticancer properties.

The result of the increased Caspase-3 activity with the treatment of Luteolin aligns with previous studies. Chen et al. showed that 20 μM of Luteolin resulted in a nearly 3-fold increase in the Caspase-3 activity of EC1 cells, esophageal carcinoma cells, after 72 hours of exposure, thereby inducing apoptosis of esophageal carcinoma cells (P. Chen et al. 2017). Also, Zhang et al. demonstrated that Luteolin increased the level of cleaved Caspase-3 to 1.5 fold, 2-fold, and 2.5-fold when applied in 5,10 and 20 μM, respectively, concentrations after 72 hours in NCI-H1975 and NCI-H165 (Zhang et al. 2021).

3.5. The Effect of Luteolin on the Mitochondrial Membrane Potential of MOLT-4 Cells

The effect of the 72 hours of Luteolin application at different concentrations (3-, 8-, and 16 μM) on the membrane potential of mitochondria of MOLT-4 cells was examined by utilizing a JC-1 dye-based assay, and the analysis of the change in the membrane potential of mitochondria of cells with the flow cytometry.

Applying Luteolin for 72 hours to MOLT-4 cells resulted in a remarkable change in MOLT-4 cells' mitochondrial membrane potential (Figure 3.7.). The P6 and P7 percentages for each result were given along with the result for the CCCP application (Figure 3.7.E); CCCP is a known disrupter of the mitochondrial membrane potential that is used for controlling whether the JC-1 response was sensitive to changes in the membrane potential, to MOLT-4 cells, and the results gathered from the CCCP control were used to normalize the results collected from the control (without Luteolin

treatment) and Luteolin-exposed groups. According to the analysis of flow cytometry, the percentages of cells located at P7 were divided into P6 to get the P7/P6 ratio, which demonstrated the cytoplasmic/mitochondrial JC-1 dye ratio, an indicator of the loss of mitochondrial membrane potential based on the principle of the JC-1 dye-based detection (Sivandzade, Bhalerao, and Cucullo 2019) (Figure 3.7.A-E). The calculated and normalized P7/P6 ratios of Luteolin-exposed groups in comparison to the control group to calculate the relative change in the cytoplasmic/mitochondrial JC-1 ratio (Figure 3.7.F).

Compared to the control group, there was no remarkable difference in the cytoplasmic/mitochondrial JC-1 ratio when MOLT-4 cells were exposed to 3 and 8 μM Luteolin (2-fold change in the 8 μM Luteolin application); however, there was a significant relative change in the cytoplasmic/mitochondrial JC-1 ratio in the cells exposed to 16 μM Luteolin, compared to control approximately 12 fold change was observed (Figure 3.7.F), suggesting that at high concentrations of Luteolin after 72 hours exposure, the loss of mitochondrial membrane potential is higher compared to low concentrations.

The reduction in the membrane potential of mitochondria caused by Luteolin was also observed in different cancer cells, such as esophageal carcinoma cells, neuroblastoma, lung, and colon cancer cells at different concentrations but found to have a significant impact at concentrations equal to or higher than 20 μM Luteolin (P. Chen et al. 2017; F. Wang et al. 2014; Q. Chen et al. 2012; H. Yang et al. 2020).

The changes in the mitochondrial membrane potential, or other words, in the permeability of the outer membrane of mitochondria, are known to be the indicator of mitochondrial damage induced by the intrinsic (mitochondrial) apoptotic pathway (Eskandari and Eaves 2022). According to the results from the JC-1 experiment (Figure 3.7.), it can be said that Luteolin induced mitochondrial apoptotic pathway in MOLT-4 cells, which needs further clarification with the certain expression levels of proteins that control the mitochondrial outer membrane permeability, including the levels of antiapoptotic Bcl-xL, Bcl-2 proteins, and the proapoptotic proteins like Bim, Bak, and Bax. Also, the levels of cytochrome c from the mitochondria and cleaved Caspase-9 and PARP levels should be quantified to be able to confirm that Luteolin induces mitochondrial apoptotic pathway in MOLT-4 cells (Ahmed et al. 2019).

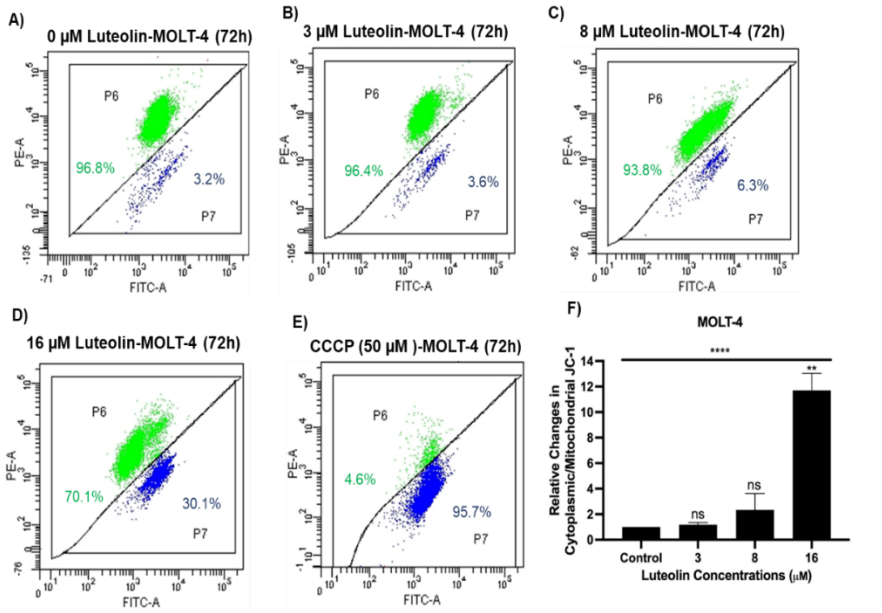

Figure 3.7. The impact of Luteolin on the membrane potential of mitochondria of MOLT-4 cells' cell cycle profile after 72 hours of exposure. Experiments were independently performed three times (n=3). The statistical analysis was performed by using a paired t-test to compare the experimental groups with the control group and using one-way ANOVA to compare all groups, where $p<0.05$:*, $p=0.0051$:** and $p<0.0001$:**** was accepted to be significant, and ns is used for the abbreviation of non-significant, and with the error bars, standard deviation (SD) is represented.

In studies conducted by different cancer cells, as identified that Luteolin can result in the induction of apoptosis through both intrinsic and extrinsic pathways, and the apoptosis induction by Luteolin through the intrinsic pathway is associated with enhanced Bax expression and cleaved levels of Caspase-3/-9 and PARP, and decreased Bcl-2, and Bcl-xL levels (Çetinkaya and Baran 2023). Therefore, it is likely that the induction of apoptosis in MOLT-4 cells by Luteolin is through the intrinsic apoptotic pathway.

3.6. The Effect of Luteolin on the Cell Cycle Profile of MOLT-4 Cells

The impact of Luteolin MOLT-4 cells was examined at different Luteolin concentrations (3-, 8-, and 16 µM) by PI staining and analysis of the cell cycle profile by flow cytometry after 72 hours of exposure.

Based on the results, 53.19% of the control cells were identified in the G1 phase, 40.53% in the S phase, and 6.28% in the phase of G2 (Figure 3.8.A). When 3 μM Luteolin was applied after 72 hours, it was identified that Luteolin promoted the arrest of the cell cycle at the G2/M phase, as the cell percentage in the phase of G2 was determined as 10.76%, while 50.48% were in G1 and 38.76% were in the S phase (Figure 3.8.B). On the other hand, applying 8 μM Luteolin enhanced cell cycle arrest at the S phase, as the cell percentage was measured as 50.79%, while 12.28% were in G2 and 36.93% were in the G1 phase (Figure 3.8.C). Similarly, 16 μM Luteolin dosage resulted in the cell cycle arrest at the S phase with 52.99%, while 4.57% of MOLT-4 cells were in the G2 phase, and 42.44% were in the G1 phase (Figure 3.8.D). Collectively, it can be said that Luteolin, after 72 hours of exposure, demonstrated a cytostatic effect on MOLT-4 cells, with 3 μM of Luteolin demonstrating the MOLT-4 cell arrest at the G2 stage and 8μM and 16 μM Luteolin resulting MOLT-4 cell arrest at the S phase (Figure 3.8.E).

The cytostatic impact of Luteolin was examined in different cancer cells. In the study by Cai et al., 20,40, and 60 μM Luteolin application was exhibited to cause arrest in the cell cycle of A549, non-small cell lung cancer cells, at the phase of G2 via inhibition of the Cyclin A expression and the phosphorylation of Rb and CDC2 (X. Cai et al. 2011).

Also, George et al. revelated that, Luteolin caused cell cycle arrest at HaCaT cells, a keratinocyte line, in the G2/M phase at 37.17 μM concentration while driving a cell cycle arrest at the G1 phase in A375, melanoma cells at 115.1 μM dosage (George et al. 2013). On the other hand, in a more recent study by Huang et al., Luteolin was identified to result in the cell cycle arrest at the S phase (at 10 and 30 μM concentrations) in breast cancer cells, MDA-MB-231 via downregulating cyclin D1 and Survivin and upregulating p21 expression (Huang, Jin, and Lan 2019).

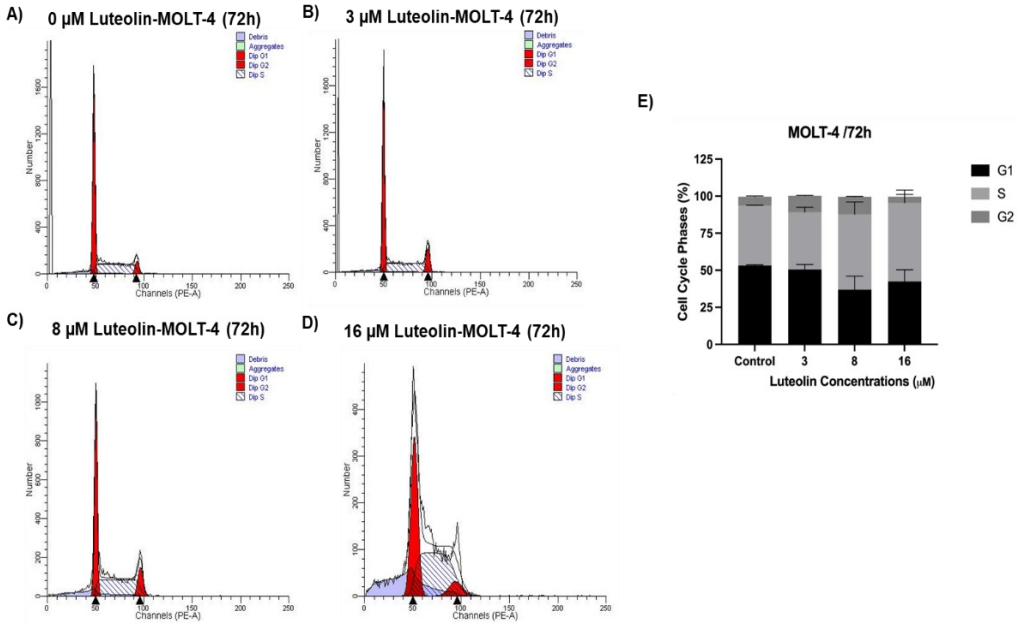

Figure 3.8. The impact of Luteolin on MOLT-4 cells at 72 hours after staining MOLT-4 cells with PI and analysis of cell population with the flow cytometry. Experiments were independently performed three times (n=3). The error bars represented the standard deviation (SD).

Therefore, it can be said that the phase at which Luteolin would cause cell cycle arrest could be associated with different factors, such as the type of cell, concentration, and the cell cycle regulatory proteins it affects, which can result in the arrestment of cells at different stages of the cell cycle.

Overall, it can be said that Luteolin has a cytostatic effect on MOLT-4 cells, where at 3 µM, it caused arrest at the G2/M phase, and at 8 and 16 µM, it caused cell cycle arrest at the S phase.

3.7. The Macromolecular Changes Caused by Luteolin on MOLT-4 Cells

Polyphenolic compounds like Luteolin have been identified to impact different processes in cancer progression by affecting enormously different signaling pathways or molecular targets, which can be dependent on various factors, thus using a broader

analysis in terms of macromolecular changes was thought to facilitate the research about the molecular pathways affected by Luteolin on MOLT-4 cells.

FTIR spectroscopy was used to investigate the macromolecular changes caused 72 hours after the Luteolin application to MOLT-4 cells. FTIR is a necessary tool in terms of the examination of different biological systems, such as cancer cells at different levels, such as at the levels of molecule and functional groups, as it gives valuable data regarding the structure of other macromolecular structural ingredients of the cancer cells like, carbohydrates, nucleic acids, and proteins (Derenne et al. 2013). Therefore, it was aimed to use this valuable tool to gain a broad understanding of the macromolecular changes on MOLT-4 cells in response to Luteolin treatment.

In Figure 3.9. , the control MOLT-4 cells' average FTIR spectra after 72 hours in the spectral region of 3960-870 cm^{-1} were shown. The numbered bands from one to fifteen in Figure 3.9., were decided to be the major bands in the infrared spectra of control MOLT-4 cells, and the assignment of these major bands was exhibited by mentioning the possible contribution of the macromolecules and their functional groups in Figure 3.9. were given and presented in Table 3.1.

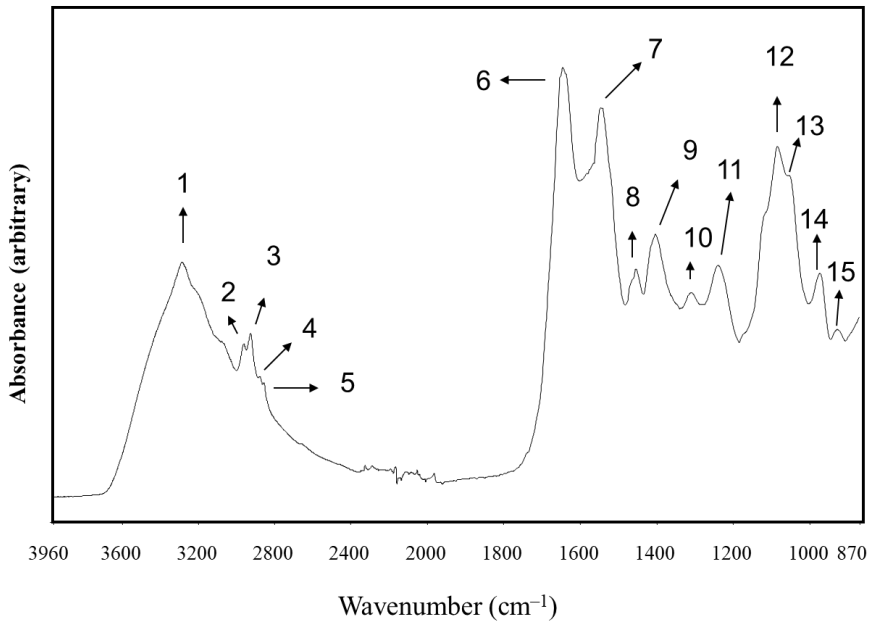

Figure 3.9. The general FTIR spectrum of the untreated MOLT-4 cells in 3960-870 cm^{-1} region after 72 hours (n=3).

Table 3.1. The general assignment of FTIR bands of MOLT-4 cells.

Number of Bands	Wavenumbers (cm^{-1})	Definitions for the Spectral Assignments	Citations
1	3282	Amide A; is primarily found in the stretching of N-H of phospholipids, cholesterol, and proteins, vibrations of CH_2 stretching.	(Grdadolnik 2003)
2	2959	Vibrations of CH_3 asymmetric stretching; are primarily found in fatty acids and protein components of cells.	(Garidel and Schott 2006)
3	2923	The CH_2 asymmetric stretching of various lipids and a small contribution from nucleic acids, carbohydrates, and proteins.	(Ceylan, Camgoz, and Baran 2012; Yandim et al. 2016)
4	2876	The CH_3 symmetric stretching of the side chains of proteins, along with a small contribution of nucleic acids, proteins, and carbohydrates.	(Yandim et al. 2016)
5	2852	The symmetric CH_2 stretching of side chains of saturated lipids, alongside the meager contribution from proteins, carbohydrates, and nucleic acids.	(Arrondo and Goni 1998)
6	1645	Amide I; is primarily found in the stretching of the carbonyl group at the peptide bond (The stretch of C = O and N-H bend), specifically sensitive to the proteins' secondary structure.	(Arrondo and Goni 1998)
7	1544	Amide II (The N-H bend and the C-N stretch), indicating the deformation of the protein amide N-H bound, nearly 60% is from the vibrations of amide N-H bending, while the rest is coupled to vibrations of C-N stretching.	(DeFlores et al. 2009)

Table 3.1. (cont.).

8	1454	Side chains of various amino acids and fatty acids; The CH_2 bending comes primarily from lipids, and a small part may be contributed from the proteins, The CH_3 asymmetric bending; indicates the proteins' methyl groups.	(Faramarzi et al. 2023)
10	1308	Amide III of proteins.	(Yandim et al. 2016; Gault and Lefaix 2003)
11	1238	The characteristics of the asymmetric stretching of phosphodiester (PO^{-2}) and a small contribution from the phospholipids' PO^{-2} groups	(Wood et al. 2004)
12	1082	The symmetric PO_4 vibrations from the linked phosphate groups to the nucleic acids (DNA and RNA).	(Balan et al. 2019)
13	1054	The C-O stretch of glycogen	(Balan et al. 2019)
14	972	The A-form of the DNA, helix formation	(Taboury, Liquier, and Taillandier 1985)
15	925	The C-N-C stretching of the skeleton of phosphate-ribose and Z form of the DNA	(Mello and Vidal 2012)

The FTIR spectrum of the MOLT-4 cells involves various bands, indicating the presence of various functional groups in macromolecules. Gathered spectra were analyzed in two sections, 3000-2800 cm^{-1} was used for the examination of lipids and proteins (Figure 3.10.), and 1780-1200 cm^{-1} for proteins' and lipids' analysis (Figure 3.12.) that includes bands derived from carbohydrates, nucleic acids, proteins, and

lipids. All the presented spectra have been normalized based on the selected bands and were used solely for illustration.

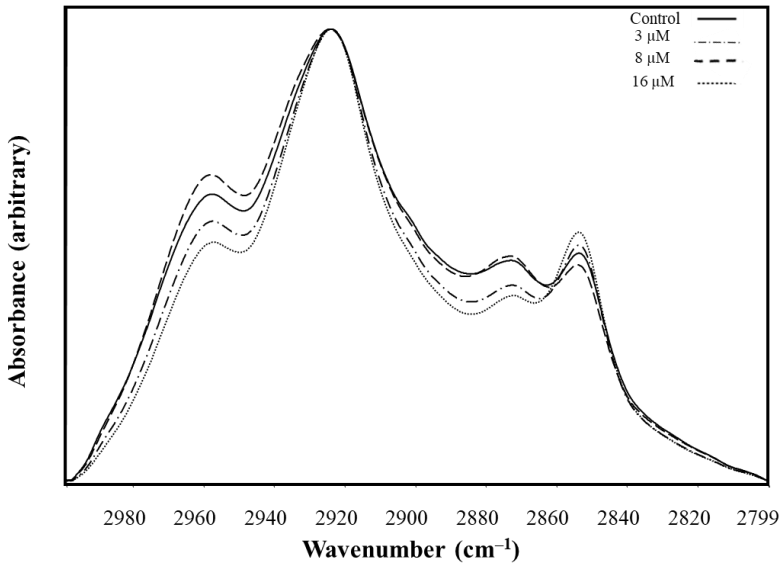

Figure 3.10. The average FTIR spectra of the control and Luteolin-treated MOLT-4 cells between the region of 3000-2800 cm^{-1} after 72 hours. (The spectra were normalized concerning the mode of CH_2 asymmetric, which was observed at 2923 cm^{-1}.) Experiments were independently performed three times (n=3).

The MOLT-4 were treated with Luteolin at different doses (IC_{25} (3 μM), IC_{50} (8 μM), and IC_{75} (16 μM)), and the control groups' average FTIR spectra between the 3000-2800 cm^{-1} region were demonstrated in Figure 3.10., in which different bands were located, for instance, the band located at 2959 cm^{-1} was due to the stretching of CH_3 which was asymmetric and contributed from proteins and lipids, the band located at 2923 cm^{-1} was due to the asymmetric stretching of CH_2 contributed from lipids, the symmetric band observed at 2876 cm^{-1} was due to the side chains of proteins along with a small contribution from nucleic acids, carbohydrates, and lipids and the symmetric CH_2 band located at 2852 cm^{-1} location was used to detect lipids primarily, as it also has a small donation from nucleic acids, carbohydrates, and proteins (Ceylan, Camgoz, and Baran 2012). As seen in Figure 3.10., a significant reduction in the intensity of 2959 cm^{-1} and 2876 cm^{-1} with respect to the increasing concentrations of Luteolin. The comparisons for the band intensity values for the changes in the region of 3000-2800

cm^{-1} in the Luteolin-treated MOLT-4 cells compared to control MOLT-4 cells were given in Figure 3.11.

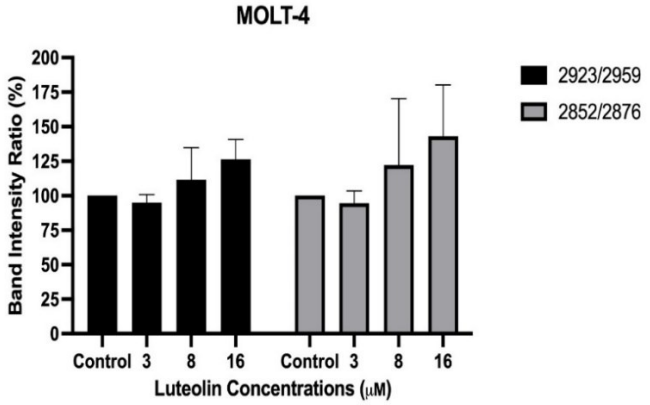

Figure 3.11. The 2923/2959 and 2852/2876 band intensity-ratio values for the control and Luteolin-treated MOLT-4 cells after 72 hours. Experiments were independently performed three times (n=3). Error bars in the graph represent the standard deviation (SD).

In Figure 3.11., the changes in the band intensity values in Luteolin-exposed groups compared to control MOLT-4 cells were given, and as can be seen, the 2923/2959 and 2852/2876 ratios increased as the Luteolin concentration increased in the MOLT-4 cells. The ratio of the intensity of CH_2 asymmetric to the stretching of CH_3 asymmetric (2923/2959) is known to indicate the hydrocarbon chain length of the acyl chains of lipids (Gupta et al. 2014) and found that Luteolin treatment led to an increment in the hydrocarbon chain length of the acyl chains of lipids in MOLT-4 cells (Figure 3.11.), demonstrating the decrease in the absorption intensity of the vibrations of CH_3 asymmetric. The reduction in the absorption intensity of the vibrations of CH_3 asymmetric is known to demonstrate the reducing freedom of the acyl chains, which are located at the heart of the phospholipid bilayer, as the mode of asymmetric stretching of CH_3 is correlated with the order of the membrane's deep interior (Severcan et al. 2000). Thus, the Luteolin treatment at the increasing concentrations caused an increment in the order in the deep interior of the plasma membrane in the leftover MOLT-4 cells (Figure 3.11.), which can be related to the mechanism of resistance to Luteolin after specific concentrations which affected the order of the lipid plasma membrane, but needs further examinations.

Furthermore, based on Figure 3.11., it can be seen that the intensity ratio of the stretching of CH_2 symmetric to the CH_3 symmetric (2852/2876) has increased as the Luteolin concentration increased in MOLT-4 cells. The intensity ratio of stretching of CH_2 symmetric to the CH_3 symmetric is known to be useful for the estimation of the lipid-to-protein ratio of the cell (Dogan et al. 2007). Based on the results from Figure 3.11., it has been found that the Luteolin treatment resulted in an increment in the lipid-to-protein ratio in the MOLT-4 cells, indicating that Luteolin might cause a rise in the content of lipids of MOLT-4 cells, which is an exceptional result in the aspect of the anticancer effects of Luteolin in cancer, as Luteolin was previously revealed to show anti-lipogenic functions in different cancer cells, meaning that Luteolin results in the decrement of lipid levels, which in turn is related to its ability to induce fatty acid oxidation and suppress the synthesis of fatty acids (Samec et al. 2023).

For instance, Brusselmans et al. have exhibited that Luteolin resulted in the inhibition of lipogenesis in a prostate cancer cell line, LNCaP, and breast cancer cells, MDA-MB-231 cells via inhibiting the activity of the enzyme fatty acid synthase, and Luteolin's ability to suppress the action of the fatty acid synthase was remarkably associated with its ability to inhibit the growth of prostate and breast cancer cells and increment in the apoptosis in those cancer cells (Brusselmans et al. 2005). Similarly, Luteolin was found to suppress the synthesis of fatty acids palmitate via inhibiting the activity of fatty acid synthase in a cell line of pancreatic cancer, MIA PaCa-2, thereby resulting in the decrease of the proliferation of the pancreatic cancer cells (D. M. Harris et al. 2012). Also, in the study of Liu et al., in the liver cancer cell line, HepG2 cell line, Luteolin was identified to result in a remarkable decrease in lipid accumulation (Liu et al. 2011). This lipid-lowering effect of it was found to be related to the upregulation of the carnitine palmitoyl transferase 1 (CPT-1), which is an enzyme that limits the rate in the mitochondrial fatty acid β-oxidation and downregulation in the fatty acid synthase and sterol regulatory element binding protein 1c (SREBP-1c), the upstream molecule that is regulating fatty acid synthase, which was all found to be related with the activation of the pathway of the AMPK signaling and substantially via the antioxidative actions of Luteolin (Liu et al. 2011). Recently, the Luteolin application was found to decrease the proliferation and result in a promoted induction in the apoptosis of human choriocarcinoma cells, JAR and JEG-3 cells, via inhibiting the pathway of PI3K/AKT/mTOR/SREBP and decreasing the expression of the lipogenic genes, including SREBP1 (Lim et al. 2016). Therefore, it was thought that another pathway

than AMPK and PI3K/Akt, well-known pathways in the regulation of lipid metabolism in cancer cells, or target, might be responsible for the increase in the lipid levels caused by Luteolin in the MOLT-4 cells (Figure 3.11.).

Even though the general trend and also the general behavior of Luteolin as an anticancer agent is the decrease in the lipid-to-protein ratio inside the cancer cells, one possible explanation for the increase in this ratio in response to Luteolin treatment in the MOLT-4 cells (Figure 3.11.), can be related with the ability of Luteolin to function as an agonist of peroxisome proliferator-activated receptor gamma (PPARγ), a receptor present at the nucleus, that is involved in the regulation of glucose and lipid metabolisms in cancer cells (Chi et al. 2021). PPARγ has been primarily found to be expressed in adipose tissue to promote lipogenesis and adipocyte differentiation; however, its broad expression of it has been proved in various other cell types, including skeletal muscle, liver, and immune cells, including T and B cells, mast cells and macrophages, as well as in several lymphomas and leukemias (Garcia-Bates et al. 2008). PPARγ has been widely studied in cancer cells; its expression leads to the inhibition of cancer cell proliferation, promotion of apoptosis, and arrest of the cell cycle in the cancer cells, highlighting the importance of the usage of PPARγ agonists for cancer treatment (Grygiel-Górniak 2014).

The agonists of PPARγ were identified to function in the regulation of genes that are participated in lipid metabolism, as they have been found to cause upregulation of fatty acid transport proteins, fatty acid-binding proteins, and various other proteins that are associated with lipid metabolism, resulting in the increment of uptake, transport, and storage of lipids, which could be related to the increase in the lipid to protein ratio inside cells (Hernandez-Quiles, Broekema, and Kalkhoven 2021). Also, these agonists have been identified to change the membrane composition of cells via changing the lipid metabolism in a way that they had been found to increase the levels of specific lipids, like free fatty acids and triglycerides, which also found to be contributing to the increment in the lipid to protein ratio in the membranes of cells (Hong et al. 2019).

The usage of PPARγ agonists in the Jurkat cells, a T cell leukemia cell line, and in T-ALL cells, CCRF-CEM cells were examined by Harris and Phipps, and found that these ligands induced apoptosis of these cells by a mechanism that is dependent on PPARγ (S. G. Harris and Phipps 2002). Moreover, different groups have identified Luteolin as an agonist of PPARγ in various settings (Qu et al. 2014; Li et al. 2022; El-Bassossy, Abo-Warda, and Fahmy 2014). Even Luteolin has been identified to sensitize

colorectal cancer SW480 cells to Oxaliplatin via PPARγ/OCTN2 pathway (Qu et al. 2014). So, it was thought that Luteolin as an agonist of PPARγ caused an increment in the lipid-to-protein ratio in MOLT-4 cells, about which further examinations are required.

Moreover, in Figure 3.12., MOLT-4 cells that were exposed to various Luteolin concentrations (IC_{25} (3 µM), IC_{50} (8 µM), and IC_{75} (16 µM)) and the control groups' average FTIR spectra between the 1780-1200 cm^{-1} region were shown. The band located at 1741 cm^{-1} is known to represent the vibrations of C=O ester stretching from the cholesterol esters and triglycerides, where the intensity of the vibration of C=O ester stretching has increased in response to the increasing concentrations of Luteolin compared to control MOLT-4 cells (Figure 3.12.).

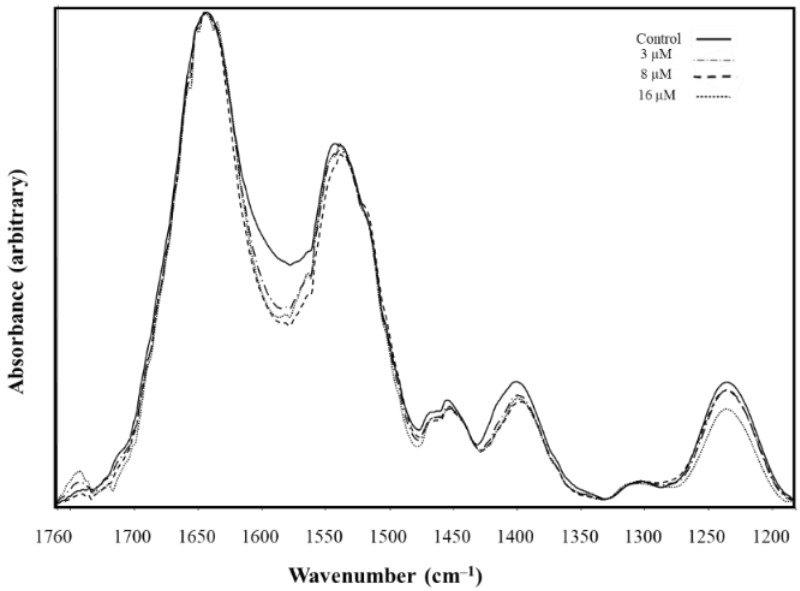

Figure 3.12. The average FTIR spectra of the control and Luteolin-treated MOLT-4 cells between 1780-1200 cm^{-1} region after 72 hours (the normalization of the spectra was done with respect to the Amide I band, observed at 1645 cm^{-1}). (n=3)

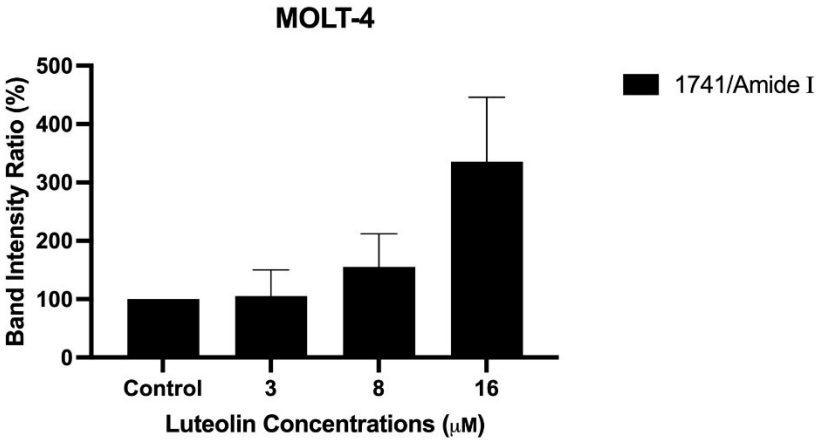

Figure 3.13. The 1741/Amide I band intensity-ratio values for the control and Luteolin-treated MOLT-4 cells after 72 hours. Experiments were independently performed three times (n=3). Error bars represented standard deviation (SD).

In Figure 3.13., changes in the band intensity values in Luteolin-exposed groups in comparison to control MOLT-4 cells were given. The 1741/Amide I ratio, which is used as another indicator of the lipid to protein ratio for the biological systems, increased as the Luteolin concentration increased in the MOLT-4 cells. The results from Figure 3.13 also correlated with the 2852/2876 ratio increase, suggesting that the increasing Luteolin concentrations increased the lipid-to-protein ratio within the MOLT-4 cells. The reason and mechanism of this increase need further examination.

CHAPTER 4

CONCLUSION

ALL is a type of leukemia described by the various recurrent generic alterations blocking the differentiation of the precursor B-and T-cells, resulting in the aberrant proliferation and survival of immature lymphoblasts and accumulation of them in the blood marrow, peripheral blood, and various extramedullary sites. It is characterized by leukemic blasts' cytogenic profile and morphology into mainly B-and T-cell lymphoblastic leukemia. T-ALL is the ALL type, which is not commonly observed as the B-ALL yet is aggressive and heterogeneous. The present treatment options for treating T-ALL comprise primarily the use of the high-intensity combination of various chemotherapeutic agents, which has been observed to result in different side effects in patients which are challenging to accept or ultimately lead to death of patients. The severe side effects observed in patients have been associated with the substantial toxicities of those chemotherapeutics, as they are known to be toxic to healthy cells alongside cancer cells, highlighting the vitalism to develop non-toxic, potent, cost-effective, and readily available treatment options for T-ALL patients.

Flavonoids, the secondary metabolites of plants responsible for color and flower aromas, have been extensively searched for their therapeutic potential as an anticancer drug and demonstrated to have various anticancer effects on different cancer types. Among flavonoids, Luteolin is an extensively explored natural compound with multiple biological activities, including anticancer effects. Its anticancer potential has been demonstrated in various cancer types, which have been associated with its function in the suppression of the growth of tumors via targeting several processes, including cancer cell proliferation, apoptosis, migration, angiogenesis, and the cancer cell cycle progression. Yet, no research demonstrated the anticancer potential of Luteolin on T-ALL cells.

This study demonstrated the anticancer potential of Luteolin shown in various terms on T-ALL cells for the first time. It has been found that Luteolin exhibited dose- and time-dependent antiproliferative effects on MOLT-4 cells, a T-ALL cell line, with a more potent effect compared to other established studies. Furthermore, Luteolin was

found to remarkably decrease MOLT-4 cells' viability depending on dose and time, as shown with the Trypan Blue Dye Exclusion Method. Luteolin also caused significant time-and dose-dependent apoptosis induction in MOLT-4 cells, as exhibited with the Annexin V/PI double staining and also verified with the increased Caspase-3 activities in the MOLT-4 cells upon the Luteolin treatment. The induction of apoptosis in MOLT-4 cells by Luteolin was thought to be likely through the mitochondrial apoptotic pathway, as the Luteolin treatment caused a rise in the loss of membrane potential of mitochondria in a fashion dependent on dose, shown with the JC-1 dye-based assay. Moreover, Luteolin has been identified to have cytostatic effects on MOLT-4 cells, as 72 hours of application of 3 μM Luteolin resulted in an arrest at the cell cycle in the stage of G2/M, while 8- and 16 μM Luteolin concentrations caused the arrest at the S phase.

When the macromolecular changes on MOLT-4 cells in exchange for Luteolin were investigated for the first time in the literature, it was found that Luteolin caused an increase in lipid to protein ratio of MOLT-4 cells, which was shown with an increase in 2852/2876 and 1741/Amide I ratios. Also, increasing concentrations of Luteolin were identified to increase the hydrocarbon chain length of the lipid acyl chains of MOLT-4 cells. The possible reasoning and mechanisms that are responsible for the increase in lipid-to-protein ratio and the hydrocarbon chain length of the lipid acyl chains of MOLT-4 cells need further examination.

In conclusion, Luteolin has been identified to have antiproliferative, apoptotic, and cytostatic effects on MOLT-4 cells, offering the use of as therapeutics for T-ALL cells as a novel and natural cancer therapeutics that would avoid the untargeted toxicity of chemotherapeutics to healthy cells, preventing the severe side effects of the chemotherapy regimen to T-ALL patients.

REFERENCES

Abdul-Hamid, Gamal. 2011. “Classification of Acute Leukemia.” In *Acute Leukemia-The Scientist’s Perspective and Challenge*. IntechOpen.

Abuasab, Tareq, Jacob Rowe, and Ariella Tvito. 2021. “Emerging Monoclonal Antibody Therapy for the Treatment of Acute Lymphoblastic Leukemia.” *Biologics: Targets and Therapy*, 419–31.

Advani, Anjali S, Shannon McDonough, Steven Coutre, Brent Wood, Jerald Radich, Martha Mims, Margaret O’Donnell, Stephanie Elkins, Michael Becker, and Megan Othus. 2014. “SWOG S0910: A Phase 2 Trial of Clofarabine/Cytarabine/Epratuzumab for Relapsed/Refractory Acute Lymphocytic Leukaemia.” *British Journal of Haematology* 165 (4): 504–9.

Ahmed, Salman, Haroon Khan, Deborah Fratantonio, Muhammad Mohtasheemul Hasan, Simin Sharifi, Nazanin Fathi, Hammad Ullah, and Luca Rastrelli. 2019. “Apoptosis Induced by Luteolin in Breast Cancer: Mechanistic and Therapeutic Perspectives.” *Phytomedicine* 59: 152883. https://doi.org/https://doi.org/10.1016/j.phymed.2019.152883.

Ambasta, Rashmi K, Rohan Gupta, Dhiraj Kumar, Saurabh Bhattacharya, Aditi Sarkar, and Pravir Kumar. 2019. “Can Luteolin Be a Therapeutic Molecule for Both Colon Cancer and Diabetes?” *Briefings in Functional Genomics* 18 (4): 230–39.

Angiolillo, Anne L, Alice L Yu, Gregory Reaman, Ashish M Ingle, Rita Secola, and Peter C Adamson. 2009. “A Phase II Study of Campath-1H in Children with Relapsed or Refractory Acute Lymphoblastic Leukemia: A Children’s Oncology Group Report.” *Pediatric Blood & Cancer* 53 (6): 978–83.

Arber, Daniel A, Attilio Orazi, Robert Hasserjian, Jürgen Thiele, Michael J Borowitz, Michelle M Le Beau, Clara D Bloomfield, Mario Cazzola, and James W Vardiman. 2016. “The 2016 Revision to the World Health Organization

Classification of Myeloid Neoplasms and Acute Leukemia." *Blood, The Journal of the American Society of Hematology* 127 (20): 2391–2405.

Arrondo, Jose Luis R, and Félix M Goni. 1998. "Infrared Studies of Protein-Induced Perturbation of Lipids in Lipoproteins and Membranes." *Chemistry and Physics of Lipids* 96 (1–2): 53–68.

Azam, Mohammad, Robert R Latek, and George Q Daley. 2003. "Mechanisms of Autoinhibition and STI-571/Imatinib Resistance Revealed by Mutagenesis of BCR-ABL." *Cell* 112 (6): 831–43.

Aziz, Nur, Mi-Yeon Kim, and Jae Youl Cho. 2018. "Anti-Inflammatory Effects of Luteolin: A Review of in Vitro, in Vivo, and in Silico Studies." *Journal of Ethnopharmacology* 225: 342–58.

Balan, Vera, Cosmin-Teodor Mihai, Florina-Daniela Cojocaru, Cristina-Mariana Uritu, Gianina Dodi, Doru Botezat, and Ioannis Gardikiotis. 2019. "Vibrational Spectroscopy Fingerprinting in Medicine: From Molecular to Clinical Practice." *Materials* 12 (18): 2884.

Bandala-Sanchez, Esther, Yuxia Zhang, Simone Reinwald, James A Dromey, Bo-Han Lee, Junyan Qian, Ralph M Böhmer, and Leonard C Harrison. 2013. "T Cell Regulation Mediated by Interaction of Soluble CD52 with the Inhibitory Receptor Siglec-10." *Nature Immunology* 14 (7): 741–48.

Bayón-Calderón, Fátima, María L Toribio, and Sara González-García. 2020. "Facts and Challenges in Immunotherapy for T-Cell Acute Lymphoblastic Leukemia." *International Journal of Molecular Sciences* 21 (20): 7685.

Bennett, J M, D Catovsky, Marie-Theregse Daniel, G Flandrin, D A G Galton, H R Gralnick, and C Sultan. 1976. "Proposals for the Classification of the Acute Leukaemias French-American-British (FAB) Co-Operative Group." *British Journal of Haematology* 33 (4): 451–58. https://doi.org/https://doi.org/10.1111/j.1365-2141.1976.tb03563.x.

Board, P D Q Pediatric Treatment Editorial. 2022. “Childhood Acute Lymphoblastic Leukemia Treatment (PDQ®).” In *PDQ Cancer Information Summaries [Internet]*. National Cancer Institute (US).

Boer, Monique L Den, Marjon van Slegtenhorst, Renée X De Menezes, Meyling H Cheok, Jessica GCAM Buijs-Gladdines, Susan TCJM Peters, Laura J C M Van Zutven, H Berna Beverloo, Peter J Van der Spek, and Gaby Escherich. 2009. “A Subtype of Childhood Acute Lymphoblastic Leukaemia with Poor Treatment Outcome: A Genome-Wide Classification Study.” *The Lancet Oncology* 10 (2): 125–34.

Bradeen, H A, and C A Eide. 2006. “O, Hare T, Johnson KJ, Willis SG, Lee FY, et al. Comparison of Imatinib Mesylate, Dasatinib (BMS-354825), and Nilotinib (AMN107) in an N-Ethyl-N-Nitrosourea (ENU)-Based Mutagenesis Screen: High Efficacy of Drug Combinations.” *Blood* 108 (2332): 8.

Bride, Karen L, Tiffaney L Vincent, Soo-Yeon Im, Richard Aplenc, David M Barrett, William L Carroll, Robin Carson, Yunfeng Dai, Meenakshi Devidas, and Kimberly P Dunsmore. 2018. “Preclinical Efficacy of Daratumumab in T-Cell Acute Lymphoblastic Leukemia.” *Blood, The Journal of the American Society of Hematology* 131 (9): 995–99.

Brusselmans, Koen, Ruth Vrolix, Guido Verhoeven, and Johannes V Swinnen. 2005. “Induction of Cancer Cell Apoptosis by Flavonoids Is Associated with Their Ability to Inhibit Fatty Acid Synthase Activity.” *Journal of Biological Chemistry* 280 (7): 5636–45.

Cai, Qiuyin, Ronald O Rahn, and Ruiwen Zhang. 1997. “Dietary Flavonoids, Quercetin, Luteolin and Genistein, Reduce Oxidative DNA Damage and Lipid Peroxidation and Quench Free Radicals.” *Cancer Letters* 119 (1): 99–107.

Cai, Xueting, Tingmei Ye, Chao Liu, Wuguang Lu, Min Lu, Juan Zhang, Min Wang, and Peng Cao. 2011. “Luteolin Induced G2 Phase Cell Cycle Arrest and Apoptosis

on Non-Small Cell Lung Cancer Cells." *Toxicology in Vitro* 25 (7): 1385–91. https://doi.org/https://doi.org/10.1016/j.tiv.2011.05.009.

Campana, Dario, Jacques J M van Dongen, Atul Mehta, Elaine Coustan-Smith, Ingrid L M Wolvers-Tettero, Kanagasabai Ganeshaguru, and George Janossy. 1991. "Stages of T-Cell Receptor Protein Expression in T-Cell Acute Lymphoblastic Leukemia." *Blood* 77 (7): 1546–54.

Cao, Zhijia, Huainian Zhang, Xiaoyan Cai, Wei Fang, Dong Chai, Ying Wen, Hongsheng Chen, Fujiang Chu, and Yongli Zhang. 2018. "Luteolin Promotes Cell Apoptosis by Inducing Autophagy in Hepatocellular Carcinoma." *Cellular Physiology and Biochemistry* 43 (5): 1803–12.

Caporali, Sabrina, Alessandro De Stefano, Cinzia Calabrese, Alfredo Giovannelli, Massimo Pieri, Isabella Savini, Manfredi Tesauro, Sergio Bernardini, Marilena Minieri, and Alessandro Terrinoni. 2022. "Anti-Inflammatory and Active Biological Properties of the Plant-Derived Bioactive Compounds Luteolin and Luteolin 7-Glucoside." *Nutrients* 14 (6): 1155.

Capria, Saveria, Matteo Molica, Sara Mohamed, Simona Bianchi, Maria Luisa Moleti, Silvia Maria Trisolini, Sabina Chiaretti, and Anna Maria Testi. 2020. "A Review of Current Induction Strategies and Emerging Prognostic Factors in the Management of Children and Adolescents with Acute Lymphoblastic Leukemia." *Expert Review of Hematology* 13 (7): 755–69. https://doi.org/10.1080/17474086.2020.1770591.

Caracciolo, Daniele, Antonia Mancuso, Nicoletta Polerà, Caterina Froio, Giuseppe D'Aquino, Caterina Riillo, Pierosandro Tagliaferri, and Pierfrancesco Tassone. 2023. "The Emerging Scenario of Immunotherapy for T-Cell Acute Lymphoblastic Leukemia: Advances, Challenges and Future Perspectives." *Experimental Hematology & Oncology* 12 (1): 5. https://doi.org/10.1186/s40164-022-00368-w.

Çetinkaya, Melisa, and Yusuf Baran. 2023. "Therapeutic Potential of Luteolin on Cancer." *Vaccines* 11 (3): 554.

Ceylan, Cagatay, Aylin Camgoz, and Yusuf Baran. 2012. “Macromolecular Changes in Nilotinib Resistant K562 Cells; an in Vitro Study by Fourier Transform Infrared Spectroscopy.” *Technology in Cancer Research & Treatment* 11 (4): 333–44.

Charles, Winter Z, Cierra R Faries, Ya’hnis T Street, Lyrik S Flowers, and Brian R McNaughton. 2022. “Antibody-Recruitment as a Therapeutic Strategy: A Brief History and Recent Advances.” *Chembiochem* 23 (16): e202200092.

Chen, Pei-Yi, Hsin-Jung Tien, Shih-Fen Chen, Chi-Ting Horng, Huei-Lin Tang, Hui-Ling Jung, Ming-Jiuan Wu, and Jui-Hung Yen. 2018. “Response of Myeloid Leukemia Cells to Luteolin Is Modulated by Differentially Expressed Pituitary Tumor-Transforming Gene 1 (PTTG1) Oncoprotein.” *International Journal of Molecular Sciences* 19 (4): 1173.

Chen, Ping, Jing-Yang Zhang, Bei-Bei Sha, Yan-Er Ma, Tao Hu, Yang-Cheng Ma, Hao Sun, Jian-Xiang Shi, Zi-Ming Dong, and Pei Li. 2017. “Luteolin Inhibits Cell Proliferation and Induces Cell Apoptosis via Down-Regulation of Mitochondrial Membrane Potential in Esophageal Carcinoma Cells EC1 and KYSE450.” *Oncotarget* 8 (16): 27471.

Chen, Qing, Shengming Liu, Jinghong Chen, Qianqian Zhang, Shijie Lin, Zhiming Chen, and Jianwei Jiang. 2012. “Luteolin Induces Mitochondria-Dependent Apoptosis in Human Lung Adenocarcinoma Cell.” *Natural Product Communications* 7 (1): 1934578X1200700111.

Chen, Ting, Li-Ping Li, Xin-Yan Lu, Hui-Di Jiang, and Su Zeng. 2007. “Absorption and Excretion of Luteolin and Apigenin in Rats after Oral Administration of Chrysanthemum Morifolium Extract.” *Journal of Agricultural and Food Chemistry* 55 (2): 273–77.

Chevallier, Patrice, Arnaud Pigneux, Nelly Robillard, Sameh Ayari, Thierry Guillaume, Jacques Delaunay, Marion Eveillard, Pierre-Yves Dumas, Eric Lippert, and Mohamad Mohty. 2012. “Rituximab for the Treatment of Adult

Relapsed/Refractory CD20 Positive B-ALL Patients: A Pilot Series." *Leukemia Research* 36 (3): 311–15.

Chi, Tiange, Mina Wang, Xu Wang, Ke Yang, Feiyu Xie, Zehuan Liao, and Peng Wei. 2021. "PPAR-γ Modulators as Current and Potential Cancer Treatments." *Frontiers in Oncology* 11: 737776.

Choi, Chun-Whan, Hyun Ah Jung, Sam Sik Kang, and Jae Sue Choi. 2007. "Antioxidant Constituents and a New Triterpenoid Glycoside from Flos Lonicerae." *Archives of Pharmacal Research* 30: 1–7.

Chung, Elaine Y, James N Psathas, Duonan Yu, Yimei Li, Mitchell J Weiss, and Andrei Thomas-Tikhonenko. 2012. "CD19 Is a Major B Cell Receptor–Independent Activator of MYC-Driven B-Lymphomagenesis." *The Journal of Clinical Investigation* 122 (6): 2257–66.

Cohen, Martin H, Grant Williams, John R Johnson, John Duan, Jogarao Gobburu, Atiqur Rahman, Kimberly Benson, John Leighton, Sung K Kim, and Rebecca Wood. 2002. "Approval Summary for Imatinib Mesylate Capsules in the Treatment of Chronic Myelogenous Leukemia." *Clinical Cancer Research* 8 (5): 935–42.

Cooper, Matthew L, Jaebok Choi, Karl Staser, Julie K Ritchey, Jessica M Devenport, Kayla Eckardt, Michael P Rettig, Bing Wang, Linda G Eissenberg, and Armin Ghobadi. 2018. "An 'off-the-Shelf' Fratricide-Resistant CAR-T for the Treatment of T Cell Hematologic Malignancies." *Leukemia* 32 (9): 1970–83.

Cordo', Valentina, Jordy C G van der Zwet, Kirsten Canté-Barrett, Rob Pieters, and Jules P P Meijerink. 2021. "T-Cell Acute Lymphoblastic Leukemia: A Roadmap to Targeted Therapies." *Blood Cancer Discovery* 2 (1): 19–31.

Cortes, Jorge E, D-W Kim, J l Pinilla-Ibarz, P Le Coutre, R Paquette, C Chuah, F E Nicolini, J F Apperley, H J Khoury, and M Talpaz. 2013. "A Phase 2 Trial of

Ponatinib in Philadelphia Chromosome–Positive Leukemias." *New England Journal of Medicine* 369 (19): 1783–96.

Dai, Zhenyu, Wei Mu, Ya Zhao, Xiangyin Jia, Jianwei Liu, Qiaoe Wei, Taochao Tan, and Jianfeng Zhou. 2021. "The Rational Development of CD5-Targeting Biepitopic CARs with Fully Human Heavy-Chain-Only Antigen Recognition Domains." *Molecular Therapy* 29 (9): 2707–22.

Dang, Hao, Murtaza Hasan Weiwei Meng, Haiwei Zhao, Javed Iqbal, Rongji Dai, Yulin Deng, and Fang Lv. 2014. "Luteolin-Loaded Solid Lipid Nanoparticles Synthesis, Characterization, & Improvement of Bioavailability, Pharmacokinetics in Vitro and Vivo Studies." *Journal of Nanoparticle Research* 16: 1–10.

Daver, Naval, Deborah Thomas, Farhad Ravandi, Jorge Cortes, Rebecca Garris, Elias Jabbour, Guillermo Garcia-Manero, Gautam Borthakur, Tapan Kadia, and Michael Rytting. 2015. "Final Report of a Phase II Study of Imatinib Mesylate with Hyper-CVAD for the Front-Line Treatment of Adult Patients with Philadelphia Chromosome-Positive Acute Lymphoblastic Leukemia." *Haematologica* 100 (5): 653.

Davila, Marco L, Isabelle Riviere, Xiuyan Wang, Shirley Bartido, Jae Park, Kevin Curran, Stephen S Chung, Jolanta Stefanski, Oriana Borquez-Ojeda, and Malgorzata Olszewska. 2014. "Efficacy and Toxicity Management of 19-28z CAR T Cell Therapy in B Cell Acute Lymphoblastic Leukemia." *Science Translational Medicine* 6 (224): 224ra25-224ra25.

Davis, Kara L, and Crystal L Mackall. 2016. "Immunotherapy for Acute Lymphoblastic Leukemia: From Famine to Feast." *Blood Advances* 1 (3): 265–69. https://doi.org/10.1182/bloodadvances.2016000034.

DeAngelo, Daniel J, Elias Jabbour, and Anjali Advani. 2020. "Recent Advances in Managing Acute Lymphoblastic Leukemia." *American Society of Clinical Oncology Educational Book*, no. 40 (May): 330–42. https://doi.org/10.1200/EDBK_280175.

DeAngelo, Daniel J, Wendy Stock, Anthony S Stein, Andrei Shustov, Michaela Liedtke, Charles A Schiffer, Erik Vandendries, Katherine Liau, Revathi Ananthakrishnan, and Joseph Boni. 2017. “Inotuzumab Ozogamicin in Adults with Relapsed or Refractory CD22-Positive Acute Lymphoblastic Leukemia: A Phase 1/2 Study.” *Blood Advances* 1 (15): 1167–80.

DeFlores, Lauren P, Ziad Ganim, Rebecca A Nicodemus, and Andrei Tokmakoff. 2009. “Amide I′− II′ 2D IR Spectroscopy Provides Enhanced Protein Secondary Structural Sensitivity.” *Journal of the American Chemical Society* 131 (9): 3385–91.

Dehelean, Cristina Adriana, Iasmina Marcovici, Codruta Soica, Marius Mioc, Dorina Coricovac, Stela Iurciuc, Octavian Marius Cretu, and Iulia Pinzaru. 2021. “Plant-Derived Anticancer Compounds as New Perspectives in Drug Discovery and Alternative Therapy.” *Molecules* 26 (4): 1109.

Derenne, Allison, Vincent Van Hemelryck, Delphine Lamoral-Theys, Robert Kiss, and Erik Goormaghtigh. 2013. “FTIR Spectroscopy: A New Valuable Tool to Classify the Effects of Polyphenolic Compounds on Cancer Cells.” *Biochimica et Biophysica Acta (BBA)-Molecular Basis of Disease* 1832 (1): 46–56.

Dias, Maria Celeste, Diana C G A Pinto, and Artur M S Silva. 2021. “Plant Flavonoids: Chemical Characteristics and Biological Activity.” *Molecules* 26 (17): 5377.

DiJoseph, John F, Douglas C Armellino, Erwin R Boghaert, Kiran Khandke, Maureen M Dougher, Latha Sridharan, Arthur Kunz, Philip R Hamann, Boris Gorovits, and Chandrasekhar Udata. 2004. “Antibody-Targeted Chemotherapy with CMC-544: A CD22-Targeted Immunoconjugate of Calicheamicin for the Treatment of B-Lymphoid Malignancies.” *Blood* 103 (5): 1807–14.

Ding, Shixiong, Airong Hu, Yaoren Hu, Jianbo Ma, Pengjian Weng, and Jinhua Dai. 2014. “Anti-Hepatoma Cells Function of Luteolin through Inducing Apoptosis and Cell Cycle Arrest.” *Tumor Biology* 35: 3053–60.

Dogan, Ayca, Kivanc Ergen, Fatma Budak, and Feride Severcan. 2007. “Evaluation of Disseminated Candidiasis on an Experimental Animal Model: A Fourier Transform Infrared Study.” *Applied Spectroscopy* 61 (2): 199–203.

Dombret, Hervé, Jean Gabert, Jean-Michel Boiron, Françoise Rigal-Huguet, Didier Blaise, Xavier Thomas, André Delannoy, Agnes Buzyn, Chrystele Bilhou-Nabera, and Jean-Michel Cayuela. 2002. “Outcome of Treatment in Adults with Philadelphia Chromosome–Positive Acute Lymphoblastic Leukemia—Results of the Prospective Multicenter LALA-94 Trial.” *Blood, The Journal of the American Society of Hematology* 100 (7): 2357–66.

Druker, Brian J, Charles L Sawyers, Hagop Kantarjian, Debra J Resta, Sofia Fernandes Reese, John M Ford, Renaud Capdeville, and Moshe Talpaz. 2001. “Activity of a Specific Inhibitor of the BCR-ABL Tyrosine Kinase in the Blast Crisis of Chronic Myeloid Leukemia and Acute Lymphoblastic Leukemia with the Philadelphia Chromosome.” *New England Journal of Medicine* 344 (14): 1038–42.

Druker, Brian J, Shu Tamura, Elisabeth Buchdunger, Sayuri Ohno, Gerald M Segal, Shane Fanning, Jürg Zimmermann, and Nicholas B Lydon. 1996. “Effects of a Selective Inhibitor of the Abl Tyrosine Kinase on the Growth of Bcr–Abl Positive Cells.” *Nature Medicine* 2 (5): 561–66. https://doi.org/10.1038/nm0596-561.

El-Bassossy, Hany M, Shaymaa M Abo-Warda, and Ahmed Fahmy. 2014. “Chrysin and Luteolin Alleviate Vascular Complications Associated with Insulin Resistance Mainly through PPAR-γ Activation.” *The American Journal of Chinese Medicine* 42 (05): 1153–67.

Eskandari, Ebrahim, and Connie J Eaves. 2022. “Paradoxical Roles of Caspase-3 in Regulating Cell Survival, Proliferation, and Tumorigenesis.” *Journal of Cell Biology* 221 (6): e202201159.

Faderl, Stefan, Hagop M Kantarjian, Deborah A Thomas, Jorge Cortes, Francis Giles, Sherry Pierce, Maher Albitar, and Zeev Estrov. 2000. “Outcome of Philadelphia

Chromosome-Positive Adult Acute Lymphoblastic Leukemia." *Leukemia & Lymphoma* 36 (3–4): 263–73.

Faramarzi, Bahar, Martina Moggio, Nadia Diano, Marianna Portaccio, and Maria Lepore. 2023. "A Brief Review of FT-IR Spectroscopy Studies of Sphingolipids in Human Cells." *Biophysica* 3 (1): 158–80.

Farhadfar, Nosha, and Mark R Litzow. 2016. "New Monoclonal Antibodies for the Treatment of Acute Lymphoblastic Leukemia." *Leukemia Research* 49: 13–21. https://doi.org/https://doi.org/10.1016/j.leukres.2016.07.009.

Fathi, Amir T, Uma Borate, Daniel J DeAngelo, Maureen M O'Brien, Tanya Trippett, Bijal D Shah, Gregory A Hale, James M Foran, Lewis B Silverman, and Raoul Tibes. 2015. "A Phase 1 Study of Denintuzumab Mafodotin (SGN-CD19A) in Adults with Relapsed or Refractory B-Lineage Acute Leukemia (B-ALL) and Highly Aggressive Lymphoma." *Blood* 126 (23): 1328.

Ferlay J, Laversanne M, Ervik M, Lam F, Colombet M, Mery L, Piñeros M, Znaor A, Soerjomataram I, and Bray F. 2020. "Global Cancer Observatory: Cancer Tomorrow." Lyon, France: International Agency for Research on Cancer. 2020. https://gco.iarc.fr/tomorrow/en.

Franco, Yollanda E M, Carolina A de Lima, Marcela N Rosa, Viviane A O Silva, Rui M Reis, Denise G Priolli, Patricia O Carvalho, Jessyane R do Nascimento, Cláudia Q da Rocha, and Giovanna B Longato. 2021. "Investigation of U-251 Cell Death Triggered by Flavonoid Luteolin: Towards a Better Understanding on Its Anticancer Property against Glioblastomas." *Natural Product Research* 35 (22): 4807–13.

Franza, Laura, Valentina Carusi, Eleonora Nucera, and Franco Pandolfi. 2021. "Luteolin, Inflammation and Cancer: Special Emphasis on Gut Microbiota." *Biofactors* 47 (2): 181–89.

Gaikwad, Abhijeet Ramnath, Komal D Ahire, Aachal A Gosavi, K S Salunkhe, and Aditi Khalkar. 2021. “Phytosome as a Novel Drug Delivery System for Bioavailability Enhancement of Phytoconstituents and Its Applications: A Review.” *Journal of Drug Delivery and Therapeutics* 11 (3): 138–52.

Garcia-Bates, Tatiana M, Geniece M Lehmann, Patricia J Simpson-Haidaris, Steven H Bernstein, Patricia J Sime, and Richard P Phipps. 2008. “Role of Peroxisome Proliferator-Activated Receptor Gamma and Its Ligands in the Treatment of Hematological Malignancies.” *PPAR Research* 2008.

Garidel, Patrick, and Heidrun Schott. 2006. “Fourier-Transform Midinfrared Spectroscopy for Analysis and Screening of Liquid Protein Formulations. Part 1: Understanding Infrared Spectroscopy of Proteins.” *BioProcess Int* 4 (5): 40–46.

Gault, Nathalie, and Jean-Louis Lefaix. 2003. “Infrared Microspectroscopic Characteristics of Radiation-Induced Apoptosis in Human Lymphocytes.” *Radiation Research* 160 (2): 238–50. http://www.jstor.org/stable/3581173.

George, Vazhapilly Cijo, Devanga Ragupathi Naveen Kumar, Palamadai Krishnan Suresh, Sanjay Kumar, and Rangasamy Ashok Kumar. 2013. “Comparative Studies to Evaluate Relative in Vitro Potency of Luteolin in Inducing Cell Cycle Arrest and Apoptosis in HaCaT and A375 Cells.” *Asian Pacific Journal of Cancer Prevention* 14 (2): 631–37.

Golay, Josée, and Martino Introna. 2012. “Mechanism of Action of Therapeutic Monoclonal Antibodies: Promises and Pitfalls of in Vitro and in Vivo Assays.” *Archives of Biochemistry and Biophysics* 526 (2): 146–53.

Gomes-Silva, Diogo, Madhuwanti Srinivasan, Sandhya Sharma, Ciaran M Lee, Dimitrios L Wagner, Timothy H Davis, Rayne H Rouce, Gang Bao, Malcolm K Brenner, and Maksim Mamonkin. 2017. “CD7-Edited T Cells Expressing a CD7-Specific CAR for the Therapy of T-Cell Malignancies.” *Blood, The Journal of the American Society of Hematology* 130 (3): 285–96.

Grdadolnik, Jože. 2003. “Saturation Effects in FTIR Spectroscopy: Intensity of Amide I and Amide II Bands in Protein Spectra.” *Acta Chimica Slovenica* 50 (4): 777–88.

Grygiel-Górniak, Bogna. 2014. “Peroxisome Proliferator-Activated Receptors and Their Ligands: Nutritional and Clinical Implications-a Review.” *Nutrition Journal* 13: 1–10.

Gupta, Ujval, Vivek K Singh, Vinay Kumar, and Yugal Khajuria. 2014. “Spectroscopic Studies of Cholesterol: Fourier Transform Infra-Red and Vibrational Frequency Analysis.” *Materials Focus* 3 (3): 211–17.

Gurunathan, Arun, Myesa Emberesh, and Robin Norris. 2019. “A Case Report of Using Daratumumab in Refractory T-Cell Acute Lymphoblastic Leukemia.” In *PEDIATRIC BLOOD & CANCER*. Vol. 66. WILEY 111 RIVER ST, HOBOKEN 07030-5774, NJ USA.

Han, Kun, Tingyuan Lang, Zhiqi Zhang, Yi Zhang, Yongning Sun, Zan Shen, Roger W Beuerman, Lei Zhou, and Daliu Min. 2018. “Luteolin Attenuates Wnt Signaling via Upregulation of FZD6 to Suppress Prostate Cancer Stemness Revealed by Comparative Proteomics.” *Scientific Reports* 8 (1): 8537.

Harborne, Jeffrey B, and Christine A Williams. 2000. “Advances in Flavonoid Research since 1992.” *Phytochemistry* 55 (6): 481–504.

Harris, Diane M, Luyi Li, Monica Chen, F Tracy Lagunero, Vay Liang W Go, and Laszlo G Boros. 2012. “Diverse Mechanisms of Growth Inhibition by Luteolin, Resveratrol, and Quercetin in MIA PaCa-2 Cells: A Comparative Glucose Tracer Study with the Fatty Acid Synthase Inhibitor C75.” *Metabolomics* 8: 201–10.

Harris, Nancy Lee, Elaine S Jaffe, Jacques Diebold, Georges Flandrin, H Konrad Muller-Hermelink, James Vardiman, T Andrew Lister, and Clara D Bloomfield. 1999. “The World Health Organization Classification of Neoplastic Diseases of the Hematopoietic and Lymphoid Tissues: Report of the Clinical Advisory Committee

Meeting, Airlie House, Virginia, November, 1997." *Annals of Oncology* 10 (12): 1419–32.

Harris, Sarah G, and Richard P Phipps. 2002. "Prostaglandin D2, Its Metabolite 15-d-PGJ2, and Peroxisome Proliferator Activated Receptor-γ Agonists Induce Apoptosis in Transformed, but Not Normal, Human T Lineage Cells." *Immunology* 105 (1): 23–34.

Hazarika, Maitreyee, Xiaoping Jiang, Qi Liu, Shwu-Luan Lee, Roshni Ramchandani, Christine Garnett, Micheal S Orr, Rajeshwari Sridhara, Brian Booth, and John K Leighton. 2008. "Tasigna for Chronic and Accelerated Phase Philadelphia Chromosome–Positive Chronic Myelogenous Leukemia Resistant to or Intolerant of Imatinib." *Clinical Cancer Research* 14 (17): 5325–31.

Hernández, Belén, Fernando Pflüger, Najoua Derbel, Joël De Coninck, and Mahmoud Ghomi. 2010. "Vibrational Analysis of Amino Acids and Short Peptides in Hydrated Media. VI. Amino Acids with Positively Charged Side Chains: L-Lysine and L-Arginine." *The Journal of Physical Chemistry B* 114 (2): 1077–88.

Hernandez-Quiles, Miguel, Marjoleine F Broekema, and Eric Kalkhoven. 2021. "PPARgamma in Metabolism, Immunity, and Cancer: Unified and Diverse Mechanisms of Action." *Frontiers in Endocrinology* 12: 624112.

Hinman, Lois M, Philip R Hamann, Roslyn Wallace, Ana T Menendez, Frederick E Durr, and Janis Upeslacis. 1993. "Preparation and Characterization of Monoclonal Antibody Conjugates of the Calicheamicins: A Novel and Potent Family of Antitumor Antibiotics." *Cancer Research* 53 (14): 3336–42.

Hong, Fan, Shijia Pan, Yuan Guo, Pengfei Xu, and Yonggong Zhai. 2019. "PPARs as Nuclear Receptors for Nutrient and Energy Metabolism." *Molecules* 24 (14): 2545.

Huang, Liming, Ketao Jin, and Huanrong Lan. 2019. "Luteolin Inhibits Cell Cycle Progression and Induces Apoptosis of Breast Cancer Cells through

Downregulation of Human Telomerase Reverse Transcriptase." *Oncol Lett* 17 (4): 3842–50. https://doi.org/10.3892/ol.2019.10052.

Hunger, Stephen P, Xiaomin Lu, Meenakshi Devidas, Bruce M Camitta, Paul S Gaynon, Naomi J Winick, Gregory H Reaman, and William L Carroll. 2012. "Improved Survival for Children and Adolescents with Acute Lymphoblastic Leukemia between 1990 and 2005: A Report from the Children's Oncology Group." *Journal of Clinical Oncology* 30 (14): 1663.

Imran, Muhammad, Abdur Rauf, Tareq Abu-Izneid, Muhammad Nadeem, Mohammad Ali Shariati, Imtiaz Ali Khan, Ali Imran, Ilkay Erdogan Orhan, Muhammad Rizwan, and Muhammad Atif. 2019. "Luteolin, a Flavonoid, as an Anticancer Agent: A Review." *Biomedicine & Pharmacotherapy* 112: 108612.

Jabbour, Elias, Jorge Cortes, and Hagop Kantarjian. 2011. "Long-term Outcomes in the Second-line Treatment of Chronic Myeloid Leukemia: A Review of Tyrosine Kinase Inhibitors." *Cancer* 117 (5): 897–906.

Jabbour, Elias, Kantarjian Hagop, Deborah Thomas, Guillermo Garcia-Manero, Daniela Hoehn, Rebecca Garris, Stefan H Faderl, et al. 2013. "Phase II Study Of The Hyper-CVAD Regimen In Combination With Ofatumumab As Frontline Therapy For Adults With CD-20 Positive Acute Lymphoblastic Leukemia (ALL)." *Blood* 122 (21): 2664. https://doi.org/https://doi.org/10.1182/blood.V122.21.2664.2664.

Jabbour, Elias, Hagop Kantarjian, and Jorge Cortes. 2015. "Use of Second-and Third-Generation Tyrosine Kinase Inhibitors in the Treatment of Chronic Myeloid Leukemia: An Evolving Treatment Paradigm." *Clinical Lymphoma Myeloma and Leukemia* 15 (6): 323–34.

Jain, Nitin, Wendy Stock, Amer Zeidan, Ehab Atallah, James McCloskey, Leonard Heffner, Benjamin Tomlinson, et al. 2020. "Loncastuximab Tesirine, an Anti-CD19 Antibody-Drug Conjugate, in Relapsed/Refractory B-Cell Acute Lymphoblastic Leukemia." *Blood Advances* 4 (3): 449–57. https://doi.org/10.1182/bloodadvances.2019000767.

Jiao, Ying, Ming Yi, Linping Xu, Qian Chu, Yongxiang Yan, Suxia Luo, and Kongming Wu. 2020. “CD38: Targeted Therapy in Multiple Myeloma and Therapeutic Potential for Solid Cancers.” *Expert Opinion on Investigational Drugs* 29 (11): 1295–1308.

Jones, Dan, Deborah Thomas, C Cameron Yin, Susan O’Brien, Jorge E Cortes, Elias Jabbour, Megan Breeden, Francis J Giles, Weiqiang Zhao, and Hagop M Kantarjian. 2008. “Kinase Domain Point Mutations in Philadelphia Chromosome-positive Acute Lymphoblastic Leukemia Emerge after Therapy with BCR-ABL Kinase Inhibitors.” *Cancer* 113 (5): 985–94.

Kantarjian, Hagop M, Daniel J DeAngelo, Matthias Stelljes, Michaela Liedtke, Wendy Stock, Nicola Gökbuget, Susan M O’Brien, Elias Jabbour, Tao Wang, and Jane Liang White. 2019. “Inotuzumab Ozogamicin versus Standard of Care in Relapsed or Refractory Acute Lymphoblastic Leukemia: Final Report and Long-term Survival Follow-up from the Randomized, Phase 3 INO-VATE Study.” *Cancer* 125 (14): 2474–87.

Kantarjian, Hagop M, Daniel J DeAngelo, Matthias Stelljes, Giovanni Martinelli, Michaela Liedtke, Wendy Stock, Nicola Gökbuget, Susan O’Brien, Kongming Wang, and Tao Wang. 2016. “Inotuzumab Ozogamicin versus Standard Therapy for Acute Lymphoblastic Leukemia.” *New England Journal of Medicine* 375 (8): 740–53.

Kantarjian, Hagop M, Bruno Lioure, Stella K Kim, Ehab Atallah, Thibaut Leguay, Kevin Kelly, Jean-Pierre Marolleau, Martine Escoffre-Barbe, Xavier G Thomas, and Jorge Cortes. 2016. “A Phase II Study of Coltuximab Ravtansine (SAR3419) Monotherapy in Patients with Relapsed or Refractory Acute Lymphoblastic Leukemia.” *Clinical Lymphoma Myeloma and Leukemia* 16 (3): 139–45.

Kantarjian, Hagop, Deborah Thomas, Jeffrey Jorgensen, Partow Kebriaei, Elias Jabbour, Michael Rytting, Sergernne York, Farhad Ravandi, Rebecca Garris, and Monica Kwari. 2013. “Results of Inotuzumab Ozogamicin, a CD22 Monoclonal

Antibody, in Refractory and Relapsed Acute Lymphocytic Leukemia." *Cancer* 119 (15): 2728–36.

Karschnia, Philipp, Justin T Jordan, Deborah A Forst, Isabel C Arrillaga-Romany, Tracy T Batchelor, Joachim M Baehring, Nathan F Clement, L Nicolas Gonzalez Castro, Aline Herlopian, and Marcela V Maus. 2019. "Clinical Presentation, Management, and Biomarkers of Neurotoxicity after Adoptive Immunotherapy with CAR T Cells." *Blood, The Journal of the American Society of Hematology* 133 (20): 2212–21.

Khan, Junaid, Swarnlata Saraf, and Shailendra Saraf. 2016. "Preparation and Evaluation of Luteolin–Phospholipid Complex as an Effective Drug Delivery Tool against GalN/LPS Induced Liver Damage." *Pharmaceutical Development and Technology* 21 (4): 475–86.

Kure, Ayako, Kiyotaka Nakagawa, Momoko Kondo, Shunji Kato, Fumiko Kimura, Akio Watanabe, Naoki Shoji, Sakiko Hatanaka, Tojiro Tsushida, and Teruo Miyazawa. 2016. "Metabolic Fate of Luteolin in Rats: Its Relationship to Anti-Inflammatory Effect." *Journal of Agricultural and Food Chemistry* 64 (21): 4246–54.

Labarthe, Adrienne de, Philippe Rousselot, Françoise Huguet-Rigal, Eric Delabesse, Francis Witz, Sébastien Maury, Delphine Réa, Jean-Michel Cayuela, Marie-Christine Vekemans, and Oumedaly Reman. 2007. "Imatinib Combined with Induction or Consolidation Chemotherapy in Patients with de Novo Philadelphia Chromosome–Positive Acute Lymphoblastic Leukemia: Results of the GRAAPH-2003 Study." *Blood* 109 (4): 1408–13.

Lai, Raymond, Cheryl F Hirsch-Ginsberg, and Carlos Bueso-Ramos. 2000. "Pathologic Diagnosis of Acute Lymphocytic Leukemia." *Hematology/Oncology Clinics of North America* 14 (6): 1209–35. https://doi.org/https://doi.org/10.1016/S0889-8588(05)70183-0.

Le, Robert Q, Liang Li, Weishi Yuan, Stacy S Shord, Lei Nie, Bahru A Habtemariam, Donna Przepiorka, Ann T Farrell, and Richard Pazdur. 2018. “FDA Approval Summary: Tocilizumab for Treatment of Chimeric Antigen Receptor T Cell-induced Severe or Life-threatening Cytokine Release Syndrome.” *The Oncologist* 23 (8): 943–47.

Lee, Daniel W, Bianca D Santomasso, Frederick L Locke, Armin Ghobadi, Cameron J Turtle, Jennifer N Brudno, Marcela V Maus, Jae H Park, Elena Mead, and Steven Pavletic. 2019. “ASTCT Consensus Grading for Cytokine Release Syndrome and Neurologic Toxicity Associated with Immune Effector Cells.” *Biology of Blood and Marrow Transplantation* 25 (4): 625–38.

Lee, Hye-Sung, Bong-Soo Park, Hae-Mi Kang, Jung-Han Kim, Sang-Hun Shin, and In-Ryoung Kim. 2021. “Role of Luteolin-Induced Apoptosis and Autophagy in Human Glioblastoma Cell Lines.” *Medicina* 57 (9): 879.

Li, Lu, Guanghua Pan, Rong Fan, Dalei Li, Lei Guo, Lili Ma, Hui Liang, and Jiaoxue Qiu. 2022. “Luteolin Alleviates Inflammation and Autophagy of Hippocampus Induced by Cerebral Ischemia/Reperfusion by Activating PPAR Gamma in Rats.” *BMC Complementary Medicine and Therapies* 22 (1): 176. https://doi.org/10.1186/s12906-022-03652-8.

Liao, Yuexia, Yang Xu, Mengyao Cao, Yuanyuan Huan, Lei Zhu, Ye Jiang, Weigan Shen, and Guoqiang Zhu. 2018. “Luteolin Induces Apoptosis and Autophagy in Mouse Macrophage ANA-1 Cells via the Bcl-2 Pathway.” *Journal of Immunology Research* 2018.

Lim, Whasun, Changwon Yang, Fuller W Bazer, and Gwonhwa Song. 2016. “Luteolin Inhibits Proliferation and Induces Apoptosis of Human Placental Choriocarcinoma Cells by Blocking the PI3K/AKT Pathway and Regulating Sterol Regulatory Element Binding Protein Activity.” *Biology of Reproduction* 95 (4): 81–82.

Lin, Yong, Ranxin Shi, Xia Wang, and Han-Ming Shen. 2008. “Luteolin, a Flavonoid with Potential for Cancer Prevention and Therapy.” *Current Cancer Drug Targets* 8 (7): 634–46.

Liu, Jin-Feng, Ying Ma, Ying Wang, Zhi-Yan Du, Jing-Kang Shen, and Hong-Li Peng. 2011. “Reduction of Lipid Accumulation in HepG2 Cells by Luteolin Is Associated with Activation of AMPK and Mitigation of Oxidative Stress.” *Phytotherapy Research* 25 (4): 588–96. https://doi.org/https://doi.org/10.1002/ptr.3305.

López-Lázaro, Miguel. 2009. “Distribution and Biological Activities of the Flavonoid Luteolin.” *Mini Reviews in Medicinal Chemistry* 9 (1): 31–59.

Lozanski, Gerard, Ben Sanford, Daohai Yu, Rebecca Pearson, Colin Edwards, John C Byrd, Richard A Larson, Clara D Bloomfield, and Wendy Stock. 2006. “CD52 Expression in Adult Acute Lymphoblastic Leukemia (ALL): Quantitative Flow Cytometry Provides New Insights.” *Blood* 108 (11): 2293.

Luca, Dragoș C. 2021. “Update on Lymphoblastic Leukemia/Lymphoma.” *Clinics in Laboratory Medicine* 41 (3): 405–16. https://doi.org/https://doi.org/10.1016/j.cll.2021.04.003.

Lussana, Federico, Giuseppe Gritti, and Alessandro Rambaldi. 2021. “Immunotherapy of Acute Lymphoblastic Leukemia and Lymphoma With T Cell–Redirected Bispecific Antibodies.” *Journal of Clinical Oncology* 39 (5): 444–55. https://doi.org/10.1200/JCO.20.01564.

Malard, Florent, and Mohamad Mohty. 2020. “Acute Lymphoblastic Leukaemia.” *The Lancet* 395 (10230): 1146–62.

Malavasi, Fabio, Silvia Deaglio, Ada Funaro, Enza Ferrero, Alberto L Horenstein, Erika Ortolan, Tiziana Vaisitti, and Semra Aydin. 2008. “Evolution and Function of the ADP Ribosyl Cyclase/CD38 Gene Family in Physiology and Pathology.” *Physiological Reviews* 88 (3): 841–86.

Mamonkin, Maksim, Rayne H Rouce, Haruko Tashiro, and Malcolm K Brenner. 2015. "A T-Cell–Directed Chimeric Antigen Receptor for the Selective Treatment of T-Cell Malignancies." *Blood, The Journal of the American Society of Hematology* 126 (8): 983–92.

Marchand, Loïc Le. 2002. "Cancer Preventive Effects of Flavonoids—a Review." *Biomedicine & Pharmacotherapy* 56 (6): 296–301.

Maude, Shannon L, Noelle Frey, Pamela A Shaw, Richard Aplenc, David M Barrett, Nancy J Bunin, Anne Chew, et al. 2014. "Chimeric Antigen Receptor T Cells for Sustained Remissions in Leukemia." *New England Journal of Medicine* 371 (16): 1507–17. https://doi.org/10.1056/NEJMoa1407222.

Maude, Shannon L, Theodore W Laetsch, Jochen Buechner, Susana Rives, Michael Boyer, Henrique Bittencourt, Peter Bader, et al. 2018. "Tisagenlecleucel in Children and Young Adults with B-Cell Lymphoblastic Leukemia." *New England Journal of Medicine* 378 (5): 439–48. https://doi.org/10.1056/NEJMoa1709866.

Maury, Sébastien, Françoise Huguet, Thibaut Leguay, Francis Lacombe, Marc Maynadié, Sandrine Girard, Adrienne de Labarthe, Emilienne Kuhlein, Emmanuel Raffoux, and Xavier Thomas. 2010. "Adverse Prognostic Significance of CD20 Expression in Adults with Philadelphia Chromosome-Negative B-Cell Precursor Acute Lymphoblastic Leukemia." *Haematologica* 95 (2): 324–28.

Mehrabadi, Ali Zarezadeh, Reza Ranjbar, Mahdieh Farzanehpour, Alireza Shahriary, Ruhollah Dorostkar, Mohammad Ali Hamidinejad, and Hadi Esmaeili Gouvarchin Ghaleh. 2022. "Therapeutic Potential of CAR T Cell in Malignancies: A Scoping Review." *Biomedicine & Pharmacotherapy* 146: 112512.

Mello, Maria Luiza S, and B C Vidal. 2012. "Changes in the Infrared Microspectroscopic Characteristics of DNA Caused by Cationic Elements, Different Base Richness and Single-Stranded Form."

Mohanty, Rimjhim, Chitran Roy Chowdhury, Solomon Arega, Prakriti Sen, Pooja Ganguly, and Niladri Ganguly. 2019. “CAR T Cell Therapy: A New Era for Cancer Treatment.” *Oncology Reports* 42 (6): 2183–95.

Muruganathan, Nandakumar, Anand Raj Dhanapal, Venkidasamy Baskar, Pandiyan Muthuramalingam, Dhivya Selvaraj, Husne Aara, Mohamed Zubair Shiek Abdullah, and Iyyakkannu Sivanesan. 2022. “Recent Updates on Source, Biosynthesis, and Therapeutic Potential of Natural Flavonoid Luteolin: A Review.” *Metabolites* 12 (11): 1145.

Narayanan, Sujata, and Paul J Shami. 2012. “Treatment of Acute Lymphoblastic Leukemia in Adults.” *Critical Reviews in Oncology/Hematology* 81 (1): 94–102.

Ning, Bo-Tao, Yong-Min Tang, Ying-Hu Chen, Hong-Qiang Shen, and Bai-Qin Qian. 2005. “Comparison between CD19 and CD20 Expression Patterns on Acute Leukemic Cells.” *Zhongguo Shi Yan Xue Ye Xue Za Zhi* 13 (6): 943–47.

Norzila, I, J Shajarahtunnur, and A Hasmah. 2016. “Natural Luteolin from Methanolic Extract of Malaysian Brucea Javanica Leaves Induces Apoptosis in HeLa Cell Lines.” *Health* 7 (2): 116–36.

Nowell, Peter C. 2007. “Discovery of the Philadelphia Chromosome: A Personal Perspective.” *The Journal of Clinical Investigation* 117 (8): 2033–35.

Oehler, Vivian G, Roland B Walter, Carrie Cummings, Olga Sala-Torra, Derek L Stirewalt, Min Fang, Jerald P Radich, and Brent Wood. 2010. “CD52 Expression in Leukemic Stem/Progenitor Cells.” *Blood* 116 (21): 2743.

Ofran, Yishai, Shimrit Ringelstein-Harlev, Ilana Slouzkey, Tsila Zuckerman, Dana Yehudai-Ofir, Israel Henig, Ofrat Beyar-Katz, Michal Hayun, and Avraham Frisch. 2020. “Daratumumab for Eradication of Minimal Residual Disease in High-Risk Advanced Relapse of T-Cell/CD19/CD22-Negative Acute Lymphoblastic Leukemia.” *Leukemia* 34 (1): 293–95. https://doi.org/10.1038/s41375-019-0548-z.

Panche, Archana N, Arvind D Diwan, and Sadanandavalli R Chandra. 2016. "Flavonoids: An Overview." *Journal of Nutritional Science* 5: e47.

Park, Jae H, Isabelle Rivière, Mithat Gonen, Xiuyan Wang, Brigitte Sénéchal, Kevin J Curran, Craig Sauter, Yongzeng Wang, Bianca Santomasso, and Elena Mead. 2018. "Long-Term Follow-up of CD19 CAR Therapy in Acute Lymphoblastic Leukemia." *New England Journal of Medicine* 378 (5): 449–59.

Pettitt, David, Zeeshaan Arshad, James Smith, Tijana Stanic, Georg Holländer, and David Brindley. 2018. "CAR-T Cells: A Systematic Review and Mixed Methods Analysis of the Clinical Trial Landscape." *Molecular Therapy* 26 (2): 342–53.

Pinz, Kevin G, Elizabeth Yakaboski, Alexander Jares, Hua Liu, Amelia E Firor, Kevin H Chen, Masayuki Wada, Huda Salman, William Tse, and Nabil Hagag. 2017. "Targeting T-Cell Malignancies Using Anti-CD4 CAR NK-92 Cells." *Oncotarget* 8 (68): 112783.

Pinz, Kevin, Hua Liu, Marc Golightly, Alexander Jares, Fengshuo Lan, Gary W Zieve, Nabil Hagag, Michael Schuster, Amelia E Firor, and Xun Jiang. 2016. "Preclinical Targeting of Human T-Cell Malignancies Using CD4-Specific Chimeric Antigen Receptor (CAR)-Engineered T Cells." *Leukemia* 30 (3): 701–7.

Png, Yi Tian, Natasha Vinanica, Takahiro Kamiya, Noriko Shimasaki, Elaine Coustan-Smith, and Dario Campana. 2017. "Blockade of CD7 Expression in T Cells for Effective Chimeric Antigen Receptor Targeting of T-Cell Malignancies." *Blood Advances* 1 (25): 2348–60.

Porkka, Kimmo, Perttu Koskenvesa, Tuija Lundán, Johanna Rimpiläinen, Satu Mustjoki, Richard Smykla, Robert Wild, Roger Luo, Montserrat Arnan, and Benoit Brethon. 2008. "Dasatinib Crosses the Blood-Brain Barrier and Is an Efficient Therapy for Central Nervous System Philadelphia Chromosome–Positive Leukemia." *Blood, The Journal of the American Society of Hematology* 112 (4): 1005–12.

Pottier, Charles, Margaux Fresnais, Marie Gilon, Guy Jérusalem, Rémi Longuespée, and Nor Eddine Sounni. 2020. “Tyrosine Kinase Inhibitors in Cancer: Breakthrough and Challenges of Targeted Therapy.” *Cancers* 12 (3): 731.

Prasher, Parteek, Mousmee Sharma, Sachin Kumar Singh, Monica Gulati, Dinesh Kumar Chellappan, Flavia Zacconi, Gabriele De Rubis, et al. 2022. “Luteolin: A Flavonoid with a Multifaceted Anticancer Potential.” *Cancer Cell International* 22 (1): 386. https://doi.org/10.1186/s12935-022-02808-3.

Pratheeshkumar, Poyil, Young-Ok Son, Amit Budhraja, Xin Wang, Songze Ding, Lei Wang, Andrew Hitron, Jeong-Chae Lee, Donghern Kim, and Sasidharan Padmaja Divya. 2012. “Luteolin Inhibits Human Prostate Tumor Growth by Suppressing Vascular Endothelial Growth Factor Receptor 2-Mediated Angiogenesis.” *PloS One* 7 (12): e52279.

Pui, Ching-Hon, Frederick G Behm, and William M Crist. 1993. “Clinical and Biologic Relevance of Immunologic Marker Studies in Childhood Acute Lymphoblastic Leukemia.”

Pulte, E Dianne, Haiyan Chen, Lauren S L Price, Ramadevi Gudi, Hongshan Li, Olanrewaju O Okusanya, Lian Ma, Lisa Rodriguez, Jonathon Vallejo, and Kelly J Norsworthy. 2022. “FDA Approval Summary: Revised Indication and Dosing Regimen for Ponatinib Based on the Results of the OPTIC Trial.” *The Oncologist* 27 (2): 149–57.

Qing, Weixia, Yong Wang, Huan Li, Fanyi Ma, Jinhua Zhu, and Xiuhua Liu. 2017. “Preparation and Characterization of Copolymer Micelles for the Solubilization and in Vitro Release of Luteolin and Luteoloside.” *Aaps Pharmscitech* 18: 2095–2101.

Qu, Qiang, Jian Qu, Yong Guo, Bo-Ting Zhou, and Hong-Hao Zhou. 2014. “Luteolin Potentiates the Sensitivity of Colorectal Cancer Cell Lines to Oxaliplatin through the PPARγ/OCTN2 Pathway.” *Anti-Cancer Drugs* 25 (9): 1016–27.

Raetz, Elizabeth A, Mitchell S Cairo, Michael J Borowitz, Susan M Blaney, Mark D Krailo, Tarek A Leil, Joel M Reid, David M Goldenberg, William A Wegener, and William L Carroll. 2008. “Chemoimmunotherapy Reinduction with Epratuzumab in Children with Acute Lymphoblastic Leukemia in Marrow Relapse: A Children’s Oncology Group Pilot Study.” *Journal of Clinical Oncology* 26 (22): 3756.

Raina, Ritu, Sreepoorna Pramodh, Naushad Rais, Shafiul Haque, Jasmin Shafarin, Khuloud Bajbouj, Mawieh Hamad, and Arif Hussain. 2021. “Luteolin Inhibits Proliferation, Triggers Apoptosis and Modulates Akt/MTOR and MAP Kinase Pathways in HeLa Cells.” *Oncology Letters* 21 (3): 1.

Ravandi, Farhad, Susan M O’Brien, Jorge E Cortes, Deborah M Thomas, Rebecca Garris, Stefan Faderl, Jan A Burger, Michael E Rytting, Alessandra Ferrajoli, and William G Wierda. 2015. “Long-term Follow-up of a Phase 2 Study of Chemotherapy plus Dasatinib for the Initial Treatment of Patients with P Hiladelphia Chromosome–Positive Acute Lymphoblastic Leukemia.” *Cancer* 121 (23): 4158–64.

Roberts, Kathryn G. 2018. “Genetics and Prognosis of ALL in Children vs Adults.” *Hematology* 2018 (1): 137–45. https://doi.org/10.1182/asheducation-2018.1.137.

Rosenblatt, Jacalyn, and David Avigan. 2010. “Immunotherapy for Acute Lymphocytic Leukemia.” In *Adult Acute Lymphocytic Leukemia: Biology and Treatment*, 351–63. Springer.

Ruhayel, Sandra, and Santosh Valvi. 2020. “Daratumumab in T-Cell Acute Lymphoblastic Leukaemia: A Case Report and Review of the Literature.” *Authorea Preprints*.

Sak, Katrin. 2022. “Anticancer Action of Plant Products: Changing Stereotyped Attitudes.” *Exploration of Targeted Anti-Tumor Therapy* 3 (4): 423.

Sak, Katrin, Kristi Kasemaa, and Hele Everaus. 2016. “Potentiation of Luteolin Cytotoxicity by Flavonols Fisetin and Quercetin in Human Chronic Lymphocytic Leukemia Cell Lines.” *Food & Function* 7 (9): 3815–24.

Samec, Marek, Alena Mazurakova, Vincent Lucansky, Lenka Koklesova, Renata Pecova, Martin Pec, Olga Golubnitschaja, et al. 2023. “Flavonoids Attenuate Cancer Metabolism by Modulating Lipid Metabolism, Amino Acids, Ketone Bodies and Redox State Mediated by Nrf2.” *European Journal of Pharmacology* 949: 175655. https://doi.org/https://doi.org/10.1016/j.ejphar.2023.175655.

Samra, Bachar, Elias Jabbour, Farhad Ravandi, Hagop Kantarjian, and Nicholas J Short. 2020. “Evolving Therapy of Adult Acute Lymphoblastic Leukemia: State-of-the-Art Treatment and Future Directions.” *Journal of Hematology & Oncology* 13 (1): 70. https://doi.org/10.1186/s13045-020-00905-2.

Saqlio, G. 2010. “Nilotinib versus Imatinib for Newly Diagnosed Chronic Myeloid Leukemia.” *N Engl J Med* 362: 2251–59.

Sasaki, Koji, Elias J Jabbour, Farhad Ravandi, Nicholas J Short, Deborah A Thomas, Guillermo Garcia-Manero, Naval G Daver, Tapan M Kadia, Marina Y Konopleva, and Nitin Jain. 2016. “Hyper-CVAD plus Ponatinib versus Hyper-CVAD plus Dasatinib as Frontline Therapy for Patients with Philadelphia Chromosome-positive Acute Lymphoblastic Leukemia: A Propensity Score Analysis.” *Cancer* 122 (23): 3650–56.

Sayre, Casey L, Karen D Gerde, Jaime A Yáñez, and Neal M Davies. 2012. “Clinical Pharmacokinetics of Flavonoids.” *Flavonoid Pharmacokinetics: Methods of Analysis, Preclinical and Clinical Pharmacokinetics, Safety, and Toxicology*, 195–247.

Schrappe, Martin, and Martin Stanulla. 2010. “Current Treatment Approaches in Childhood Acute Lymphoblastic Leukemia.” *International Society of Paediatric Oncology*, 25.

Schultz, K R, A Carroll, N A Heerema, W P Bowman, A Aledo, W B Slayton, H Sather, M Devidas, H W Zheng, and S M Davies. 2014. “Long-Term Follow-up of Imatinib in Pediatric Philadelphia Chromosome-Positive Acute Lymphoblastic Leukemia: Children’s Oncology Group Study AALL0031.” *Leukemia* 28 (7): 1467–71.

Severcan, Feride, Neslihan Toyran, Neşe Kaptan, and Belma Turan. 2000. “Fourier Transform Infrared Study of the Effect of Diabetes on Rat Liver and Heart Tissues in the C-H Region.” *Talanta* 53 (1): 55–59.

Shah, Neil P, John M Nicoll, Bhushan Nagar, Mercedes E Gorre, Ronald L Paquette, John Kuriyan, and Charles L Sawyers. 2002. “Multiple BCR-ABL Kinase Domain Mutations Confer Polyclonal Resistance to the Tyrosine Kinase Inhibitor Imatinib (STI571) in Chronic Phase and Blast Crisis Chronic Myeloid Leukemia.” *Cancer Cell* 2 (2): 117–25.

Shah, Neil P, Chris Tran, Francis Y Lee, Ping Chen, Derek Norris, and Charles L Sawyers. 2004. “Overriding Imatinib Resistance with a Novel ABL Kinase Inhibitor.” *Science* 305 (5682): 399–401.

Shang, Yufeng, and Fuling Zhou. 2019. “Current Advances in Immunotherapy for Acute Leukemia: An Overview of Antibody, Chimeric Antigen Receptor, Immune Checkpoint, and Natural Killer.” *Frontiers in Oncology* 9: 917.

Shimoi, Kayoko, Hisae Okada, Michiyo Furugori, Toshinao Goda, Sachiko Takase, Masayuki Suzuki, Yukihiko Hara, Hiroyo Yamamoto, and Naohide Kinae. 1998. “Intestinal Absorption of Luteolin and Luteolin 7-O-β-Glucoside in Rats and Humans.” *FEBS Letters* 438 (3): 220–24.

Siegel, Rebecca L, Kimberly D Miller, Hannah E Fuchs, and Ahmedin Jemal. 2022. “Cancer Statistics, 2022.” *CA: A Cancer Journal for Clinicians* 72 (1): 7–33.

Singh Tuli, Hardeep, Prangya Rath, Abhishek Chauhan, Katrin Sak, Diwakar Aggarwal, Renuka Choudhary, Ujjawal Sharma, Kanupriya Vashishth, Sheetu Sharma, and

Manoj Kumar. 2022. “Luteolin, a Potent Anticancer Compound: From Chemistry to Cellular Interactions and Synergetic Perspectives.” *Cancers* 14 (21): 5373.

Sivandzade, Farzane, Aditya Bhalerao, and Luca Cucullo. 2019. “Analysis of the Mitochondrial Membrane Potential Using the Cationic JC-1 Dye as a Sensitive Fluorescent Probe.” *Bio-Protocol* 9 (1): e3128–e3128.

Slayton, William B, Kirk R Schultz, John A Kairalla, Meenakshi Devidas, Xinlei Mi, Michael A Pulsipher, Bill H Chang, Charles Mullighan, Ilaria Iacobucci, and Lewis B Silverman. 2018. “Dasatinib plus Intensive Chemotherapy in Children, Adolescents, and Young Adults with Philadelphia Chromosome–Positive Acute Lymphoblastic Leukemia: Results of Children’s Oncology Group Trial AALL0622.” *Journal of Clinical Oncology* 36 (22): 2306.

Slika, Hasan, Hadi Mansour, Nadine Wehbe, Suzanne A Nasser, Rabah Iratni, Gheyath Nasrallah, Abdullah Shaito, Tarek Ghaddar, Firas Kobeissy, and Ali H Eid. 2022. “Therapeutic Potential of Flavonoids in Cancer: ROS-Mediated Mechanisms.” *Biomedicine & Pharmacotherapy* 146: 112442.

Stock, Wendy, Ben Sanford, Gerard Lozanski, Ravi Vij, John C Byrd, Bayard L Powell, Meir Wetzler, Dorie Sher, Colin Edwards, and Michael Kelly. 2009. “Alemtuzumab Can Be Incorporated Into Front-Line Therapy of Adult Acute Lymphoblastic Leukemia (ALL): Final Phase I Results of a Cancer and Leukemia Group B Study (CALGB 10102).” *Blood* 114 (22): 838.

Taboury, J A, J Liquier, and E Taillandier. 1985. “Characterization of DNA Structures by Infrared Spectroscopy: Double Helical Forms of Poly (DG-DC)• Poly (DG-DC), Poly (DD8G-DC)• Poly (DD8G-DC), and Poly (DG-Dm5C)• Poly (DG-Dm5C).” *Canadian Journal of Chemistry* 63 (7): 1904–9.

Taylor, Ronald P, and Margaret A Lindorfer. 2016. “Cytotoxic Mechanisms of Immunotherapy: Harnessing Complement in the Action of Anti-Tumor Monoclonal Antibodies.” In *Seminars in Immunology*, 28:309–16. Elsevier.

Tembhare, Prashant Ramesh, Harshini Sriram, Twinkle Khanka, Gaurav Chatterjee, Devasis Panda, Sitaram Ghogale, Yajamanam Badrinath, Nilesh Deshpande, Nikhil V Patkar, and Gaurav Narula. 2020. "Flow Cytometric Evaluation of CD38 Expression Levels in the Newly Diagnosed T-Cell Acute Lymphoblastic Leukemia and the Effect of Chemotherapy on Its Expression in Measurable Residual Disease, Refractory Disease and Relapsed Disease: An Implication for Anti-CD38 Immunotherapy." *Journal for Immunotherapy of Cancer* 8 (1).

Terwilliger, T, and M Abdul-Hay. 2017. "Acute Lymphoblastic Leukemia: A Comprehensive Review and 2017 Update." *Blood Cancer Journal* 7 (6): e577. https://doi.org/10.1038/bcj.2017.53.

Thomas, Deborah A, Susan O'Brien, Stefan Faderl, Guillermo Garcia-Manero, Alessandra Ferrajoli, William Wierda, Farhad Ravandi, Srdan Verstovsek, Jeffrey L Jorgensen, and Carlos Bueso-Ramos. 2010. "Chemoimmunotherapy with a Modified Hyper-CVAD and Rituximab Regimen Improves Outcome in de Novo Philadelphia Chromosome–Negative Precursor B-Lineage Acute Lymphoblastic Leukemia." *Journal of Clinical Oncology* 28 (24): 3880.

Thomas, Deborah A, Susan O'Brien, Jeffrey L Jorgensen, Jorge Cortes, Stefan Faderl, Guillermo Garcia-Manero, Srdan Verstovsek, Charles Koller, Sherry Pierce, and Yang Huh. 2009. "Prognostic Significance of CD20 Expression in Adults with de Novo Precursor B-Lineage Acute Lymphoblastic Leukemia." *Blood, The Journal of the American Society of Hematology* 113 (25): 6330–37.

Tibes, Raoul, Michael J Keating, Alessandra Ferrajoli, William Wierda, Farhad Ravandi, Guillermo Garcia-Manero, Susan O'Brien, Jorge Cortes, Srdan Verstovsek, and Mary L Browning. 2006. "Activity of Alemtuzumab in Patients with CD52-positive Acute Leukemia." *Cancer: Interdisciplinary International Journal of the American Cancer Society* 106 (12): 2645–51.

Ullah, Asad, Sidra Munir, Syed Lal Badshah, Noreen Khan, Lubna Ghani, Benjamin Gabriel Poulson, Abdul-Hamid Emwas, and Mariusz Jaremko. 2020. "Important Flavonoids and Their Role as a Therapeutic Agent." *Molecules* 25 (22): 5243.

Vale, Andre M, and Harry W Schroeder Jr. 2010. “Clinical Consequences of Defects in B-Cell Development.” *Journal of Allergy and Clinical Immunology* 125 (4): 778–87.

Vardiman, James W, Jüergen Thiele, Daniel A Arber, Richard D Brunning, Michael J Borowitz, Anna Porwit, Nancy Lee Harris, Michelle M Le Beau, Eva Hellström-Lindberg, and Ayalew Tefferi. 2009. “The 2008 Revision of the World Health Organization (WHO) Classification of Myeloid Neoplasms and Acute Leukemia: Rationale and Important Changes.” *Blood, The Journal of the American Society of Hematology* 114 (5): 937–51.

Wang, F, F Gao, S Pan, S Zhao, and Y Xue. 2014. “Luteolin Induces Apoptosis, G0/G1 Cell Cycle Growth Arrest and Mitochondrial Membrane Potential Loss in Neuroblastoma Brain Tumor Cells.” *Drug Research*, 91–95.

Wang, Liping, Qingwei Chen, Lijun Zhu, Qiang Li, Xuejun Zeng, Linlin Lu, Ming Hu, Xinchun Wang, and Zhongqiu Liu. 2017. “Metabolic Disposition of Luteolin Is Mediated by the Interplay of UDP-Glucuronosyltransferases and Catechol-O-Methyltransferases in Rats.” *Drug Metabolism and Disposition* 45 (3): 306–15.

Wang, Qiang, Handong Wang, Yue Jia, Hui Ding, Li Zhang, and Hao Pan. 2017. “Luteolin Reduces Migration of Human Glioblastoma Cell Lines via Inhibition of the P-IGF-1R/PI3K/AKT/MTOR Signaling Pathway.” *Oncology Letters* 14 (3): 3545–51.

Wang, Xiaodong, Qi Wang, and Marilyn E Morris. 2008. “Pharmacokinetic Interaction between the Flavonoid Luteolin and γ-Hydroxybutyrate in Rats: Potential Involvement of Monocarboxylate Transporters.” *The AAPS Journal* 10: 47–55.

Watanabe, Norihiro, Feiyan Mo, Rong Zheng, Royce Ma, Vanesa C Bray, Dayenne G van Leeuwen, Juntima Sritabal-Ramirez, Hongxiang Hu, Sha Wang, and Birju Mehta. 2023. “Feasibility and Preclinical Efficacy of CD7-Unedited CD7 CAR T Cells for T Cell Malignancies.” *Molecular Therapy* 31 (1): 24–34.

Wierda, William G, Swaminathan Padmanabhan, Geoffrey W Chan, Ira V Gupta, Steen Lisby, Anders Österborg, and Hx-CD20-406 Study Investigators. 2011. "Ofatumumab Is Active in Patients with Fludarabine-Refractory CLL Irrespective of Prior Rituximab: Results from the Phase 2 International Study." *Blood, The Journal of the American Society of Hematology* 118 (19): 5126–29.

Wood, Bayden Robert, Luis Chiriboga, H Yee, Michael A Quinn, Donald McNaughton, and Max Diem. 2004. "Fourier Transform Infrared (FTIR) Spectral Mapping of the Cervical Transformation Zone, and Dysplastic Squamous Epithelium." *Gynecologic Oncology* 93 (1): 59–68.

Wu, Wenying, Kexin Li, Chen Zhao, Xiaohua Ran, Yu Zhang, and Tianhong Zhang. 2022. "A Rapid HPLC–MS/MS Method for the Simultaneous Determination of Luteolin, Resveratrol and Their Metabolites in Rat Plasma and Its Application to Pharmacokinetic Interaction Studies." *Journal of Chromatography B* 1191: 123118.

Yandim, Melis Kartal, Cagatay Ceylan, Efe Elmas, and Yusuf Baran. 2016. "A Molecular and Biophysical Comparison of Macromolecular Changes in Imatinib-Sensitive and Imatinib-Resistant K562 Cells Exposed to Ponatinib." *Tumor Biology* 37: 2365–78.

Yang, Huan, Bing-Fang Liu, Fu-Jia Xie, Wei-Lin Yang, and Nong Cao. 2020. "Luteolin Induces Mitochondrial Apoptosis in HT29 Cells by Inhibiting the Nrf2/ARE Signaling Pathway." *Experimental and Therapeutic Medicine* 19 (3): 2179–87.

Yang, Kedi, Yi Song, Li Ge, Jing Su, Yanxuan Wen, and Yunfei Long. 2013. "Measurement and Correlation of the Solubilities of Luteolin and Rutin in Five Imidazole-Based Ionic Liquids." *Fluid Phase Equilibria* 344: 27–31.

Yasuda, Michiko Torii, Kotone Fujita, Takahiro Hosoya, Shinjiro Imai, and Kayoko Shimoi. 2015. "Absorption and Metabolism of Luteolin and Its Glycosides from

the Extract of Chrysanthemum Morifolium Flowers in Rats and Caco-2 Cells." *Journal of Agricultural and Food Chemistry* 63 (35): 7693–99.

Yin, Lei, Meiyun Shi, Yantong Sun, Xiaocheng Sun, Huan Meng, J Paul Fawcett, Yan Yang, and Jingkai Gu. 2013. "A Liquid Chromatography–Tandem Mass Spectrometric Method for the Simultaneous Quantitation of Five Components of Ixeris Sonchifoliain (Bge.) Hance in Rat Plasma and Its Application to a Pharmacokinetic Study." *Journal of Chromatography B* 931: 12–16.

Younes, Anas, Stella Kim, Jorge Romaguera, Amanda Copeland, Silvana de Castro Farial, Larry W Kwak, Luis Fayad, Frederick Hagemeister, Michelle Fanale, and Sattva Neelapu. 2012. "Phase I Multidose-Escalation Study of the Anti-CD19 Maytansinoid Immunoconjugate SAR3419 Administered by Intravenous Infusion Every 3 Weeks to Patients with Relapsed/Refractory B-Cell Lymphoma." *Journal of Clinical Oncology* 30 (22): 2776.

Zang, Ming-de, Lei Hu, Zhi-yuan Fan, He-xiao Wang, Zheng-lun Zhu, Shu Cao, Xiong-yan Wu, Jian-fang Li, Li-ping Su, and Chen Li. 2017. "Luteolin Suppresses Gastric Cancer Progression by Reversing Epithelial-Mesenchymal Transition via Suppression of the Notch Signaling Pathway." *Journal of Translational Medicine* 15 (1): 1–11.

Zang, Mingde, Lei Hu, Baogui Zhang, Zhenglun Zhu, Jianfang Li, Zhenggang Zhu, Min Yan, and Bingya Liu. 2017. "Luteolin Suppresses Angiogenesis and Vasculogenic Mimicry Formation through Inhibiting Notch1-VEGF Signaling in Gastric Cancer." *Biochemical and Biophysical Research Communications* 490 (3): 913–19.

Zang, Yanqing, Kiharu Igarashi, and Yu Li. 2016. "Anti-Diabetic Effects of Luteolin and Luteolin-7-O-Glucoside on KK-A y Mice." *Bioscience, Biotechnology, and Biochemistry* 80 (8): 1580–86.

Zhang, Man, Rui Wang, Jie Tian, Mengqiu Song, Ran Zhao, Kangdong Liu, Feng Zhu, Jung-Hyun Shim, Zigang Dong, and Mee-Hyun Lee. 2021. "Targeting LIMK1

with Luteolin Inhibits the Growth of Lung Cancer in Vitro and in Vivo." *Journal of Cellular and Molecular Medicine* 25 (12): 5560–71. https://doi.org/https://doi.org/10.1111/jcmm.16568.

Zhou, Tianjun, Lois Commodore, Wei-Sheng Huang, Yihan Wang, Mathew Thomas, Jeff Keats, Qihong Xu, Victor M Rivera, William C Shakespeare, and Tim Clackson. 2011. "Structural Mechanism of the Pan-BCR-ABL Inhibitor Ponatinib (AP24534): Lessons for Overcoming Kinase Inhibitor Resistance." *Chemical Biology & Drug Design* 77 (1): 1–11.

Zubiaur, Mercedes, Olga Fernández, Enza Ferrero, Javier Salmerón, Bernard Malissen, Fabio Malavasi, and Jaime Sancho. 2002. "CD38 Is Associated with Lipid Rafts and upon Receptor Stimulation Leads to Akt/Protein Kinase B and Erk Activation in the Absence of the CD3-ζ Immune Receptor Tyrosine-Based Activation Motifs." *Journal of Biological Chemistry* 277 (1): 13–22.